

Politecnico di Torino

Master's degree in
Automotive Engineering



Master's thesis

Calibration and optimization of a 1D SI light-duty
engine model - PHOENICE H2020 Project

Candidate

Daniele SANTILLI

Supervisors

Prof. Federico MILLO

Prof. Luciano ROLANDO

Dr. Giuseppe CASTELLANO

Company Supervisors:

Dr. Giuseppe SAMMITO

Dr. Marco SPAGNUOLI

Dr. Alessandro PERAZZO

July 2022

A tutti coloro che mi sono stati accanto e mi hanno supportato in questo magnifico percorso.

Index

INDEX	2
ABSTRACT	3
1 AUTOMOTIVE FRAMEWORK	4
1.1 GLOBAL FRAMEWORK ON SUSTAINABLE USE OF ENERGY	4
1.2 ROAD TRANSPORT CONTRIBUTION TO CO ₂ EMISSIONS AND FUTURE PREVISION	5
1.3 INTERNAL COMBUSTION ENGINE ROLE IN FUTURE YEARS	9
2 STATE OF ART OF GASOLINE INTERNAL COMBUSTION ENGINE: INTRODUCTION TO PHOENICE	13
2.1 EXAMPLE OF REFERENCE GASOLINE ENGINE FOR PASSENGER CAR: STELLANTIS GSE-T4	13
2.2 A HORIZON 2020 PROJECT: PHOENICE	24
3 ROLE OF 1D CFD SIMULATION FOR ECU DEVELOPMENT: INTRODUCTION OF GT-SUITE TOOL	31
3.1 CFD MODELS FOR HARDWARE IN THE LOOP ECU DEVELOPMENT	31
3.2 GT-SUITE: MODELLING AND SIMULATION PRINCIPLES	34
4 GSE-T4 MODEL CALIBRATION	39
4.1 THE BASELINE MODEL	39
4.2 CALIBRATION PARAMETERS	42
4.3 FULL LOAD CALIBRATION	52
4.3.1 <i>Calibration methodology and results analysis</i>	53
4.4 PART LOAD CALIBRATION	57
4.4.1 <i>Calibration methodology and results analysis</i>	57
5 IMPLEMENTATION OF THE PHOENICE FEATURES	66
5.1 MODEL UPDATES	66
5.2 CONTROL STRATEGY DEFINITION	67
5.3 OPTIMIZATION METHODOLOGY	72
5.4 RESULTS AND ANALYSIS	75
CONCLUSION	80
REFERENCES	81

Abstract

Today's society is undergoing a major transition, problems related to the environment and climate change have become increasingly evident, and various countries are mobilizing to implement new regulations for increasingly sustainable development for the environment as well. The Paris Treaty is a prime example of what the world needs, but it provides a path, the one toward carbon balancing by 2050, that is out of reach with current regulations. Further efforts will therefore be needed, and the automotive sector is not exempt. The European Parliament has voted to make the abolition of the sale of cars containing a combustion engine from 2035, decreeing what could be the end of this technology. The motivation is to reduce the emissions of greenhouse gases (GHGs) that internal combustion cars emit directly (tail pipe emissions) but it is unclear whether this is the correct way to achieve this goal. The world energy agency (WEO) has for years been involved in compiling a World Energy Outlook report from which various scenarios based on different assumptions emerge. This report serves as a guide for the countries of the world to understand the possible ways to achieve their goals. The report shows that in the best case scenario in 2030, 80 percent of vehicles will be equipped with an internal combustion engine, and this is enough to make it clear how important it is to continue developing this technology by incentivizing as much research as possible toward increasingly efficient powertrains. In this thesis work, after an initial detailed look at the future and current automotive framework, we will move on to an analysis of current technologies that have brought today's vehicles to an efficiency, and thus fuel consumption, in line with the emissions road map dictated by the European Union. In this context, the gasoline-powered internal combustion engine produced by Stellantis, the GSE-T4, which powers some of the group's cars is a clear example. But in a future where hybridization will be crucial to increase the overall efficiency of the vehicle, the combustion engine will have to be developed specifically for these architectures thus favoring the integration of the latter while at the same time having the goal of making the most of the synergy between these different technologies. PHOENICE, a Horizon 2020 project funded by the European Commission, aims to do just that. Based on one of the Stellantis cars and the GSE-T4, it will develop a 'Plug in Hybrid car, seeking to maximize the vehicle's energy efficiency while minimizing pollutant emissions. To do so, the project will strongly focus on an initial virtual development that will then give the basis and accompany the prototyping of the vehicle to minimize development time. In this context, the thesis work carried out at FEV Italia s.r.l, one of the companies involved, aims to calibrate a virtual model of the GSE-T4 engine on data provided by Stellantis. This model will then be used as a virtual environment for an initial setup of a Hardware in the Loop (HiL), a technology that will allow software development of the future ECU without the need for the presence of the engine prototype. Finally, this model will then be updated with the technologies provided by the PHOENICE project for an initial analysis of the possible theoretical benefits in terms of improved efficiency and thus less fuel consumption.

1 Automotive framework

1.1 Global framework on sustainable use of energy

The automotive sector is in the midst of the transition towards a cleaner use of energy. It is playing a very important role on transportation sector and together with others energy sectors to meet the targets of Green House Gases (GHG) and pollutant emissions. [1] The 26th Conference of the Parties (COP26) to the United Nations Framework Convention on Climate Change (UNFCCC) has set some key objectives like gather new 2030 emissions reduction pledges from countries to follow the line of the Paris Agreement that entered in to force in 2016 [2]. The last is a legally binding international treaty on climate change adopted by 196 Parties in COP 21 in Paris and its goal is to limit the global warming to 1.5 degrees Celsius compared to pre-industrial levels. To achieve this long-term temperature goal, the countries must reach a global net zero CO₂ emission by 2050.

To understand better what are the policies to adopt to reach this important target, every year the International Energy Agency (IEA) publish a report called “The World Energy Outlook (WEO) [1]” which provides critical analysis and insights on trends in energy demand and supply, and what they mean for energy security, environmental protection, and economic development. The WEO uses a scenario-based approach to highlight the key choices, consequences and contingencies that lie ahead, and to illustrate how the course of the energy system might be affected by changing some of the key variables, chief among them the energy policies adopted by governments around the world:

- Stated Policies Scenario (STEPS) reflects existing policies and measures, as well as policy ambitions and targets that have been legislated by governments around the world. It includes as example current Electric Vehicle (EV)-related policies and regulations and future developments based on the expected impacts of announced deployments and plans from industry stakeholders. The Stated Policies Scenario aims to hold up a mirror to the plans of policy makers and illustrate their consequences.
- Announced Pledges Scenario (APS) assumes that the announced ambitions and targets made by governments around the world, including the most recent ones, are met in full and on time. With regards to electromobility as example, it includes all recent major announcements of electrification targets and longer-term net zero emissions and other pledges, regardless of whether or not these have been anchored in legislation or in updated Nationally Determined Contributions.
- Net Zero Emissions by 2050 Scenario (NZE) is a normative scenario that sets out a narrow but achievable pathway for the global energy sector to achieve net zero CO₂ emissions by 2050. The scenario is compatible with limiting the global temperature rise to 1.5 °C with no or limited temperature overshoot, in line with reductions assessed in the Intergovernmental Panel on Climate Change in its Special Report on Global Warming of 1.5 °C.

The figure 1.1 resume the prediction in terms of Gigatons of CO₂ emission based on this different scenario and the respective temperature increase that the world can register in 2100.

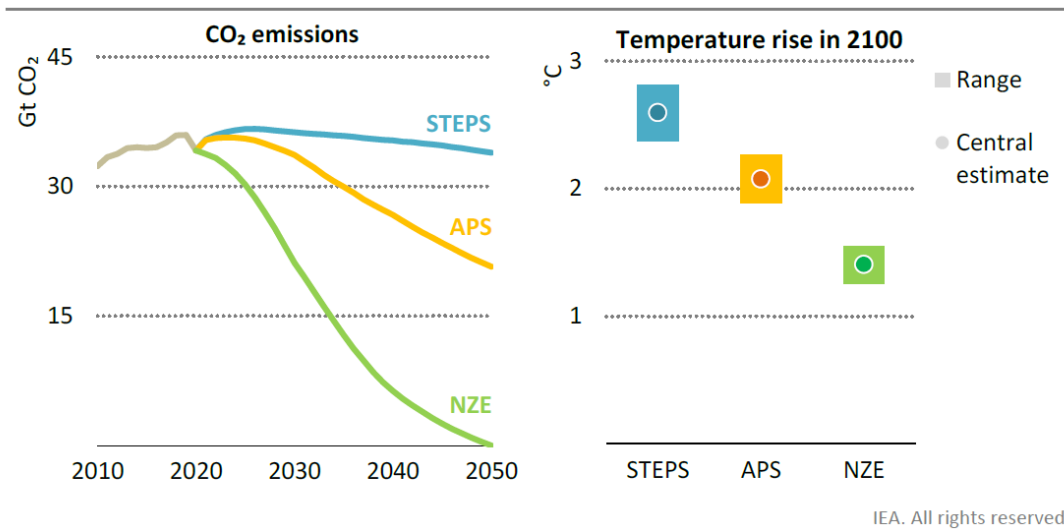


Figure 1.1 Total CO₂ emissions in Gigatons (Gt) by scenario and the corresponding prevision about temperature rise in 2100 [1]

1.2 Road transport contribution to CO₂ emissions and future prevision

In this framework the road transport sectors account for over 15% of total energy-related CO₂ emission (figure 1.2) and the previsions for the next years are quite different [1].

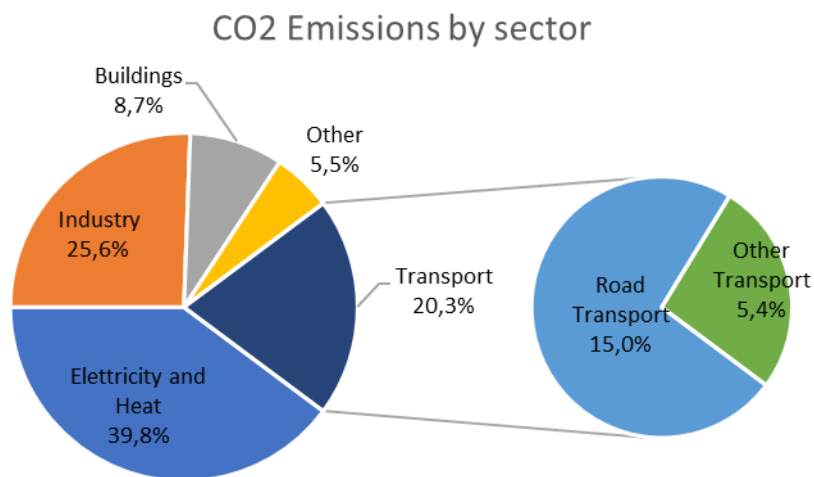


Figure 1.2 Total CO₂ emissions by sector in percentage

When analyzing CO₂ emissions in this sector usually it is referred to two types: well to tank (WTT) and tank to wheels (TTW) emissions. These analyses lead to obtain the total amount of energy derived from fossil fuels spent to operate the vehicle (figure 1.3) [3] from which GHG emissions can then be obtained. WTT includes the analysis of the energy costs of producing, transporting, and distributing the fuel while TTW considers the fuel used by the vehicle itself.

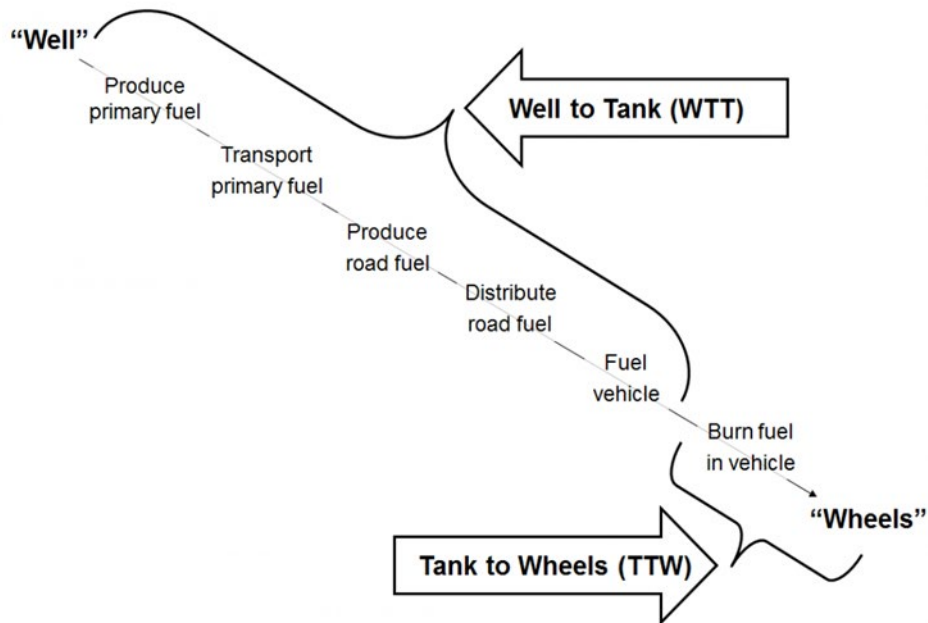
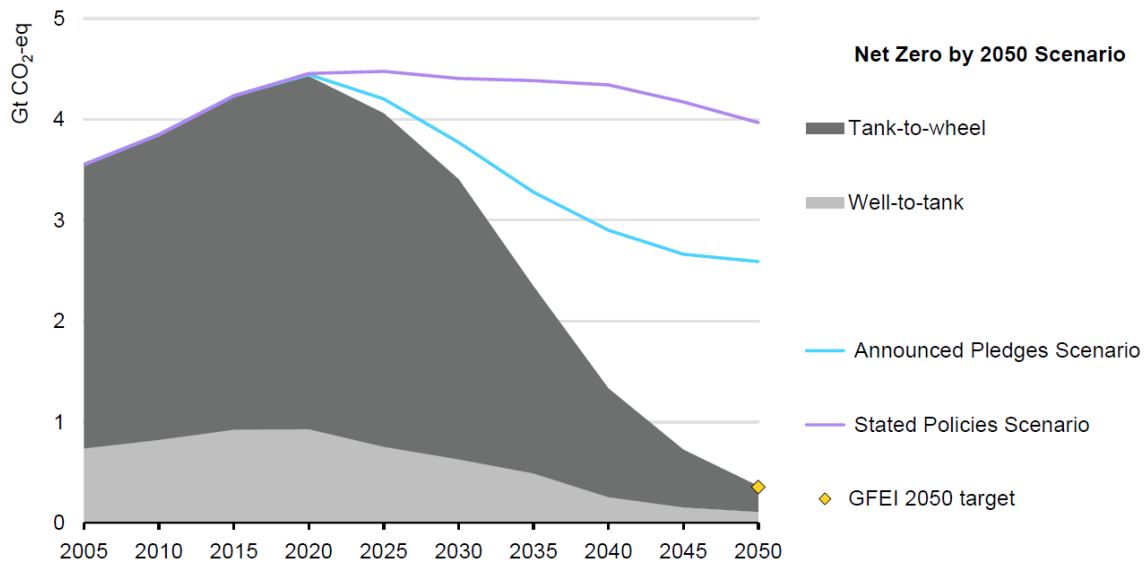


Figure 1.3 WTT and TTW analysis explained [3]

For example, in the case of a battery electric vehicle (BEV), TTW emissions will be zero because no fuel is burned during use while WTT emissions depend on how much electricity is produced using fossil fuels. Looking at the light duty vehicle sector, the graph (figures 1.4) shows us that most of the CO₂ emissions from the road transport sector are due to direct fuel use [4]. The trend predicted by the NZE calls for a very high abatement especially of this form of GHG emission due mainly to an increase of electric propulsion in the market at the expense of conventional propulsion. The other two scenarios call for much less abatement, the difference between NZE and APS, called the “the ambition gap”, correspond to 0.5 Gt of CO₂ emission in 2030 and become almost 2.2 Gt in 2050.



IEA. All rights reserved.

Figure 1.4 Global well-to-wheel emissions reductions in the light-duty fleet, GFEI target and IEA Scenarios, 2005-2050 [4]

One of the major reasons behind the higher emissions in APS is strong demand growth in emerging market and developing economies, many of which do not have net zero pledges. For example, over 40% of global car sales in 2030 take place in emerging market and developing economies without pledges. For instance,

emerging market and developing economies rely heavily on the second-hand market, which is unlikely to have many Electric Vehicles until 2030.

To achieve these goals stringent regulations about fuel consumption are going to be set and even in Europe on 8 June 2022 the European Parliament voted to ban sales of new internal combustion engine (ICE) cars and vans in the European Union from 2035 onward [5]. Apart from niche luxury cars, no more gasoline or diesel engines will be allowed, nor even hybrid, gas (LPG, CNG), agrofuel (ethanol, agrodiesel) or synthetic fuel engines. This is only the first step in bringing the legislation into force, but it's a clear signal of what the legislation think it can be the needs to achieve the "Fit for 55" (table 1.1) [6].

Table 1.1 Previous and current EU CO₂ emissions standards for light-duty vehicles [6]

Category	Passenger cars		Light commercial vehicles	
	Previous	New	Previous	New
Year/target				
2020 (base)	95 g CO ₂ /km		147 g CO ₂ /km	
2025	15%	15%	15%	15%
2030	37.5%	55%	31%	50%
2035	--	100%	--	100%

Notes: 2020 emissions are measured with the NEDC. Percentage reductions are benchmarked to the 2020 base year.

Several car makers announce their intention to go throw the production of mainly BEV and plug-in Hybrid (P-HEV) vehicles in the next years (figure 1.5) following the European intentions [7].

Battery and fuel cell electric vehicles (BEVs / FCEVs)

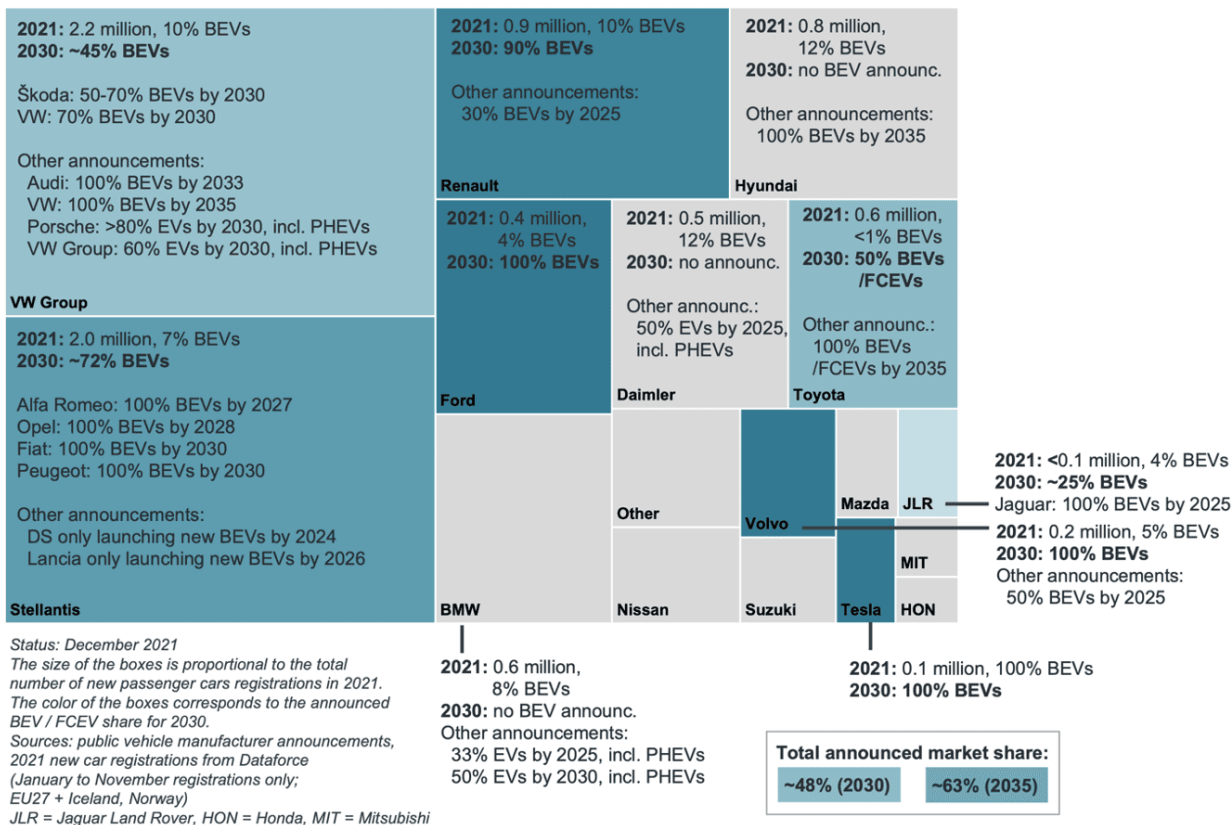


Figure 1.5 Passenger car vehicle manufacturer announcements for Europe [7]

There is no doubt that the electrification of the road sector with the increasing introduction of BEV, and P-HEV in the market will play a very important role in the reduction of GHG emission. Indeed, in the figure 1.6 [4] is illustrated the potential GHG emission reduction compared to what would otherwise be a continued reliance on ICE vehicles powered by liquid or gaseous fossil fuels.

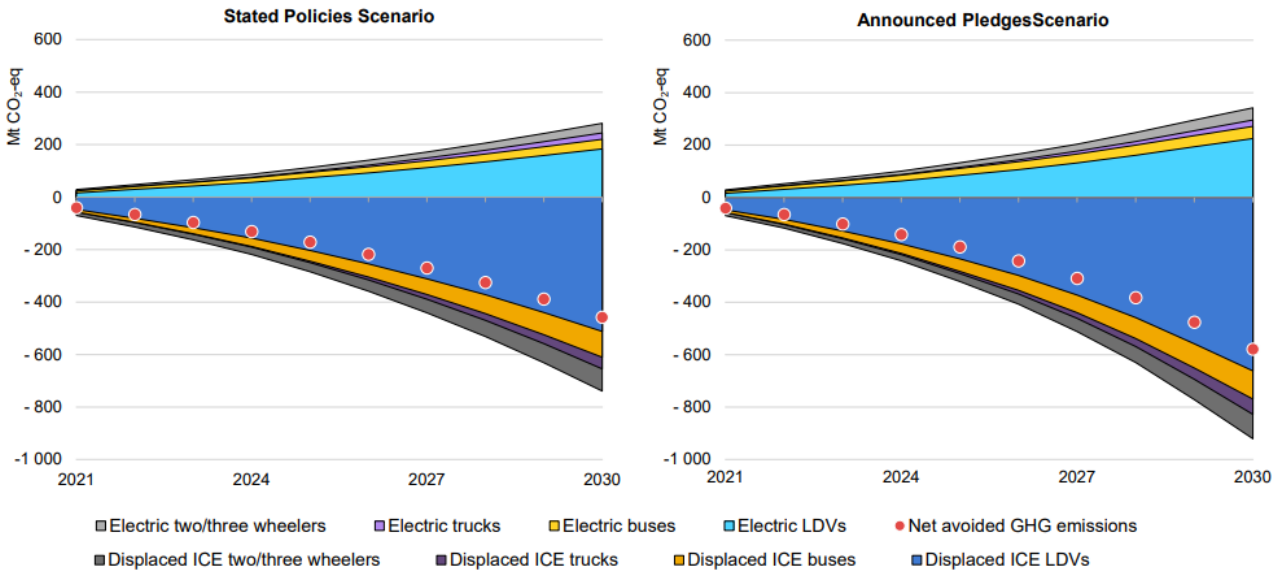


Figure 1.6 Well-to-wheel GHG emissions from the global EV fleet by scenario, 2021-2030 [4]

The analysis is carried out on a Well to Wheel basis, so also considering the electric energy consumption of the vehicle and so of the energy production mix that tends to decarbonize (i.e. to depend less on fossil fuels) during the years while the stock of EVs (that include the P-HEV) rise. In detail, the figure 1.7 permit to appreciate the expected grow of the EVs:

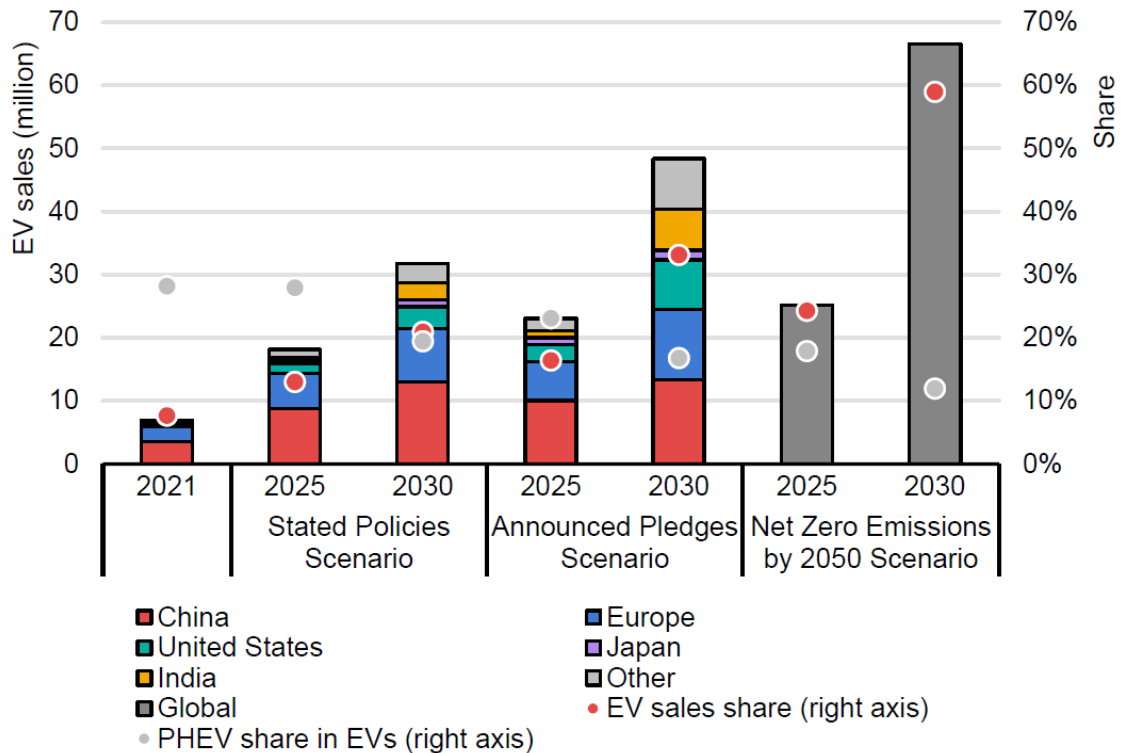
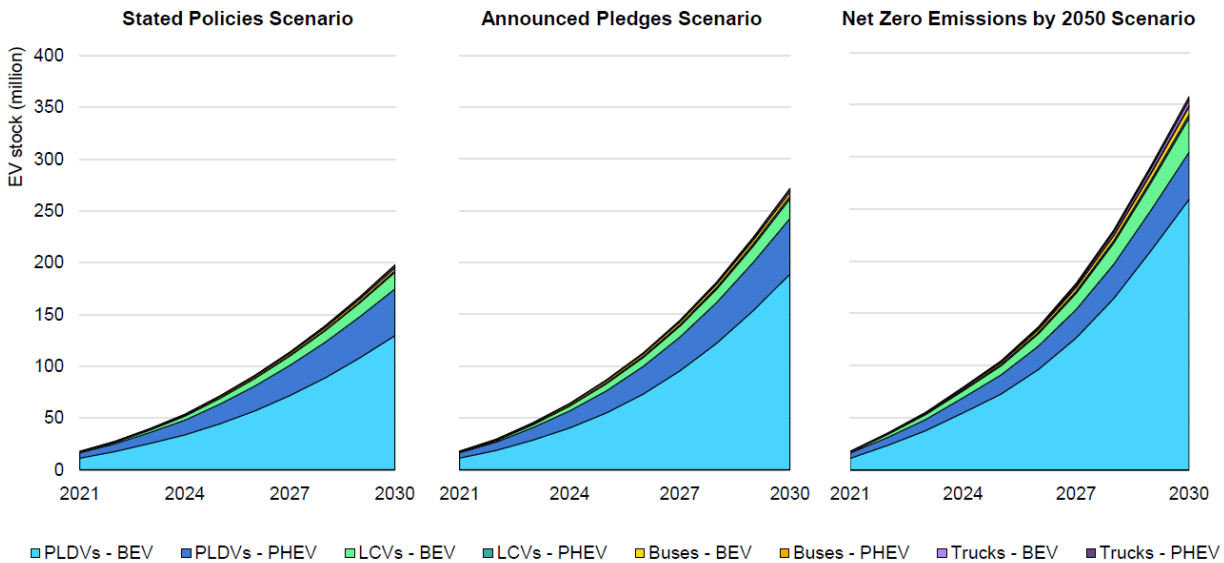


Figure 1.7 Global EV sales by scenario, 2021 – 2030 [4]

The bar indicated the sales in millions (left axis) of EVs (P-HEV included) divided in regions for the first two scenarios and the dots indicate the respective share (right axis) in the market of EVs respect of the other kinds of vehicles (red dots) and of the P-HEV respect the EVs (gray dots). For instance, in the 2030 considering the NZE, the global sales of EVs would be around the 66 million, that represent the 60% of vehicles sold, among which 8 million (7,3% of total vehicle sold) are P-HEV. These values seem to be quite interesting but the point of view change if the focus goes on the total stock vehicles. Indeed, in the best-case scenario (NZE) the total EVs would represent the 20% of the total vehicle stock becoming respectively the 14% and 10% in the APS and STEPS scenarios considering a total vehicle stock of 2 billion (1.8 for NZE) as is depicted in the figure 1.8.



IEA. All rights reserved.

Figure 1.8 Global EV stock by mode and scenario, 2021-2030 [4]

Considering this outlook, the conventional ICE powered cars will represent the 80% of vehicles stock in the best-case scenario (mostly embedded in hybrid architectures and powered by alternative renewable fuels).

1.3 Internal combustion engine role in future years

Despite the intention to limit the share of vehicles powered with an internal combustion engine (or ban completely as in case of European Union market) that would lead one to think about stopping the development of this technology, there are many reasons to believe that this will not be the case at all. As shown earlier even if efforts to electrify transportation are many, at best the global coverage of BEV road vehicles will not exceed 14%. This is because the green transition of transportation enabling technologies such as [8]:

- Technological evolution of batteries: at present, the power and specific energy (in terms of both mass and volume) of the batteries is still very low, allowing BEVs to be a viable alternative especially for urban mobility due to the limited range of the vehicles when compared to conventional ones;
- Recharging infrastructure and standards (HW & SW): the deployment of charging infrastructure (especially fast charging) today is still very limited;
- Smart Grids.

Moreover, these investments must be combined with those for energy decarbonization. Indeed, an increase in electric vehicles would also lead to a higher demand for electricity, which to date is largely produced from fossil fuels and contribute to the global GHG emissions (figure 1.9) [9].

TOTAL 2019 = 26936 TWh

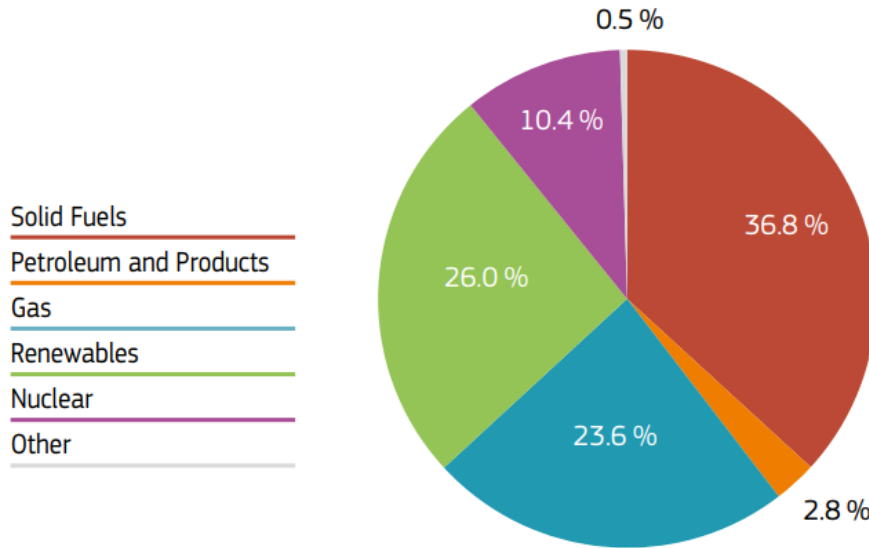


Figure 1.9 Electric energy production mix, note that about 63,2% of electricity is derived from carbon fossil sources [9]

For this reason, meeting the targets set by the NZE requires a very strong investment in clean energy technologies (figures 1.10).

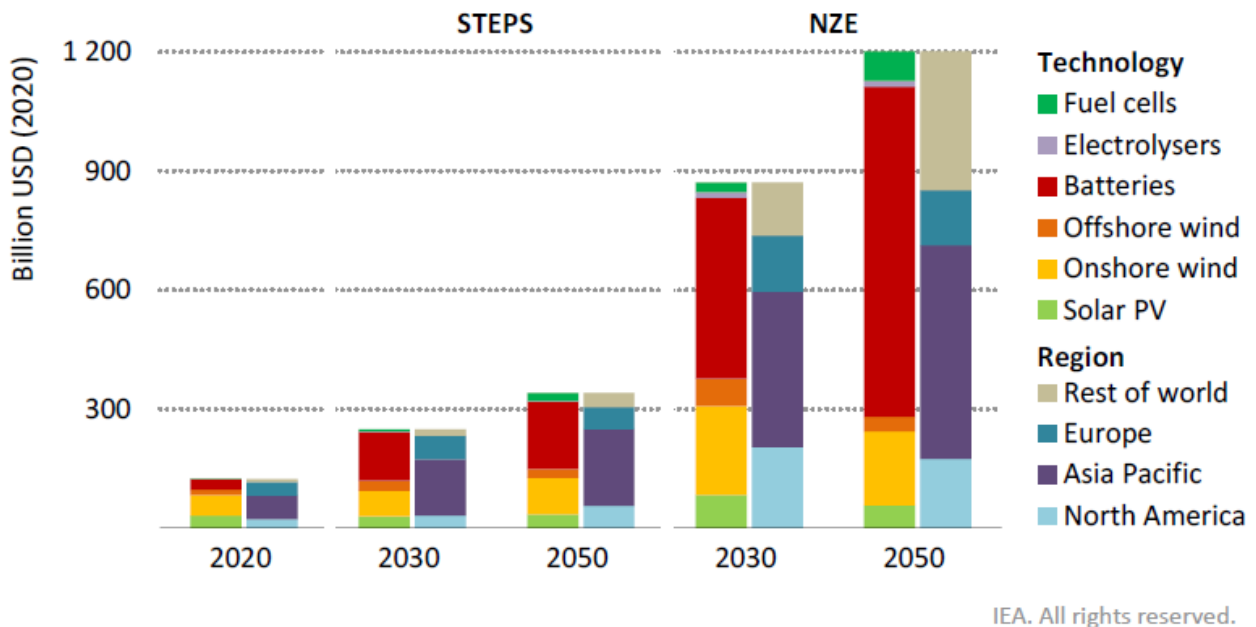
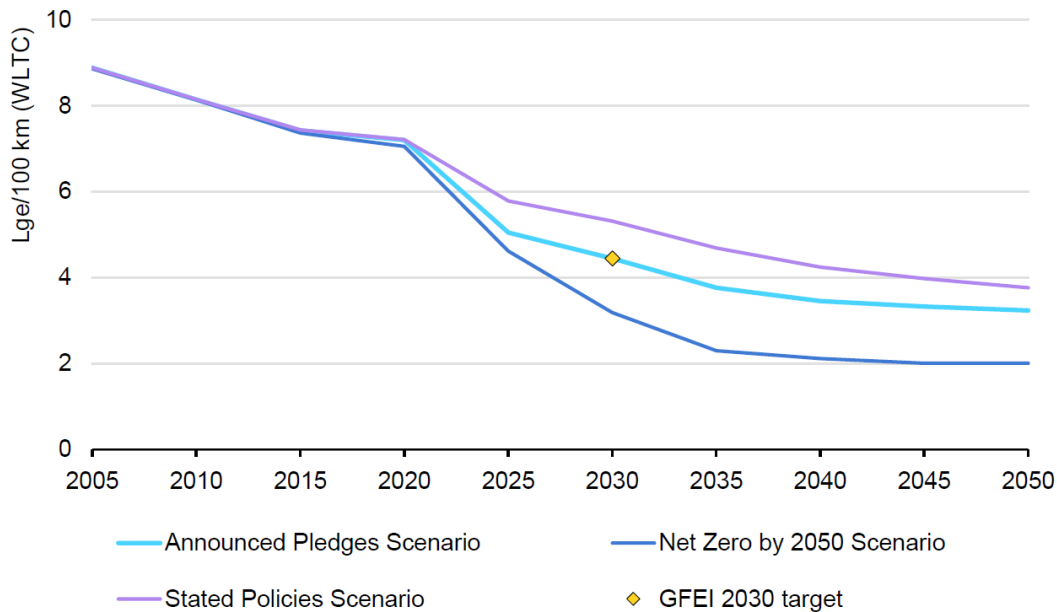


Figure 1.10 Planned investments in clean energy technologies by scenario, 2030 -2050 [1]

This presents a challenge even for industrialized countries and is likely to continue to be difficult for many emerging markets and developing economies. For these reasons, the diffusion of BEVs and P-HEVs is expected to be very limited even in the most ambitious scenario. Therefore, to reach the projected targets, it is necessary to continue developing combustion engines to increase their efficiency and reduce fuel consumption to meet the target required to achieve carbon neutrality in 2050 (figure 1.11).

1.3 - Internal combustion engine role in future years



IEA. All rights reserved.

Figure 1.11 Global fuel economy improvements in new light-duty vehicle sales, GFEI target and IEA scenarios, 2005-2050 [4]

Such a development is likely to be possible only if fuel economy standards are implemented, with sufficient stringency, not only in leading markets but also in many emerging markets and developing economies. Setting such standards is particularly important for emerging markets and developing economies, as internal combustion engine vehicles are expected to retain the majority of light-duty vehicle sales over the coming decade [4]. Standards are also needed to prevent these countries from becoming dumping grounds for used or outdated technologies and can further provide incentives to manufacturers to continue investing in fuel economy technologies.

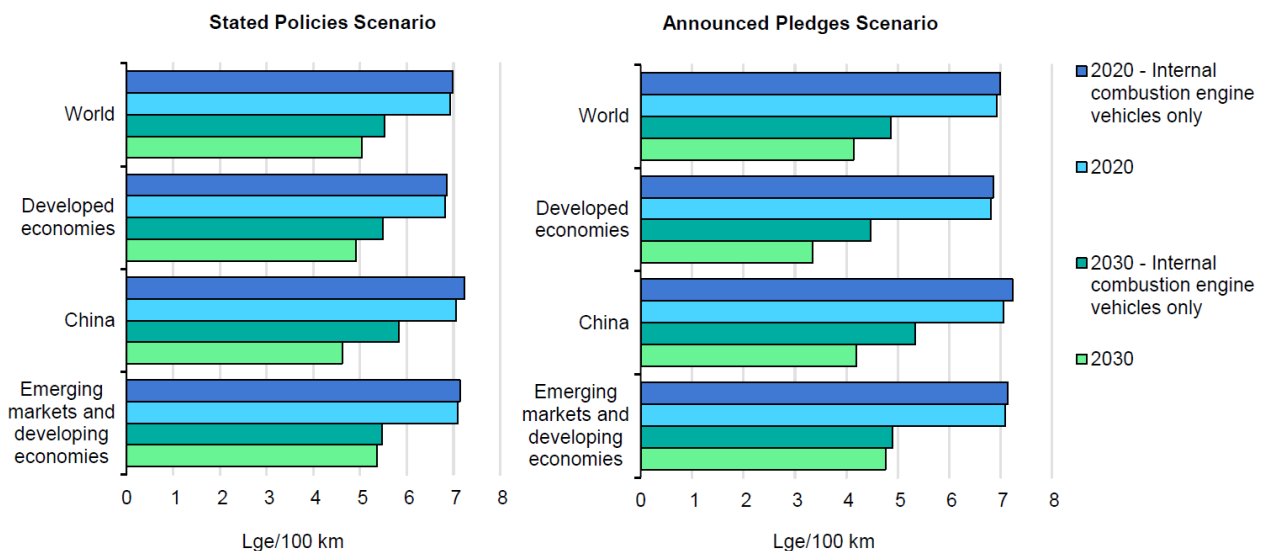


Figure 1.12 Average rated fuel consumption of new vehicles, all sales and internal combustion engine vehicles, in STEPS and APS, 2020 and 2030 [4]

As depicted in the figure 1.12 is possible to understand how much the efficiency internal combustion engine vehicles (hybrid included) must be improved to achieve the target on the APS scenario that is not even the more ambitious scenario. In detail, the figure represents the rated fuel economy (TTW) in liters of

gasoline equivalent for kilometer harmonized globally to the WLTC, the APS scenario imposes an improvement of more than 30% in fuel economy during this decade from a CO₂ consumption of 185,6 g/km to a 127,4 g/km (116,6 g/km considering developed economies like the ones of EU. Part of this improvement can be achieved by acting on the body of the vehicle: lightening and aerodynamic improvement, and part from powertrain development: increased ICE efficiency, improved hybrid control strategies.

So, despite the intentions of legislation to severely restrict the internal combustion engine (or even ban it), it would seem that the most sensible future of mobility is most likely to be a mix of technologies that will give all countries (developed and developing) the opportunity to contribute to the reduction of GHG emissions and for this the research and related investment in the combustion engine will have to continue so as to ensure not only global ecological sustainability but also economic and social sustainability.

2 State of art of gasoline internal combustion engine: introduction to PHOENICE

2.1 Example of reference gasoline engine for passenger car: Stellantis GSE-T4

In recent years, manufacturers have had to adapt to stringent legislations by offering different types of architectures (hybrids, P-HEVs, and BEVs), but as seen earlier (figure 1.8) most of the global sales share has been accounted for by conventional vehicles. Despite this if we look at Europe car makers have managed to achieve the required fleet average in terms of CO₂ emissions (figure 2.1) particularly demanding for gasoline engines. This achievement was also the result of improved efficiency of internal combustion engines.

	Target gap	New car fleet average CO ₂ (in g/km)								
		Dec 2021		2021		Compliance credits		Status 2021	Target 2021	Target gap
		WLTP	NEDC	WLTP	NEDC	EC	SC	WLTP	WLTP	WLTP
Tesla-Honda-JLR	-54%	31	26	65	54	0.0	0.0	65	143	-78
Volvo	-23%	77	64	102	85	0.0	0.0	102	132	-30
BMW Group	-6%	98	84	116	99	0.2	0.0	116	124	-8
Mercedes-Benz	-5%	105	94	116	103	0.0	0.0	116	122	-6
Kia	-4%	91	78	105	91	0.0	0.0	105	110	-5
Ford	-4%	110	89	120	97	0.2	5.7	115	120	-5
AVERAGE	-3%	101	84	115	95	0.0	0.6	114	118	-4
Hyundai	-2%	96	83	107	92	0.0	0.0	107	110	-3
Renault-Nissan-Mitsubishi	0%	94	80	110	94	0.0	0.0	110	111	-1
VW Group	0%	110	92	119	99	0.0	0.0	119	120	-1
Stellantis	0%	109	86	119	93	0.0	0.3	118	118	0
Mazda-Subaru-Suzuki-Toyota	0%	117	93	119	95	0.0	2.6	116	116	0

Notes: EC = eco-innovations, SC = super-credits; all CO₂ values are estimates, see methodology section.

Figure 2.1 New passenger car fleet average CO₂ emission level, by manufacturer pool [10]

This work will focus on the GSE-T4 engine from Stellantis. This engine represents an example of the state of the art of current gasoline internal combustion engine technology for passenger cars. The acronym stays for Global Small Engine 4 cylinders Turbo (table 2.1), and it is characterized from a 1,332 L displacement, 4 valves for cylinder and in the most powerful version has a maximum power of 132,4 kW (a specific power of almost 100 kW/L) [11]. The engine was developed with the aim to reduce as much as possible the encumbrance and the weight. The engine is equipped with a proprietary VVA system called MultiAir on the intake valves. The VVA coupled with a Turbo Compressor and a direct injection permit the downsizing without sacrificing the performance but need also of a gasoline particulate filter (GPF) in addition at the common three-way catalyst (TWC) to reduce the particulate emissions. Other technologies present are the integrated water-air-cooled intercooler (WCAC) and the exhaust manifold also water-cooled integrated into the cylinder head.

Table 2.1 Stellantis GSE-T4 Engine characteristics

Stellantis GSE-T4	
Cylinders	4 in line
Displacement	1332 cm ³
Bore/Stroke	70x86,5 cm
Valves for cylinder	4
Compression ratio	10,5
Max power	132,4 Kw at 6000 rpm
Max Torque	270 Nm at 1750 rpm
Injection system	Gasoline Direct Injection (GDI)
Valve actuation	MultiAir III (VVA)
Fuel	Gasoline
After-treatment system	TWC + GPF

The synergy between all these technologies has led to a significant increase in specific power (kW/L) and simultaneous improvement in fuel conversion efficiency due to higher flexibility in engine control. In detail these technologies are explained below:

- Downsizing: by downsizing the engine, many advantages can be obtained: apart from the obvious ones such as less weight and bulk, in terms of efficiency it is possible to "downsize" the engine map and get the same torque with a higher BMEP and thus less "throttling" with a gain in volumetric and thermodynamic efficiency. With careful analysis of what may be the most frequent operating points of engine use in the homologation cycle (such as WLTC or an RDE) one can choose the correct size to slip the points into the most efficient part of the engine map.
- VVA: Variable Valve Actuation differs from Variable Valve Timing (VVT) because it allows not only the timing but also the valve lift to be changed, increasing the flexibility of control. In gasoline engines we always refer to a VVA strategy on inlet valves given their great influence on volumetric efficiency. With fixed profile valves, a compromise must be found between reducing throttling and hence engine pumping work at low loads and optimizing performance at high rpm. In general, intake valves are opened 50 to 60 degrees after BDC and closed 15 to 10 degrees before TDC [12] (figure 2.2).

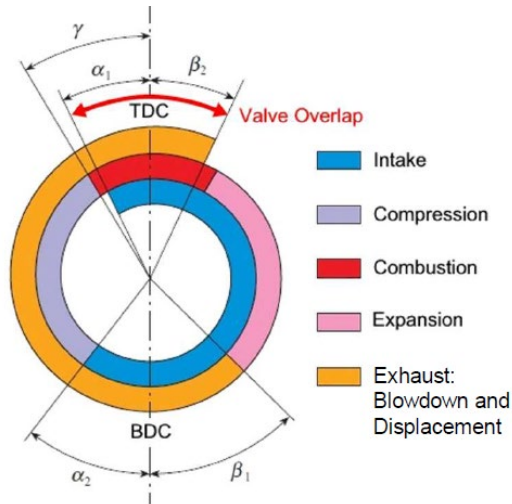


Figure 2.2 Typical valve angles [12]

The intake valves closing point (from now IVC) in part load can be set closer the BDC (early IVC or EIVC) to avoid an important back flow given by the pressure difference between the chamber and intake manifold in the final part of the intake stroke and thus decrease pumping losses (figure 2.3). Whereas a high-rpm late IVC (LIVC) allows the inertia of the flow to be exploited to draw more air into the cylinder, the so-called RAM effect (figure 2.3).

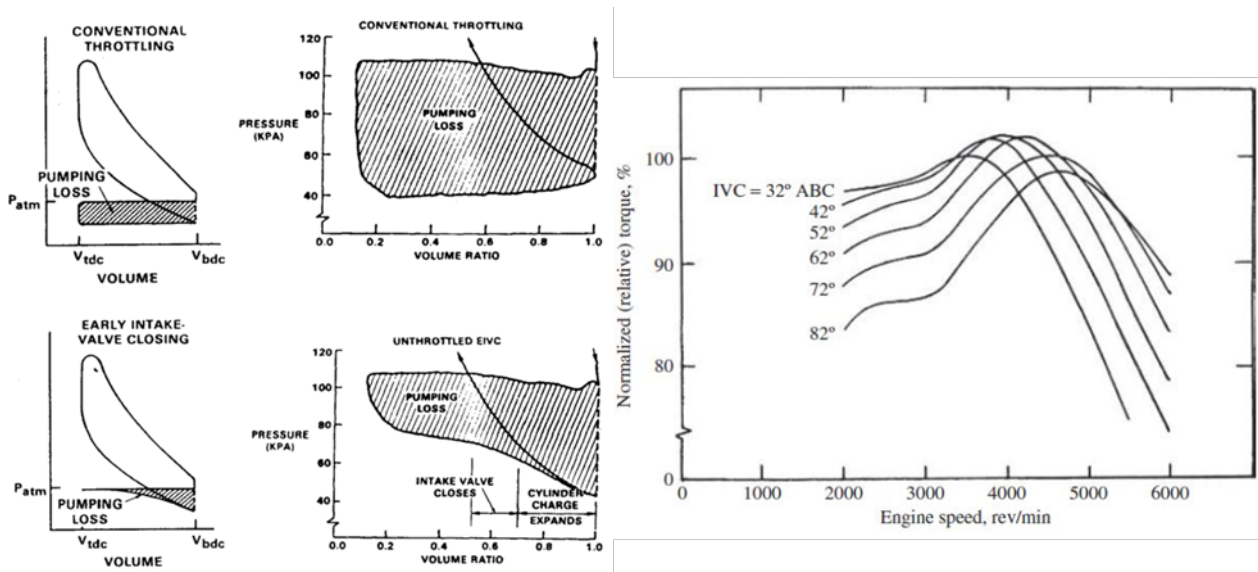


Figure 2.3 On the left, one can appreciate the reduction of pumping losses through an EIVC while on the right, one can see how as the IVC increases, the torque peak shifts to higher and higher RPM: ram effect [12]

An engine using these IVC strategies is said to adopt a Miller Cycle [13] (figure 2.4).

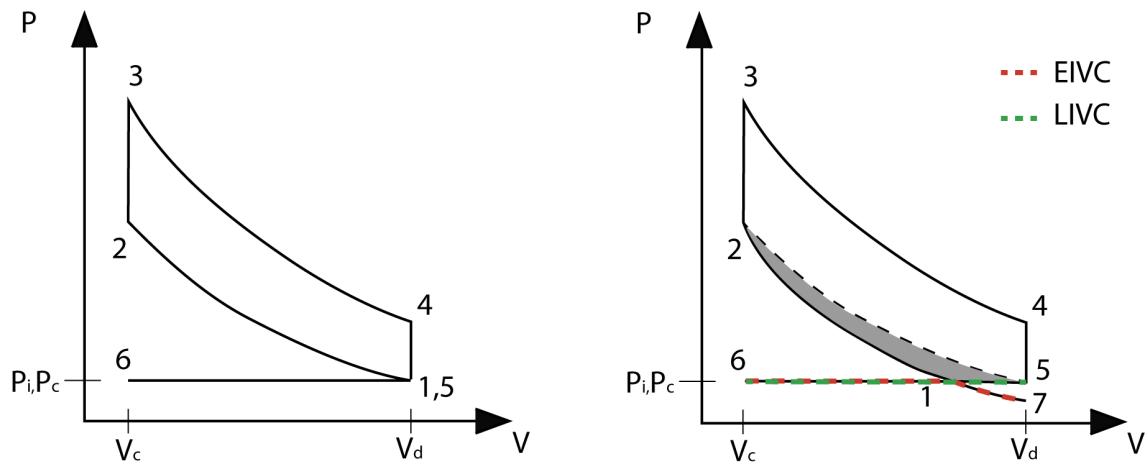


Figure 2.4 Ideal cycle comparison, with EIVC the charge experiences an over-expansion that also cool the charge, instead with LIVC the charge remains at intake pressure following the 5-6-5-1 path

In addition to the benefits already listed, there is an additional gain in thermal efficiency and indicated work per cycle due to the difference between the current compression and expansion ratios. In fact, the nominal compression ratio is defined as:

$$r = \frac{V_d}{V_c}$$

It differs from the actual ratio at the point when the valves do not close and open perfectly at TDC and BDC:

$$r_c = \frac{V_1}{V_c} \quad r_e = \frac{V_4}{V_c}$$

From figure 2.4 it's possible to appreciate the gain in indicated work through the use of both EIVC and LIVC strategies that result in a lower compression ratio respect to the expansion ratio.

Turning to the opening phase of the intake valve, an early intake valves opening (EIVO) allows for an increase in the overlap between the exhaust valve and intake valve, that is, the time in which both valves are open. At low RPM and high load this strategy allows the pressure difference between intake and exhaust to be used to move residual gases faster to the turbine increasing airflow and generating more boost increasing overall performance but most importantly reducing turbo-lag. This strategy called "scavenging", however, can only be used when coupled with a direct injection system (GDI) to avoid unburned fuel going directly into the exhaust at this stage which would lead to increased fuel consumption but more importantly to improper catalyst operation [14]. Ultimately, VVA allows all of these compromises to be eliminated, thus allowing each operating point to be optimized while maximizing efficiency and coupled with turbocharging and GDI can increase even more the performance and the global efficiency of the engine.

In the GSE-T4 the VVA system is called MultiAir and is an "electrohydraulic" system that avoids having the cam act directly on the valve by interposing between the cam and the valve a volume of lubricating oil called a control chamber (figure 2.5). This chamber faces, at the top, toward the piston moved by the cam and, at the bottom, toward the top of the valve stem. The objective is to control the connection of this volume of oil to a "low-pressure environment" (= the lubrication circuit) by means of a solenoid valve. If the solenoid valve is kept normally closed, the volume of lubricating oil is isolated and behaves as a rigid body (except for the compressibility of the oil). In

this case, the piston pushes on the oil, and once the compressibility of the oil is exceeded, the oil (as a rigid body) transmits motion from the cam to the valve and the "normal" valve lift profile is performed [14].

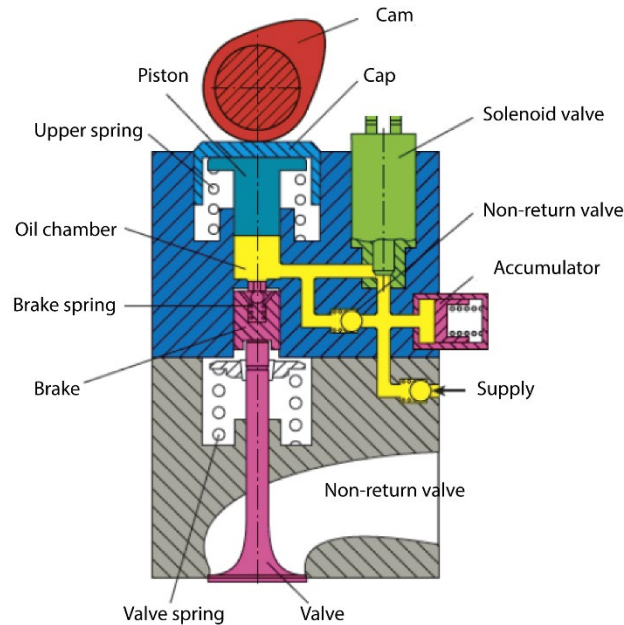


Figure 2.5 MultiAir 2D scheme

On the other hand, if the solenoid valve is opened, due to the high pressure in the control chamber, oil flows from the chamber into the lubrication circuit (immediate depressurization of the control chamber). As a result, the rigid body connection between the cam and the top of the valve stem fails: the valve is governed only by the forces of inertia and the spring. Under the action of the return spring, which overcomes the forces of inertia, the valve begins to close at very high speed. This is why a hydraulic brake is present (figure 2.5): it consists of a small layer of oil that remains between the cam piston and the valve stem. This layer acts as a "cushion" damping the impact between the valve and the seat.

Initially, the system was designed to make sure that the input valves had a way to act independently. This allowed more sophisticated strategies to be used to increase turbulence within the cylinder and thus increase combustion efficiency under part load (figure 2.6).

MULTIAIR Technology: Features / Benefits

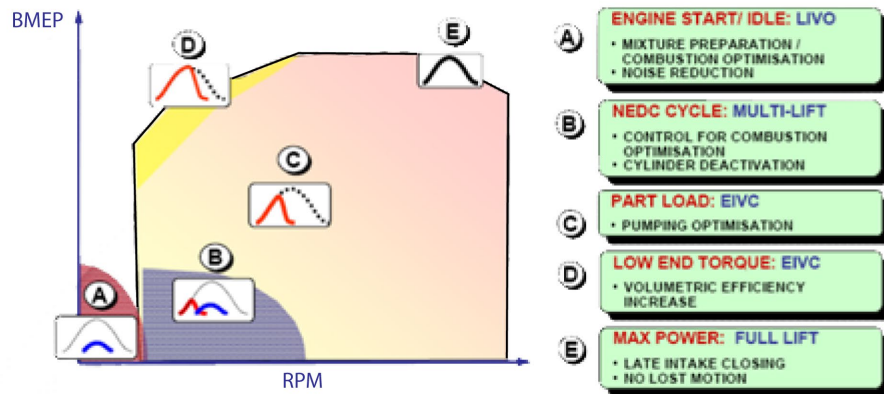


Figure 2.6 MultiAir strategies. Note that to achieve the control strategy B both valves must act independently

Today, as a matter of cost, the system in use involves only one solenoid valve and one piston acting simultaneously on both inlet valves (the so-called thunder actuation) which will then have the same lift (figure 2.7)

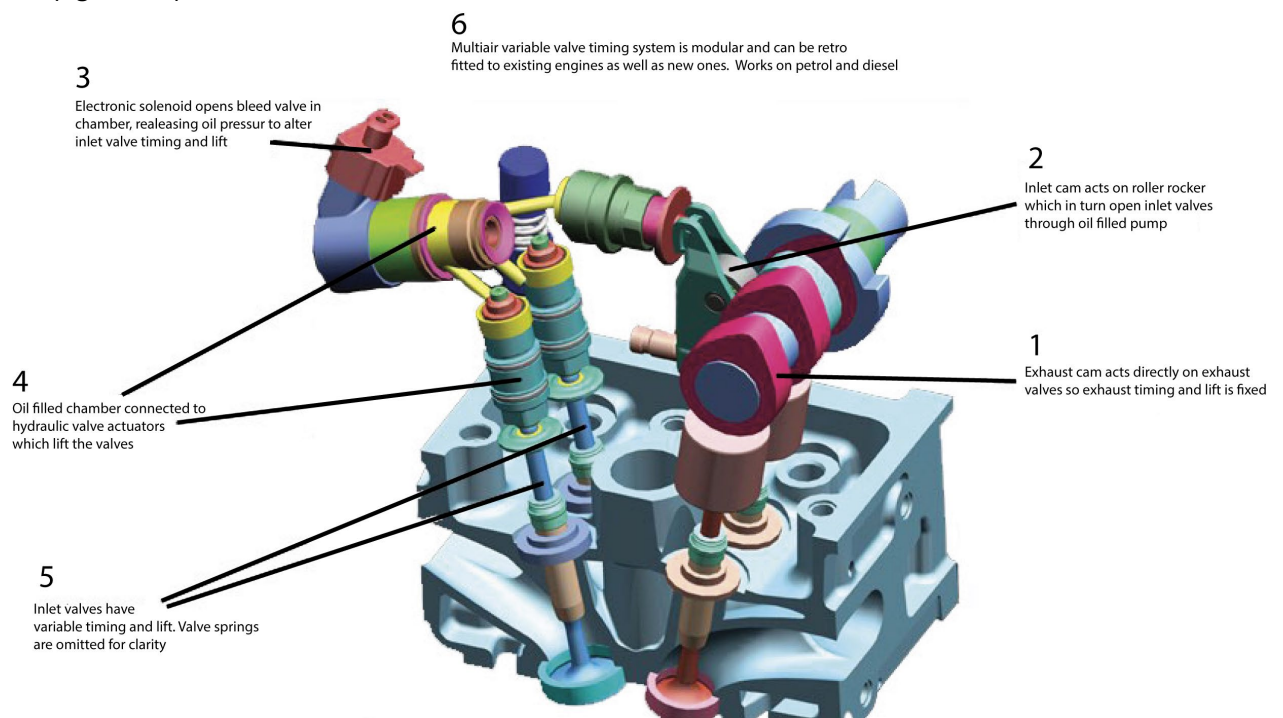


Figure 2.7 MultiAir 3D scheme

- Turbocharging: in order not to lose too much absolute power due to downsizing, turbocharging can be considered to maintain high performance if not increase it, plus this technology together with VVA to direct injection can bring additional benefits thanks to the scavenging technique. Indeed, the engine's power is limited by the amount of fuel it can burn in the efficient way each cycle and thus in turn is limited by the amount of air that enters the combustion chamber. Therefore, power is proportional to air density [8].

$$P_{ICE} = bmep * iV * \frac{n}{m} \qquad bmep = \eta_f * \lambda_v * \frac{H_L}{\alpha * v}$$

Turbocharging is one way to increase the density of air by increasing its pressure before it enters the chamber by using a compressor driven by a turbine, which in turn harnesses the energy of the exhaust gases (figure 2.8).

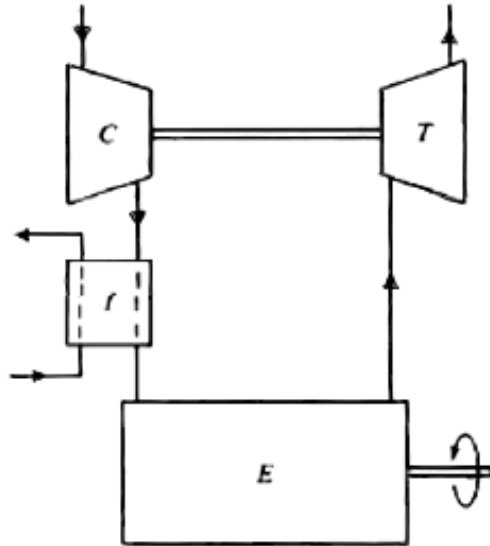


Figure 2.8 Turbo-Compressor typical layout

Often, the compressor is followed by a heat exchanger (called an aftercooler or intercooler) whose purpose is to cool the compressed air to increase the density of the mixture even more. Turbochargers adopted for passenger car application experience a wide range of operating condition and must provide excellent dynamic response. To ensure this performance, at full load the turbocharger must provide the maximum possible boost already from relatively low rpm such as torque rated speed (figure 2.9).

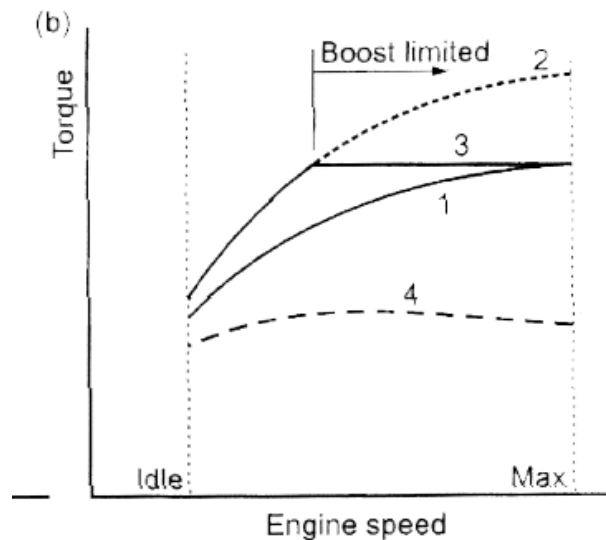


Figure 2.9 Comparison between different strategies: 1-Turbo matched at full speed; 2-Turbo matched at max torque rated speed; 3-Turbo matched a max torque rated speed boost limited; 4-Natural Aspirated engine typical torque curve

After this speed, the boost from the compressor would continue to increase, and to avoid overspeeding a boost control must be implemented. In GSE-T4, the turbine is of the fixed geometry type, and boost pressure control is handled by the electronically implemented wastegate valve or exhaust side bypass.

The system allows part of the exhaust gases to bypass the turbine ensuring boost control while improving dynamic response through improved efficiency at low flow rates as well as decreasing turbocharger inertia.

Another way to achieve boost control is to use a Variable Geometry Turbine (VGT) or Variable Nozzle Turbo (VNT). In this case, the turbine has adjustable guide vanes. The vanes are all connected to a support ring driven by a servo motor or vacuum box that sets all the vanes in motion in unison. At low speeds to increase boost, the vanes are flatter so as to narrow the cross section to the exhaust gas entering the turbine increasing its speed which allows faster rotation of the turbine promoting higher charging pressure. Conversely at high speeds when maximum boost is reached the vanes open up increasing the cross section and decreasing the flow velocity (figure 2.10).



Figure 2.10 VGT configurations at two different speeds at full load [8]

The maximum vane opening represents the emergency operation of the VGT in case of failure. VGTs are more efficient than wastegate-controlled turbos, achieve higher torque at low rpm, and reduce turbo lag. Despite these benefits in SI vehicles VGTs are usually not considered an option because of the relative high cost compared to the benefits due to the use of more exotic materials due to high exhaust gas temperatures.

- GDI: Gasoline Direct Injection and is a technology that allows fuel injection directly into the combustion chamber. This technology allows a gain in performance and efficiency over the classic multi-point injection system (MPI) (figure 2.11) [12].

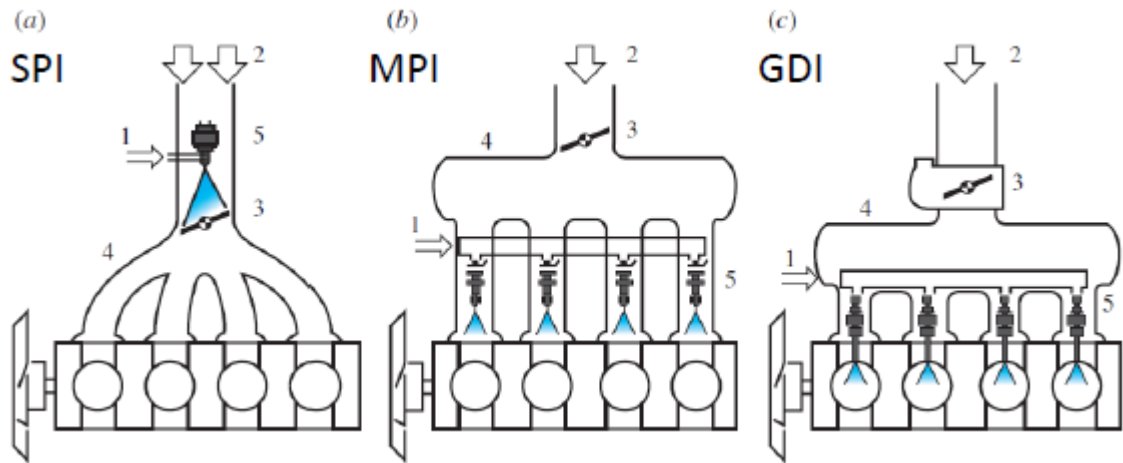


Figure 2.11 Different fuel metering systems: (a) Single point Injection: injection prior to throttle valve; (b) Multi-point Injection: each injector sprays inside cylinders intake port, also called port fuel injection (PFI); (c) Gasoline direct injection: Injector sprays directly inside the cylinder [12]

The fuel allows the fresh air from intake to cool via evaporative heat absorption, increasing volumetric efficiency and reducing knock tendency thanks to a reduction in the temperature and so the density of the mixture. This then allows the compression ratio and boost to be raised, further improving efficiency and performance. In addition, the GDI allows more precise control of the A/F ratio to increase the efficiency of the three-way catalyst (TWC) and enabling technologies such as fuel cut off in the deceleration stages or even the ability to adopt a stratified charge (overall lean) to decrease throttling in part load and increase efficiency more. However, the latter possibility increases the complexity of the control strategy as the TWC would not work at maximum efficiency and an additional NO_x catalyst could become mandatory. Among the disadvantages, GDI leads to increased soot (particulate formation), which requires the use of a gasoline particulate filter (GPF) that leads to increased engine oil dilution. Turbocharging: In order not to lose too much absolute power due to downsizing, turbocharging can be considered to maintain high performance if not increase it, plus this technology together with VVA to direct injection can bring additional benefits through the technique of scavenging.

Although the combustion engine has made so many advances in performance and efficiency in recent years to be able to meet the required GHG Emission targets (figure 2.1) car makers have had to increase the number of hybrid models. Stellantis itself has used the GSE-T4 in conjunction with a hybrid powertrain as in the case of the P-HEV Compass and Renegade.

Going in order, hybrid cars in terms of architecture can be classified into 3 types [15]:

- Series hybrids: they are distinguished to have only one powertrain with the electric machine as the torque actuator. The ICE in this case then is disconnected from the transmission and is connected to an electric machine that acts as a generator (figure 2.12)

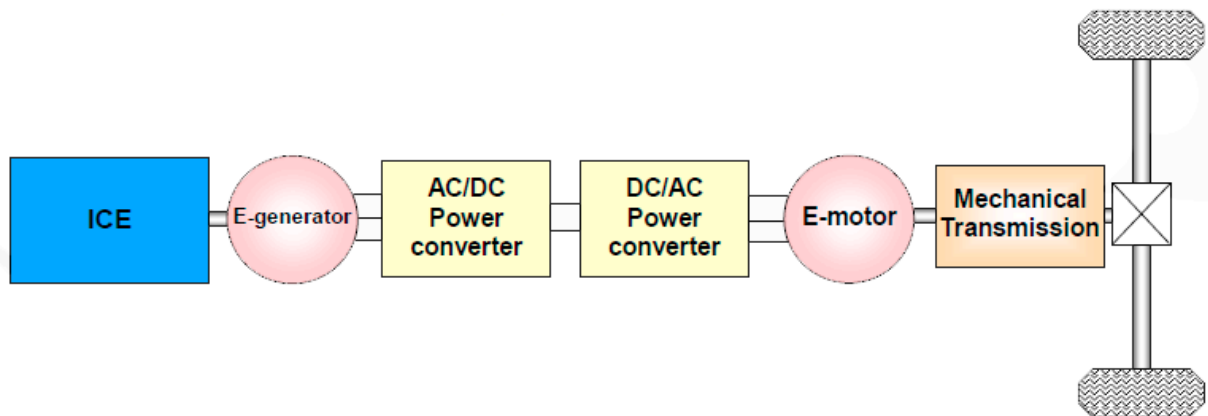


Figure 2.12 Serial Hybrid configuration; Note that a battery pack connected to the DC/AC converter can be present when the ICE works as range extender [15]

- Parallel Hybrid: these are vehicles that have two elementary traction systems, i.e., both the electric machine and the engine are connected to the final transmission and thus can independently provide power to the wheels (figure 2.13).

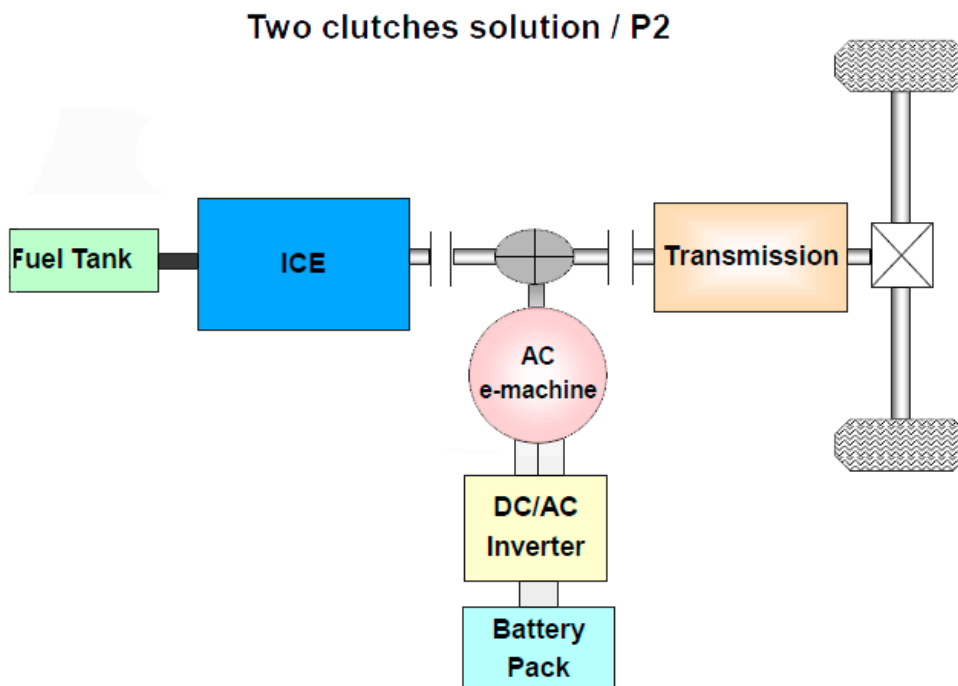


Figure 2.13 P2 Parallel Hybrid configuration; Note the presence of double clutch to allow different type of power path [15]

The way they are connected determines whether they are:

- double drive: the thermal powertrain powers one axle, while the electric powertrain powers the other axle

- double shaft: the joining of electric and thermal powertrain occurs before the differential, after their respective transmissions
- single shaft: electric motor and ICE are coaxially and non-coaxially connected. Therefore, it is not possible to choose the speeds of the two components separately since their gear ratio is always constant.

To immediately understand where the electric machines are located, the nomenclature shown in figure 2.14 is used. For example, the case of a parallel hybrid P4 refers to a double drive and the case of P2 refers to a single shaft (as report in figure 2.13).

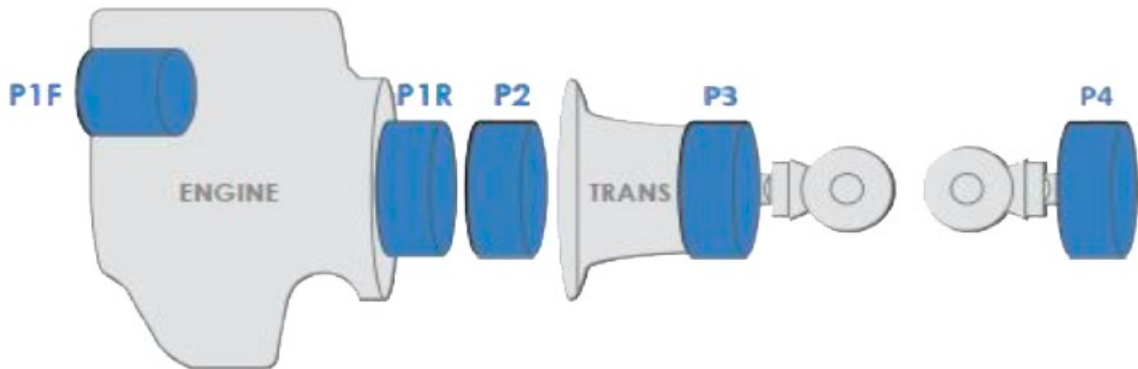


Figure 2.14 Electric motor nomenclature based on the position respect the thermal powertrain [15]

- complex hybrids: they have more than two elementary powertrains due to the presence of multiple electrical machines that allow power to flow in different types of paths (figure 2.15).

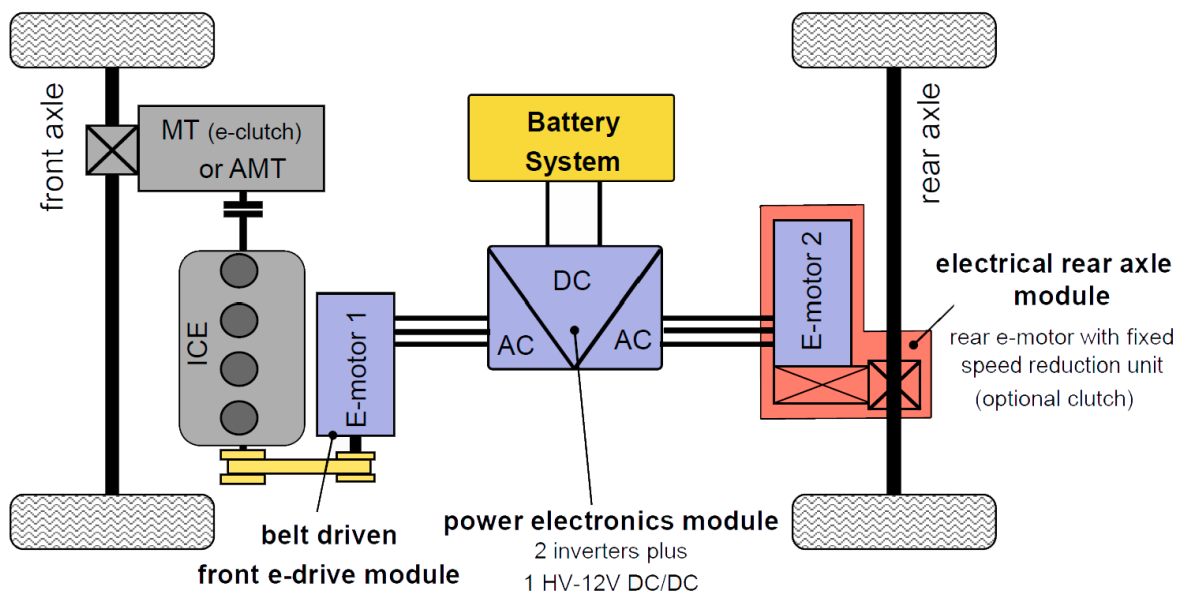


Figure 2.15 An example of complex hybrid (P1F-P4) by PSA, this platform represents also the scheme of Jeep Compass and Renegade 4Xe version, the double drive configuration allow a 4x4 mode without physical connection between axles [15]

In addition, hybrid cars can be classified by the amount of extra features they can offer and usually depend on the amount of power (electric motors and battery pack) and energy (battery pack) installed in the vehicle (Figure 2.16).

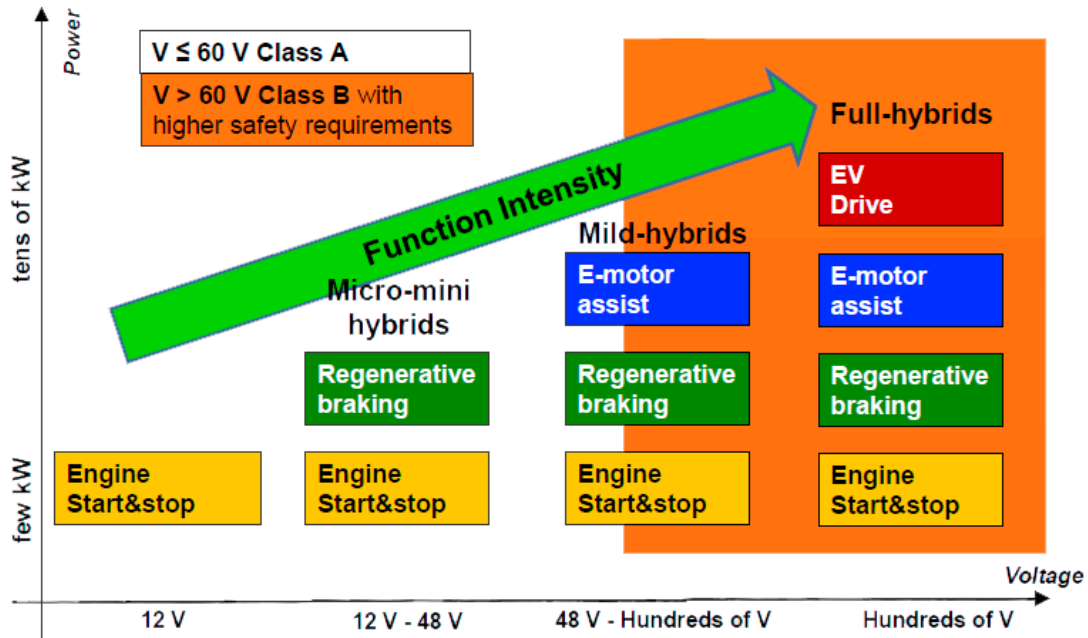


Figure 2.16 Hybrid classification based on type and number of functionalities [15]

If, for example, P-HEVs are considered such as the Jeep Compass and Jeep Renegade, these cars are complex parallel hybrids that provide a range of miles in pure electric mode (ICE off) and the ability to recharge the battery pack at dedicated charging stations. This means that the battery and electric motor are sized both in terms of power (to ensure adequate performance in pure electric mode) and in terms of energy (to ensure the required range before having to charge the battery), and the battery can operate in charge depleting mode, that is, in a way that can make it reach a low charge level. As for the evaluation of emissions a utility factor (<1), which depends directly on the range in pure electric, multiplies the calculated emissions in the hybrid mode (ICE ON) with the battery in that case keeping its charge level almost constant (charge sustaining mode).

This allows certified emission levels up to one third lower than those of an HEV operating in charge sustaining mode. However, this runs the risk of not representing real emissions since the formulation of the rules requires that the battery is recharged at the end of each mission and therefore that there is always a charging station available, time to recharge and that the driver wants to recharge. In the event that one of these cases is not verified, the calculated consumption and emissions would overestimate the benefits of P-HEVs by closing the delta with HEV ones [16].

2.2 A Horizon 2020 project: PHOENICE

The plug-in hybrid models of the Stellantis group are an example of how car makers have tried to adapt to comply with GHG emission regulations. The P-HEVs are the most direct way to reduce these emissions but require a great deal of effort to integrate the hybrid part (battery pack, converter, electric motor(s) and its transmission) together with an existing thermal powertrain without excessively increasing weight and cost.

This strategy, however, does not allow the presence of a high-voltage circuit to be fully exploited; indeed, the thermal unit is also conceived with a view to conventional use, which naturally imposes certain constraints. The next step to improve the efficiency of the entire vehicle is to think, from the outset, how to optimise the use of energy and thus develop the thermal power unit with a view to use in combination with its electric counterpart ('hybrid oriented'). [17] The PHOENICE project aims precisely at this type of approach: this thesis will focus on analysing the benefits of this, specifically regarding the combustion process. The latter will follow a new logic that takes into account the presence of the hybrid part.

PHOENICE stands for "PHEv towards zero EmissionS & ultimate ICE efficiency" and is an EU-funded project that aims at developing a C SUV-class plug-in hybrid (complex P1-P4) vehicle demonstrator whose performance, in terms of energy consumption and pollutant emissions, will be jointly optimised for real world driving conditions. The project is based on an existing plug-in vehicle, Jeep Compass 4Xe, and aims to improve the range in full electric (from 50 km to 80 km) and also the efficiency of the entire powertrain through essential modifications (figure 2.17):

- an innovative turbocharged gasoline engine based on a dual dilution combustion approach and specifically designed for hybrid architectures;
- a waste heat recovery system for optimising the overall vehicle thermal and energy management;
- a complete after-treatment system including a selective catalytic reduction and a gasoline particulate filter;
- a complete control strategy including the engine, the after-treatment, the waste heat recovery system, and the hybrid strategy with an emission-based management system.

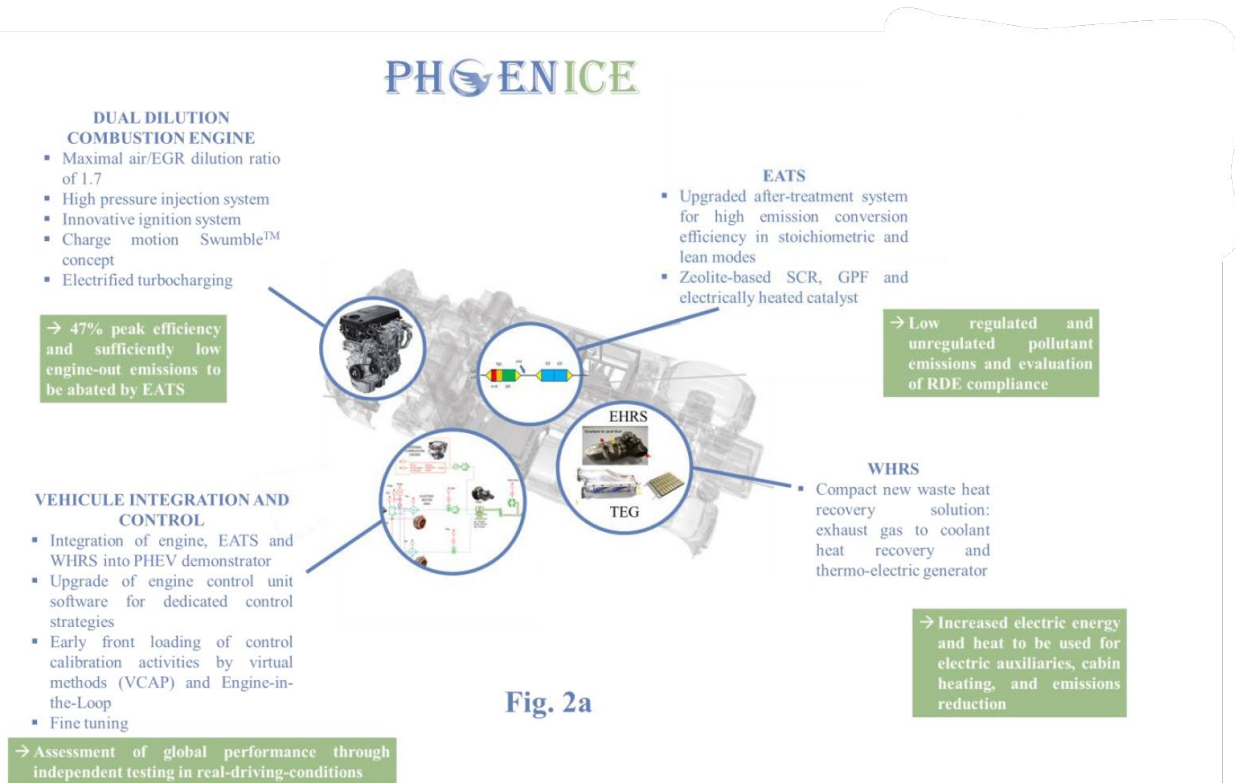


Figure 2.17 Resume of the principal PHOENICE's introduced features

Technologies developed in the frame of the PHOENICE project will achieve a TRL 7, and some of them will be usable for various powertrains and vehicle classes to maximise the economic and environmental impacts. This project will support the European automobile industry in the medium term and will speed up the transition towards a more environmentally friendly and sustainable mobility in terms of air quality and

GHG emissions. The vehicle demonstrator will enhance the knowledge to design and build engines and after-treatment systems for future market requirements with a strong focus on the cost of the proposed solutions. These enhancements will permit improved competitiveness and know-how, and possibly increased vehicle sales.

The engine is based on GSE-T4 but will implement new features to improve overall efficiency and engine out emissions. Indeed, most of gasoline spark-ignited engines currently available are running with stoichiometric air/fuel mixtures. Due to their design and operating principle, these engines are usually limited to peak efficiencies of around 40%. Some recent engine concepts resulting from intense developments have reached peak efficiencies of around 42% by combining high compression ratios with EGR, optimised valve actuation strategies together with well-structured and high-level tumble motion. However, the basic operating principle with stoichiometric mixtures imposes high pumping losses during the gas exchange process at low loads, high cooling losses because of the elevated combustion temperature, as well as important energy loss at the exhaust. For a P-HEV application, pumping losses at low load are not a major concern since the EV propulsion mode can be selected to avoid running the internal combustion engine in this very low efficiency area. However, the losses related to heat transfer and delayed combustion timings remain very high in the mid to high load region. According to this, it is reasonable to claim that stoichiometric engines can achieve peak efficiencies of 42 to 45% but not more.

From that perspective, ultra-lean burn engines can be a relevant solution to increase the peak efficiency above 45%. Firstly, thanks to air dilution, cooling losses can be significantly decreased. At the same time, diluting the air/fuel mixture improves its auto-ignition resistance and therefore the knock limits can be extended. In other words, lean burn engines can be designed with higher compression ratios than stoichiometric engines and can thus benefit from a higher thermodynamic efficiency.

The engine concept selected for the PHOENICE project will combine the strengths of air dilution and those of EGR. This Dual Dilution Combustion Approach (DDCA) aims at achieving high efficiencies and NO_x emissions sufficiently low to be abated by the after-treatment system in real driving conditions.

The low temperature of emission gases greatly lowers the enthalpy available to the turbine, and for this reason to achieve an adequate boost level an electro-assisted variable geometry turbine becomes essential. The synergy between the dual diluted combustion approach and an electrified turbocharger is particularly relevant for a hybrid architecture. On the one hand, the diluted combustion can offer high efficiencies and reduced engine-out emissions. On the other hand, the electrified turbocharger is required to achieve high dilution rates by providing the necessary boosting pressure. It can not only recover the exhaust enthalpy like any turbocharger, but also be an additional opportunity regarding the hybrid vehicle management (for example for energy recovery or even possibly for catalyst light-off). In addition, so much air dilution may lead to combustion stability problems and performance losses. To avoid these problems an innovative charge motion called Swumble™ is introduced [18]. It was developed by IFPEN and consists of the combination of tumble, cross-tumble and swirl motion, in contrary to current SI engines that generally only use tumble fluid motion. It is exclusively based on intake engine ducts and combustion chamber specific designs. The aim of this innovation is to increase the turbulence index to help the combustion process when high Miller rate and air dilution is used. Thanks to the synergy of all these solutions a peak efficiency of 49% is estimated to be achievable.

To understand better this concept the swirl and tumble motion (figure 2.18) are described below [8]:

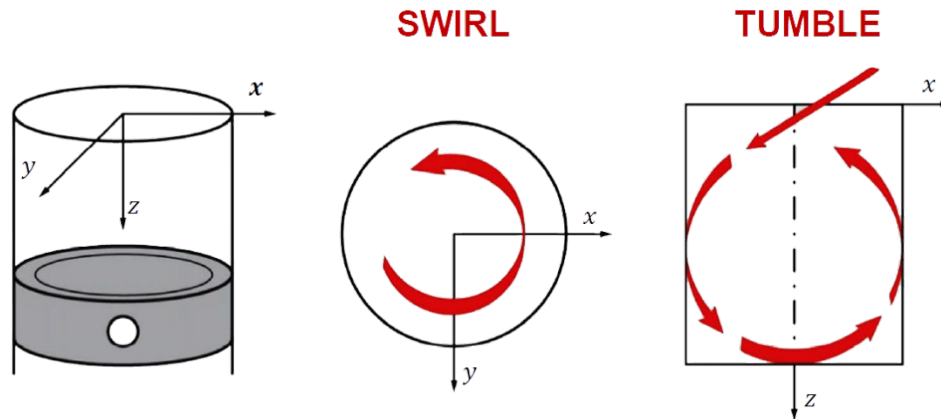


Figure 2.18 Swirl and tumble in-cylinder motions [8]

- The swirl vortex is an organized rotation of the charge about the cylinder axis. Swirl is created during the induction stroke, by bringing the intake flow into the cylinder with an initial angular momentum, for instance by means of either “directed ducts” or “helical ports”.

One possible approach to create swirl during the induction process is discharging the flow into the cylinder tangentially toward the cylinder wall, where it is deflected sideways and downward in a swirling motion. This type of motion is achieved by forcing the flow distribution around the circumference of the inlet valve to be nonuniform, so that the inlet flow has a substantial net angular momentum about the cylinder axis. The directed port and deflector wall port are two common ways of achieving this result. In the other possible approach to create swirl during the induction process, the swirl is largely generated within the inlet port: the flow is forced to rotate about the valve axis before it enters into the cylinder. This can be done by helical inlet ports (figure 2.19).



Figure 2.19 An example of intake ports geometry to increase swirl motion: direct and helical ports combo [8]

- Tumble is an organized vortex about an axis that is perpendicular to the cylinder one. It is used mainly in SI engines to enhance turbulence prior to the spark discharge. In fact, tumble is generated during expansion and, if sufficient strength persists, it can be “accelerated” during the first part of

the compression stroke. Tumble is then destroyed near TDC and converted into turbulence energy at small scales. Cross-tumble is defined when tumble motion is present also on the other perpendicular axis (figure 2.20).

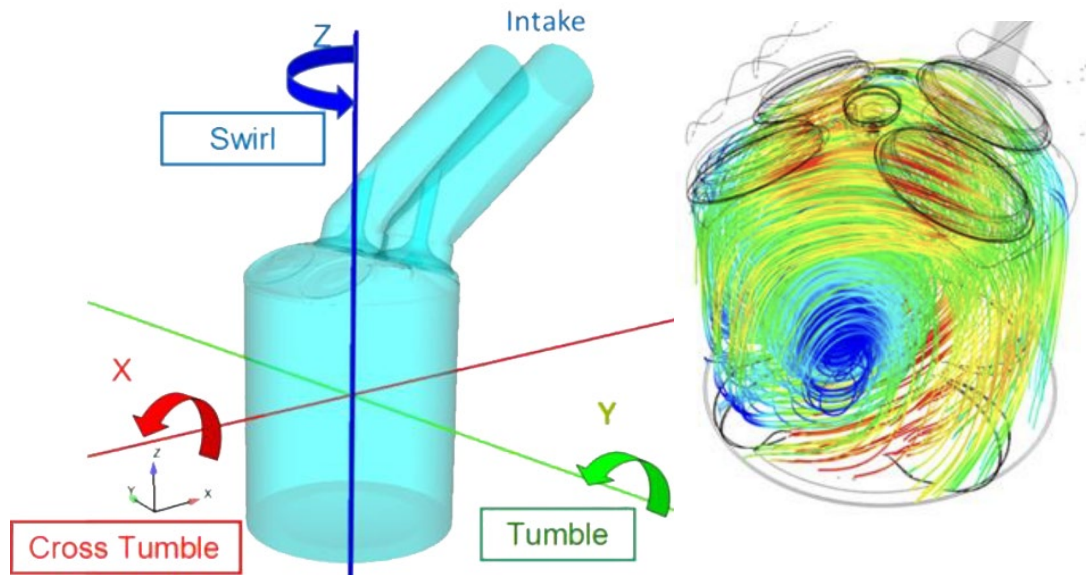


Figure 2.20 Left: $Swumble^{tm}$ is the sum of swirl, tumble, and cross tumble (tumble motion around X axis). Right: the 3D CFD results of a $Swumble^{tm}$ motion [18]

Concerning the abatement of pollutant emissions, various technologies for aftertreatment systems will be investigated. In fact, a very lean combustion can appreciably abate engine-out emissions of CO, NO_x, somewhat less HCs, but the NO_x conversion efficiency of the three-way catalyst (TWC) degenerates with a very high lambda (figures 2.21), so implanting a selective catalyst converter (SCR) with urea injection becomes indispensable to significantly abate NO_x and also unregulated pollutants such as NH₃ through an ammonia slip.

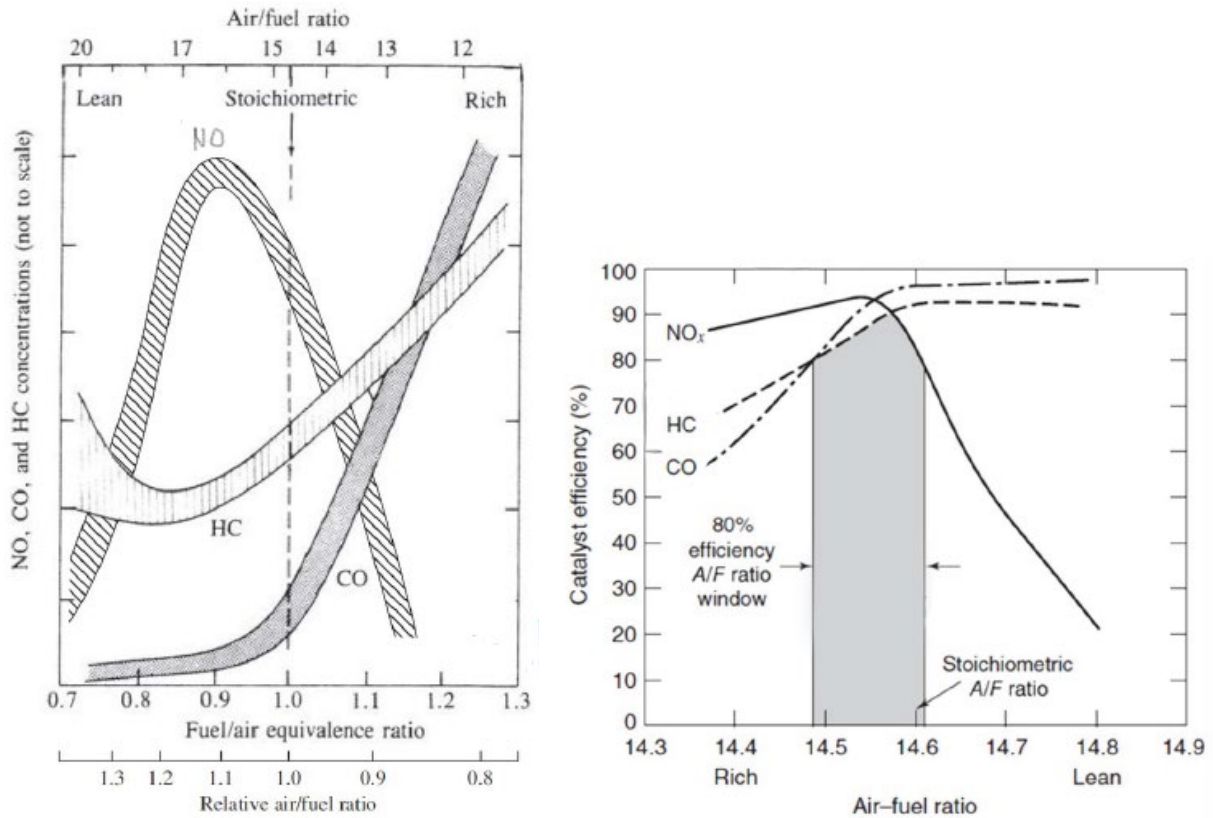


Figure 2.21 Left: Engine out emission by relative air-fuel ratio. Right: TWC efficiency based on air-fuel ratio [12]

Most emissions, however, are generated in the first moments of driving when the catalytic converters have not yet reached light-off temperature. In order to comply with the Euro 7 regulation, the project envisages the use of an e-Cat, i.e. a catalytic converter that can be heated quickly through the use of electric resistors. In conventional engines, this type of technology has always been difficult to implement, but in the case of hybrid vehicles, the availability of high-voltage electricity makes it possible. Within PHOENICE project, this technology is also essential due to the lower exhaust gas temperature caused by the high dilution rate.

Having a direct injection, a gasoline particulate filter will also be mandatory. The whole ATS would look as shown in figure 2.22.

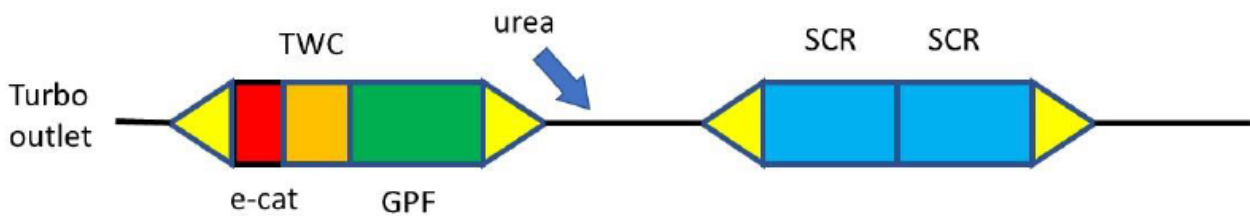


Figure 2.22 PHOENICE's after-treatment system layout

Finally, a waste heat recovery system will be integrated in the exhaust line. The solutions that are under investigation are an Exhaust gas to coolant Heat Recovery System (EHRS) and a Thermo-Electric Generator (TEG) (figure 2.23).



Figure 2.23 Left: An example of EHRS by CRF. Right: An example of a TEG

EHRS is already implemented in some hybrid vehicle and can be useful mostly in cold weather where the ICE needs to switch on just for cabin heating and the EHRS provides instant comfort by reducing the switch on time. A TEG converts waste heat to electricity. Even if not yet adopted on cars, the thermo-electric cell technology has evolved rapidly and new cells are now available with higher power density, higher temperature resistance and lifetime. Hybrid electric vehicles are particularly suited for this type of technology, which can provide electrical energy for the auxiliaries in a complete passive way and, at the same time, it recovers waste heat to be used for engine faster warm-up or for cabin heating.

Considering the implementation of all these innovations, the development of an accurate hybrid control strategy will be critical to maximize the synergy of these technologies, and that is precisely why PHOENICE will focus heavily on virtual control development. Indeed, this thesis work contributes to the setup of the HIL bench that will be used to develop and calibrate the ECU to introduce the control strategies needed to optimize energy management while ensuring minimal emissions and fuel consumption, drivability, and electrical balance.

3 Role of 1D CFD simulation for ECU development: introduction of GT-Suite tool

3.1 CFD models for Hardware in the loop ECU development

Today, the introduction of the increasingly complex architectures mentioned above has led to the development of new technologies to accelerate powertrain development. Virtual development is certainly the most important of these, and Computational Fluid Dynamics (CFD) is a prime example. Through flow analysis it is possible to analyse possible aerodynamic improvements without having to resort to the use of prototypes and wind tunnel tests or, in any case, it is possible to arrive at testing already with prototypes at an advanced stage of development. The same can be done within the study of the vehicle cooling system or, in the specific case of the combustion engine, it is possible to design the intake system to achieve the desired charge motion in the combustion chamber. All these examples refer mainly to three-dimensional (3D) analysis, i.e. a numerical calculation method that integrates the Navier-Stokes equations in space. This type of numerical calculation requires more effort in terms of time (computational power) and cost, and it generally becomes appropriate to introduce simplifications in order to obtain the best compromise. For this reason, the first numerical methods developed refer to one-dimensional (1D) models, which restrict the field to just the axial co-ordinate that allows obvious simplifications [19].

Thanks to the increase in computational power, 3D calculation is becoming more and more widespread, while 1D calculation is becoming increasingly important for the analysis of entire systems, where 3D calculation is not yet a viable route. In the case of the analysis of an internal combustion engine, a one-dimensional model can yield significant results by modelling the entire system, from intake to exhaust volumes including after-treatment systems

Besides being used for the development of the combustion engine itself, these models can be used as plant models for the development of the control hardware (the ECUs). The great complexity of vehicle architectures also increases the complexity of the control software itself, which requires development in parallel with the hardware in accordance with the V-Shape methodology (figure 3.1).

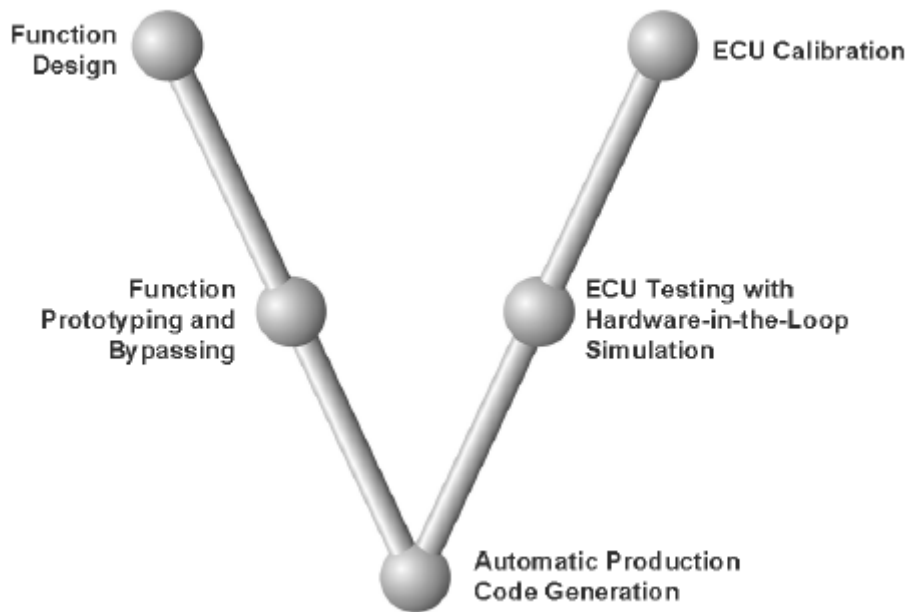


Figure 3.1 V-Shape Development for ECU [20]

The main steps for ECU software development are as follows (figure 3.2) [20]:

- **Model in the Loop (MiL):** Generally, control unit development starts with the analysis of the functions to be adopted to control the "plant", i.e. the virtual environment, which can be modelled using software such as Simulink/State flow. Since the function model is integrated into the control loop, this is often referred to as a 'model-in-the-loop'.
- **Software in the Loop (SiL):** Subsequently, the function model can be replaced directly by the C code that will later be implemented in the control unit. This type of analysis makes it possible to compare the behavior of the code against the function model in the control of the 'plant'.

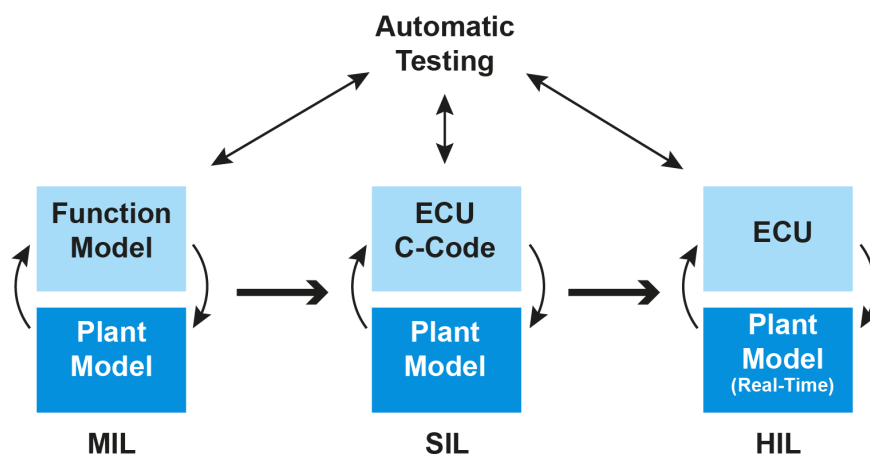


Figure 3.2 ECU software development stages

- Hardware in the Loop (HiL):** In HiL simulation software and hardware models simulate the behavior of the vehicle. Real vehicle components (real parts) are then connected, via their electrical interfaces, to a simulator, which reproduces the behavior of the real environment. Figure 3.3 shows the fundamental design of HiL systems. Instead of being connected to an actual vehicle, the ECU to be tested is connected to a simulation system. This runs a real time model of the vehicle process and associated sensors and actuators that will usually have been developed and implemented with suitable modeling tools such as 1D CFD tools. C code is generated automatically from the representation within the modeling tools and then downloaded to special real-time hardware for execution. The real-time hardware is in turn connected to the ECU's electrical interface via special I/O boards and suitable signal conditioning for level adjustment, using either simulated or real loads.

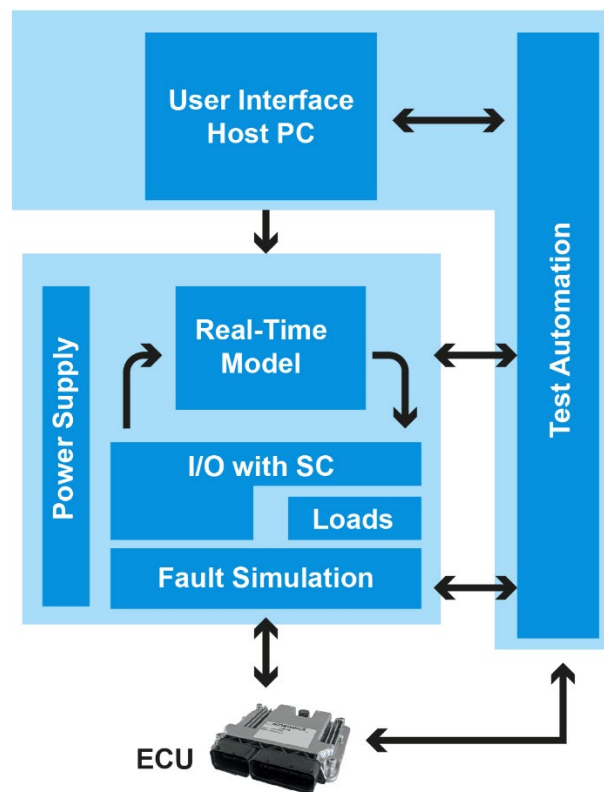


Figure 3.3 HiL design scheme

Using HiL as a parallel development method naturally allows for less time and cost than actual testing, but there are additional advantages:

- Daring situations can be partially tested through desktop experiments;
- Unusual and extreme environmental conditions can be simulated;
- Errors or damages that would have devastating consequences on the prototype can be avoided or even simulated without consequences;
- All tests can be systematically, accurately, and automatically repeated.

3.2 GT-Suite: Modelling and simulation principles

GT-Suite is a software package that allows the simulation and analysis of almost all vehicle subsystems, and through the GT-Power license, it is possible to evaluate the performance of an internal combustion engine through 1D models [21].

In this work GT-Power license is used to calibrate and validate a model on experimental data that then will be used as “real-time model” for the validation of the HiL workflow and process and to investigate how new feature on engine architecture can theoretically improve the base model.

The tool GT-ISE is the interface where models are built, it has a 2-D environment where various objects can be put inside the map and linked together. These objects called also templates are taken from the GT-ISE library and may represent geometrical parts of engine like cylinders, pipes, flow splits, turbines (figure 3.4) that can be fully customized in terms of geometry, material, and thermal properties.

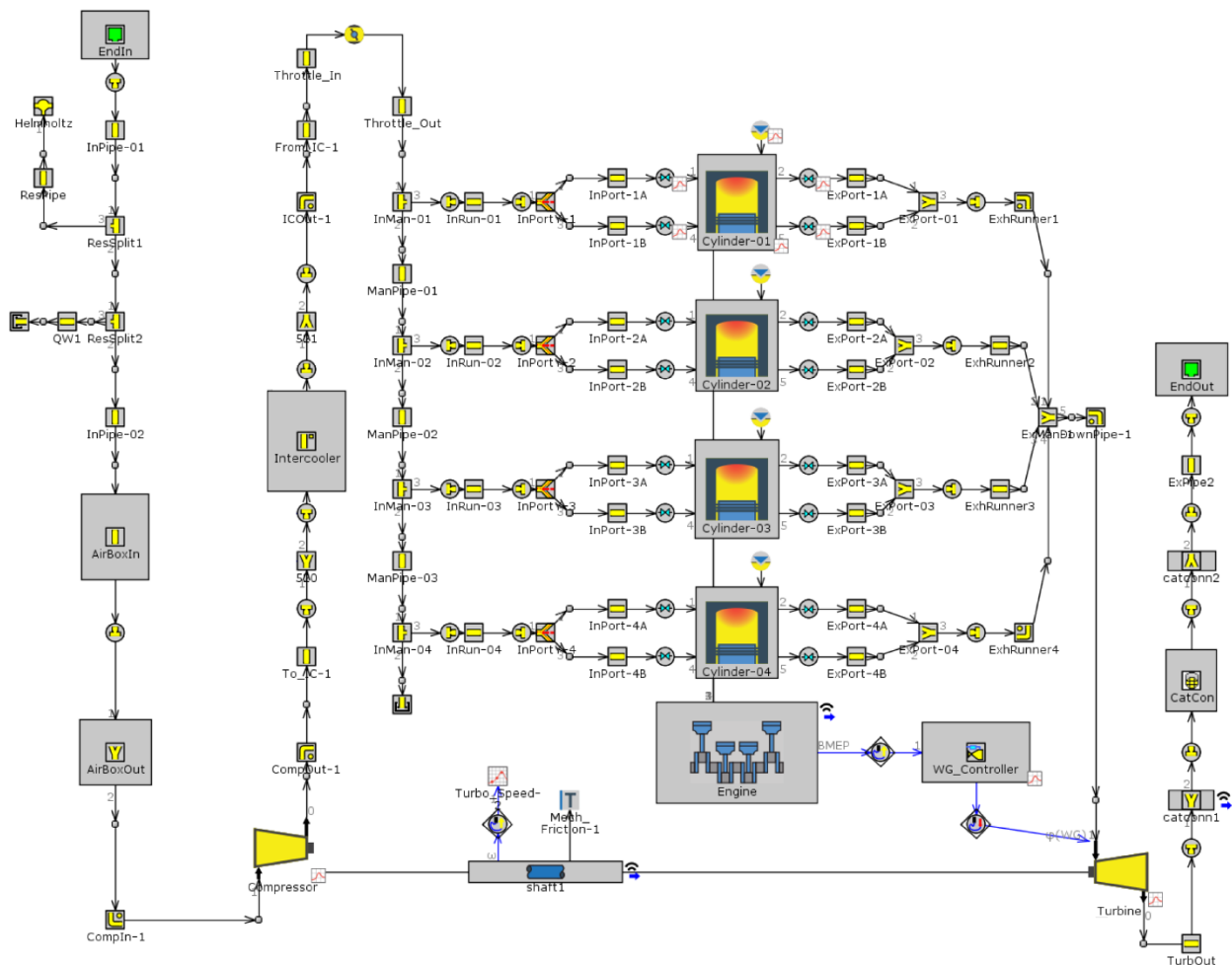


Figure 3.4 Example of a complete SI Turbo engine model

The goal is to recreate as closely as possible the real volumes on both the intake and exhaust sides with a simplified geometry using even different objects for a single real part (figure 3.5). This is to reproduce the same pressure losses, heat transfer for example or as also to reproduce the pressure waves that are used for tuning the intake system (e.g., Helmholtz resonator) or for tuning the exhaust system (e.g., pulse exhaust manifold). All this then requires a certain amount of data, depending on the level of accuracy required, such as 3D models of the components and bench tests.

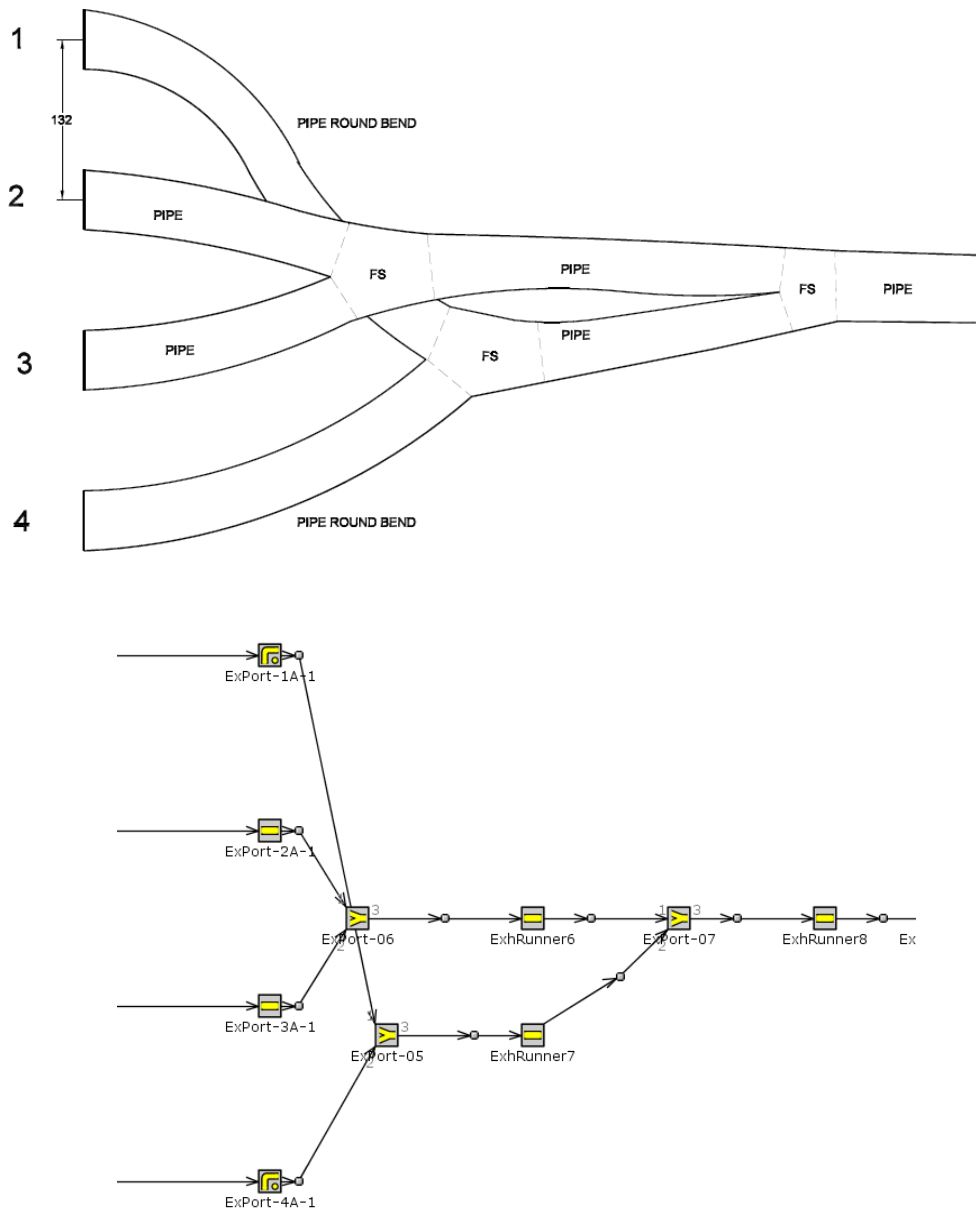


Figure 3.5 Example of how an exhaust manifold can be modeled in GT-Suite

Other templates do not represent physical parts but define aspects like combustion, turbine and compressor maps or define the control logic of the model. As an example, a PID controller can be implemented to match desired quantities like brake mean effective pressure changing the wastegate diameter of the turbine.

[22] The flow model involves the solution of Navier-Stokes equations: the conservation of continuity, momentum and energy equations that are solved in one-dimension. It means that all quantity are averages across the flow direction. The system is discretized into “staggered grid” (figure 3.6) i.e., into several volumes depending on the discretization length imposed by the user. The vector variables (mass flux, velocity, mass fraction fluxes, etc.) are calculated for each of volume boundaries whereas the scalar variables (pressure, temperature, density, internal energy, etc.) are assumed to be uniform over each volume.

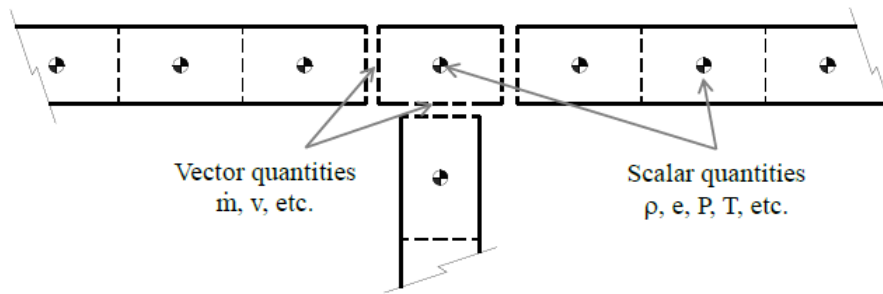


Figure 3.6 Pipe volume division: discretization into staggered grid

The part that makes combustion engine simulation software differ from regular CFD software is the combustion modeling, which becomes critical to obtaining satisfactory results. [23] The combustion is modeled in the same way for almost all the type of combustion templates present in the tool and is a two-zone combustion: every time step the cylinder volume is divided into two zones: the unburned and the burned zone. At the start of combustion (spark time in SI engines and start of injection in DI engines), the whole volume is the unburned zone that is composed by fresh air, residual gas from previous cycle and EGR. Then, every time step, a certain quantity of the unburned zone is transferred to the burned zone depending on the burn rate that is predicted by the type of combustion model chosen or imposed a-priori by the user. Then a chemical equilibrium calculation is carried out taken into account all the atoms of each species present in the burned zone to obtain an equilibrium concentration of the products of combustion species. The equilibrium concentrations of the species depend strongly on the current burned zone temperature and to a lesser degree from the pressure. Once the new burned zone is obtained, the internal energy of every species is calculated to derive the energy of the entire zone and apply the energy conservation to obtain the new temperature and pressure of the new burned and unburned zone. So, for each time step the following equations are solved:

Unburned Zone:

$$\frac{d(m_u e_u)}{dt} = -\frac{pdV_u}{dt} - Q_u + \left(\frac{dm_f}{dt} h_f + \frac{dm_a}{dt} h_a \right) + \frac{dm_{f,i}}{dt} h_{f,i}$$

Burned Zone:

$$\frac{d(m_b e_b)}{dt} = -\frac{pdV_b}{dt} - Q_b + \left(\frac{dm_f}{dt} h_f + \frac{dm_a}{dt} h_a \right)$$

The key point is the choice of the combustion model that defines the burn rate. There are several options depending first of all on the type of engine (SI and DI) and from the target of the simulation study. In general, these models can be divided into three categories [23]:

- Predictive combustion model: These models solve at each time step several physical equations that depend on several input data like cylinder's geometry, spark locations (SI engines) and timing, air motion and fuel properties and need of a robust calibration based on experimental data. These models are the most complete and complex and require also high computational time. They can be useful in case the target of the study is to evaluate changes that influence in a significant way the burn rate, such as spark timing or injection rate profile in case of a diesel engine.
- Semi-Predictive combustion model: These models can be an appropriate substitute of the predictive models because they are sensitive to significant variables that influence the combustion rate

and can respond to changes on those variables. Respect the predictive models, these do not contain any physical models but exploit trained neural networks. These neural networks predict the burn rate computing the parameters of non-predictive methodology (e.g. Wiebe) in function of the significant variables. For these reasons they need some experimental data to be trained to be strong enough out of the experimental points used.

- Non-Predictive combustion model: These models impose the burn rate regardless of the in-cylinder state, so it will be not affected by changes for an example on injection time. These models can be used to study the effect of variables that have low influence on the combustion rate like the impact of the length of the manifold runner on volumetric efficiency. If the cylinder pressure is available, the burn rate can be derived, and a specific template can be used to impose that burn rate. In case of no information about the cylinder pressure the Wiebe function can be used to impose the typical S-shape burn rate of a SI engine. The Wiebe parameters and equations are the following [23]:

AA = Anchor Angle

D = Combustion Duration

E = Wiebe Exponent

CE = Combustion efficiency (Fraction of fuel burned)

BM = Burned Fuel percentage at Anchor angle

BS = Burned Fuel percentage at Duration Start

BE = Burned Fuel percentage at Duration End

θ = Instantaneous crank angle

$$BMC = -\ln(1 - BM) \quad \text{Burned Midpoint Constant (1)}$$

$$BSC = -\ln(1 - BS) \quad \text{Burned Start Constant (2)}$$

$$BEC = -\ln(1 - BE) \quad \text{Burned End Constant (3)}$$

$$WC = \left[\frac{D}{\left(\frac{1}{BEC^{E+1}} - \frac{1}{BSC^{E+1}} \right)} \right]^{-(E+1)} \quad \text{Wiebe Constant (4)}$$

$$SOC = AA - \frac{D * (BMC)^{\frac{1}{E+1}}}{\frac{1}{BEC^{E+1}} - \frac{1}{BSC^{E+1}}} \quad \text{Start of Combustion (5)}$$

$$Combustion(\theta) = (CE) * [1 - e^{-(WC)(\theta - SOC)^{E+1}}] \quad \text{Burn rate (6)}$$

Usually, the burned fuel percentage at anchor angle (BM) is set to 50% and the other two (BS and BE) are set respectively to 10% and 90%. In this way the anchor angle (AA) corresponds to the MFB50 (angle at which the mass of fuel burned is 50% of total) and the combustion duration (D) correspond to the difference between MFB90 and MFB10 (figure 3.7).

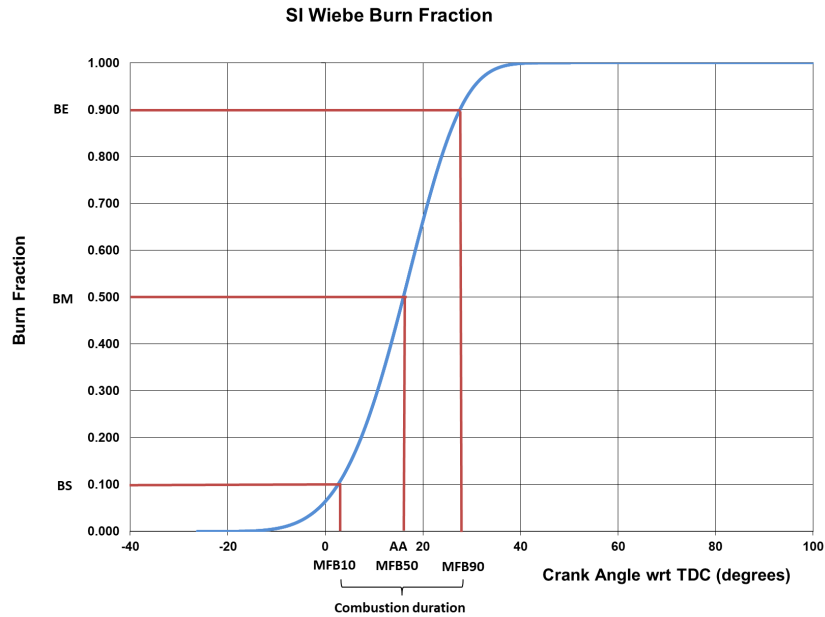


Figure 3.7 Example of a S-Shape function generated by Wiebe equations: in this case the anchor angle (AA) is set equal to MFB50 and combustion duration as MFB90-MFB10

After the creation of the model with its components and links the simulation can be run. The software allows you to vary some parameters in one simulation through the Case Setup whereas the word suggests you can create various cases where some parameters vary. The most obvious example is the analysis of a full load curve where the main parameter that changes is the motor speed and all the parameters dependent on it (such as friction or heat transfer coefficients in the chamber), or in the case of an analysis of part load points in addition to the speed also the target load can be changed (figure 3.8).

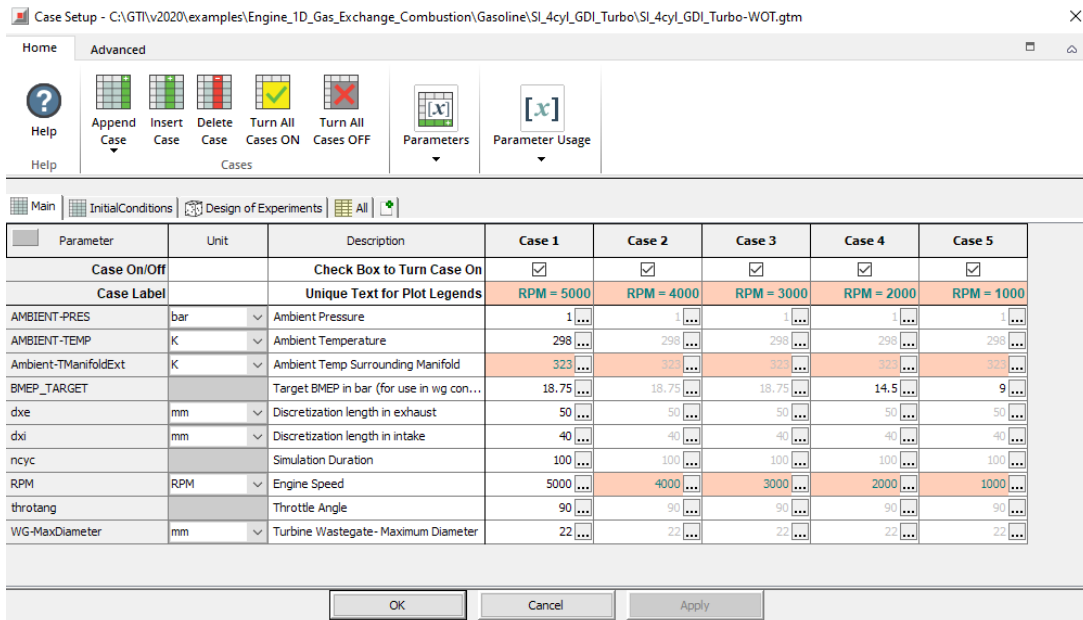


Figure 3.8 Example of the structure of the Case Setup

Once the simulation is complete, through GT-Post, a post processing tool, it is possible to analyze all the data and create useful reports and graphs and make some DOE analysis and prediction.

4 GSE-T4 Model calibration

4.1 The baseline model

As described in Chapter 2, the PHOENICE project starts from the base of the Jeep Compass 4Xe. In this context, the combustion engine will also be developed directly from the GSE-T4. The main components such as the block and cylinders will remain the same (thus same displacement) and the VVA MultiAir system will be used. Therefore, a first part of the work focuses on calibrating a 1D model of the GSE-T4 both at full load and at some points at part load. This model will be essential for the HiL bench setup and will be the basis for an initial optimization and estimation of the possible benefits of the model implementing the PHOENICE modifications.

The calibration work starts from a base model received from Stellantis and tuned by Politecnico di Torino (from now baseline model) that completely describes the GSE-T4 from intake volumes to the exhaust ones also including the entire after-treatment system.

The choice of starting from a model based on GSE-T4 also lies in the high availability of experimental data. The data used as input and validation are derived from one of the last ECU calibration checks of GSE-T4 and include 286 operating points covering the entire engine map (figure 4.1).

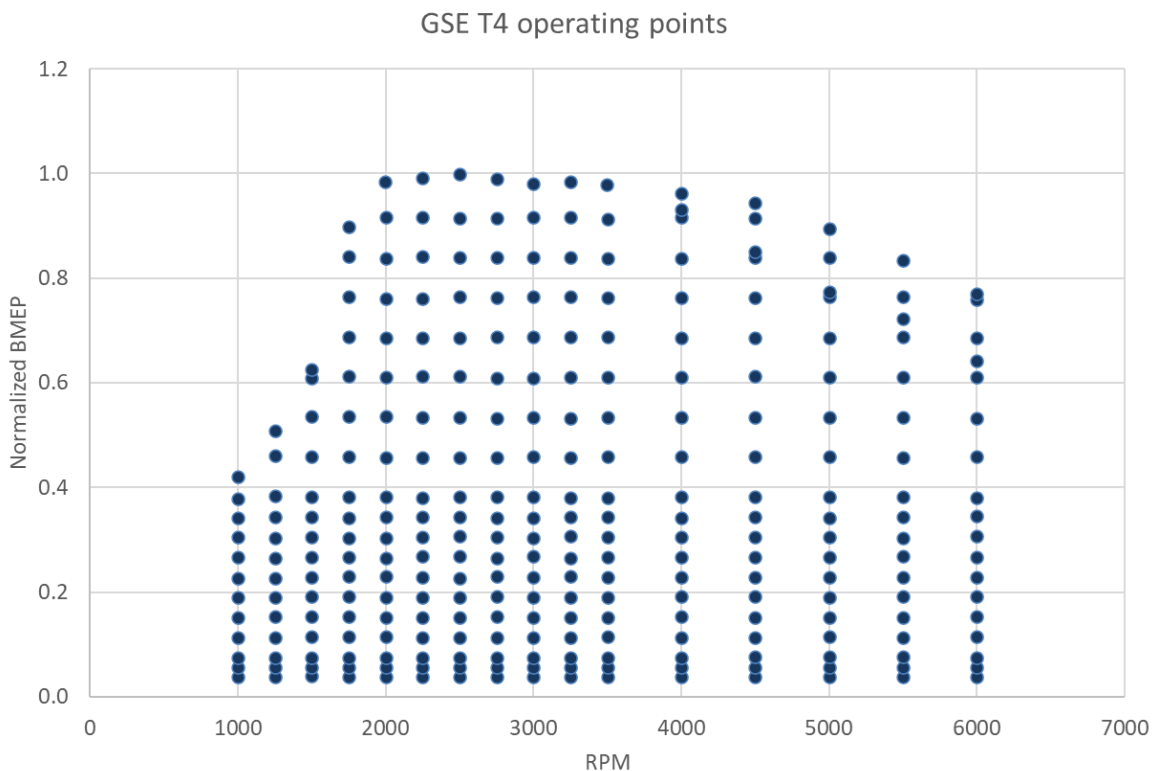


Figure 4.1 Engine map points investigated at test bench

The information for each operating point is comprehensive and includes all parameters related to combustion engine performance, pressures and temperatures at various points, tail pipe emissions information. The actual data used are a small extract of this information (table 4.1) since the calibration

activity aims to change only a few key variables in order to obtain behaviors of the validation variables (table 4.1) more similar to reality. Among these validation variables, pollutant emission variables were not included because the PHOENICE project involves a radical change in the aftertreatment system that would have made more detailed work unnecessary.

Table 4.1 Input variables set in the Case Setup and the validation data uses to plot the results

Input variables			Validation data		
Quantity	Units	Comments	Quantity	Units	Comments
Main			BMEP	bar	Only for full load cal.
Engine speed	rpm		PMEP	bar	pumping losses
FMEP	bar	friction losses	Volumetric efficiency		Computed in the manifold
Target boost pressure P2	bar		Air mass flow rate	kg/h	
Target BMEP	bar	Only for partial load calibration	BSFC		brake specific fuel consumption
Environmental condition			Turbo-compressor speed	rpm	
Ambient Temperature	C°		Boost pressure P2	bar	
Ambient Pressure	mbar		T2	C°	
Humidity	%		P3	bar	
Fuel Injection			T3	C°	
SOI	deg		P4	bar	
Injection duration	deg		T4	C°	
Injection pressure	bar		PMAX	bar	Max cylinder pressure
Air to Fuel ratio			APMAX	°CA	Angle of max cylinder pressure
Thermal					
Oil temperature	C°				
Head coolant temperature	C°				

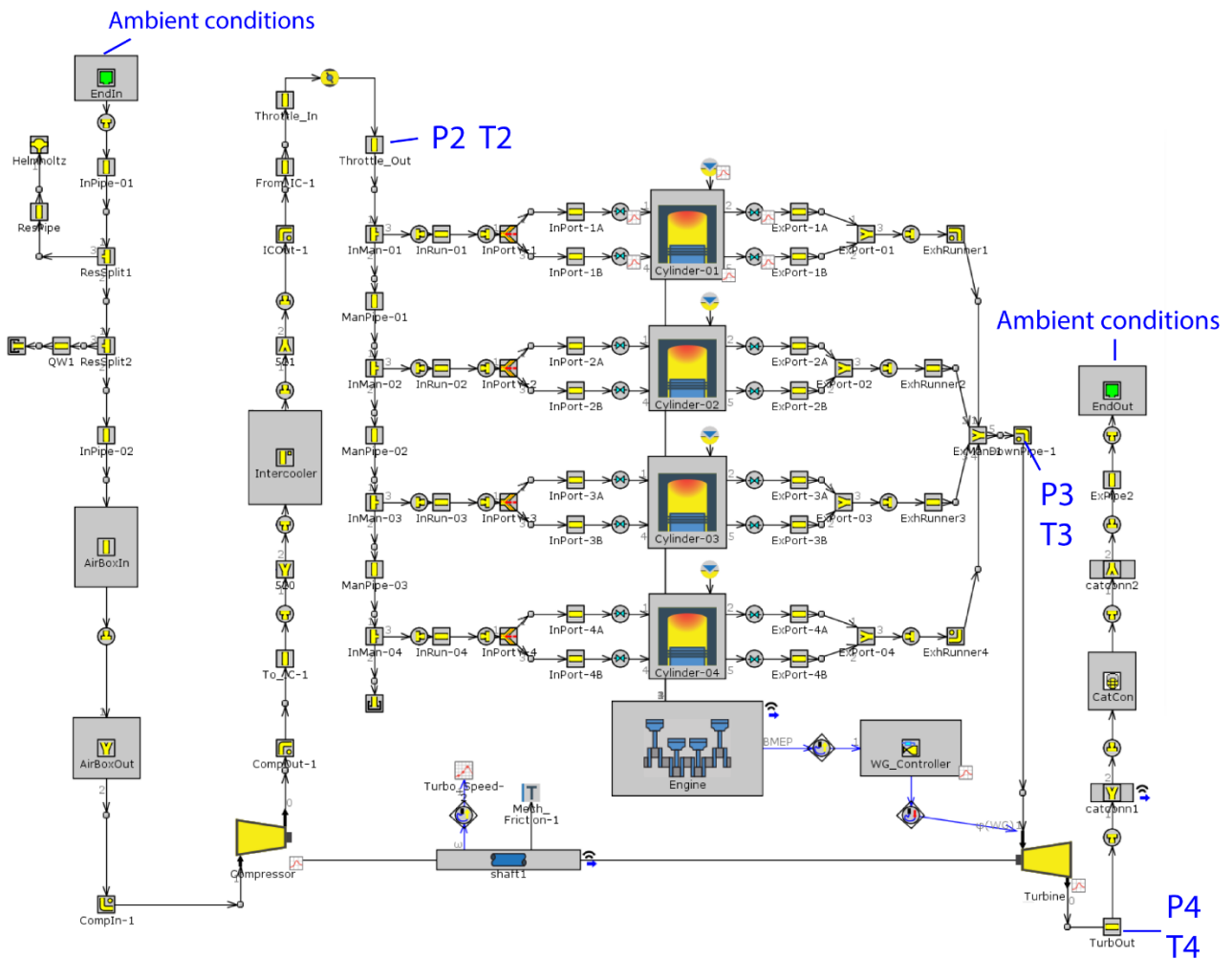


Figure 4.2 Pressures and temperatures nomenclature and position on the engine model

Temperature and pressure are taken from the points showed in the figure 4.2. The volumetric efficiency is not directly derived from experimental data but was calculated considering the following formula [12]:

$$\lambda_v = \frac{\dot{m}_a}{\rho_a * i * V_d * \frac{n}{2}}$$

Where:

- \dot{m}_a is the air flow rate in kg/s
- ρ_a is the air density in kg/m³
- i is the number of cylinders
- V_d is the cylinder displacement in m³
- n is the rotational speed of the engine in rps (round per second)

The density is calculated considering the pressure and temperature downstream of intercooler (P2 and T2 respectively) and also the humidity. In that way only the pumping performance of the inlet ports, of the

cylinders and the valves are considered and permit to isolate and evaluate better the performance of the VVA system.

4.2 Calibration parameters

The main calibration parameters that were varied to best match the experimental data are listed in table 4.2. These parameters involve quantities that cannot be measured directly experimentally but affect other parameters that can be measured instead. For example, the heat transfer coefficients between cylinder and head with coolant and engine oil affect the temperature of the gas flow upstream of the turbine (temperature T3). For calibration parameters GT-Suite allows you to choose the value you prefer for each operating point, so you can use a map of values that may depend on one or more inputs, or you can formulate a law as a function of some inputs or you can simply act on some multipliers that in turn act on the output values of physical models managed by the software.

Table 4.2 Calibration parameters

Calibration parameters		
Quantity	Units	Comments
Thermal		
Overall convection multiplier		
HTC Water-Head	W/(m ² *K)	
HTC Water-Cylinder	W/(m ² *K)	
HTC Cylinder-Oil	W/(m ² *K)	
HTC Piston-Oil	W/(m ² *K)	
Combustion		
MFB50	deg	
Combustion Duration	deg	MFB90-MFB10
Wiebe Exponent		
Fraction of fuel burn		
Other		
Turbine mass multiplier		
IVO	deg	
IVC	deg	

Thermal parameters

- Overall convection multiplier: Considering the energy balance equation [12]:

$$\dot{m}_f Q_{LHV} = P_b + \dot{Q}_{cool} + \dot{Q}_{misc} + \dot{H}_{eic} + \dot{H}_e$$

Where:

- \dot{m}_f is the fuel mass flow rate;
- Q_{LHV} is the lower heating value of the fuel;
- P_b is the engine brake power;
- \dot{Q}_{cool} is the heat transfer rate to cooling medium (including that transferred to oil);
- \dot{Q}_{misc} is the heat directly rejected to the surrounding ambient;

- \dot{H}_{eic} is the exhaust enthalpy loss due to incomplete combustion;
- \dot{H}_e is the exhaust enthalpy loss due to high temperature of exhaust gases;

The heat exchanged to the environment is an important amount that accounts for about one-third of the energy given by the fuel, which is then lost, drastically diminishing the efficiency of the process (table 4.3).

Table 4.3 Si engines percentage of utilization of the energy of the fuel [12]

SI engines typical energy balance				
P_b	\dot{Q}_{cool}	\dot{Q}_{misc}	\dot{H}_{eic}	\dot{H}_e
25-30 %	17-25 %	5-10 %	6-15 %	25-35 %

Most of this energy is released to the coolant and engine oil (\dot{Q}_{cool}) and other energy to the environment (\dot{Q}_{misc}) through conduction, convection and radiation (figure 4.3)

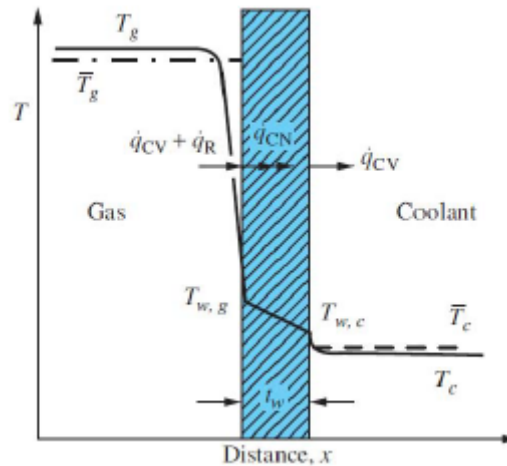


Figure 4.3 Schematization of heat transfer between gases, cylinder wall and coolant [12]

Looking specifically at the heat that the gases exchange with the surfaces of the combustion chamber (cylinder walls, head, valves, piston) in gasoline engines the bulk of it occurs through the convection phenomenon:

$$\dot{q} = h(T_g - T_w)$$

Where:

- \dot{q} is the instantaneous heat transfer per unit area
- h is the Convective heat transfer coefficient
- T_g is the gas temperature
- T_w is the walls temperature

From this relationship the instantaneous heat exchanged can be derived [8]:

$$\partial Q = -\dot{q}A \frac{d\theta}{\omega}$$

This instantaneous heat transfer changes as the crankshaft angle varies and is relevant during combustion. Experimentally, it is very complicated to obtain the value of the heat transfer coefficient (h), and for this there are some empirical relations that allow it to be estimated as a function of numerous variables. One of these is the Wolschni correlation [23]:

$$h = \frac{K_1 p^{0.8} w^{0.8}}{B^{0.2} T^{K_2}}$$

Where:

- B is the cylinder bore
- K_1, K_2 are tuning parameters
- p is the cylinder pressure
- T is the cylinder temperature
- w is the average cylinder gas velocity expressed below

$$w = C_1 \bar{S}_p + C_2 \frac{V_d T_r}{P_r V_r} (p - p_m)$$

Where:

- C_1, C_2 are other tuning parameters
- \bar{S}_p is the mean piston speed
- T_r is the working fluid temperature prior to combustion
- p is the instantaneous fluid pressure
- p_m is the motoring fluid pressure at the same angle as p
- P_r is the working fluid pressure
- V_d is the displaced volume
- V_r is the working fluid volume prior to combustion

GT-Suite allows the heat transfer to be modeled with the Wolschni correlation with already set values for the tuning coefficients [23]:

Table 4.4 Coefficients of wolschni correlation used in the WolschniGT model on GT-Suite

K_1	K_2
3.01426	0.50

$$C_1 = 2.28 + 3.9 * \text{Minimum} \left(\frac{\dot{m}_{in}}{m_{cyl} f}, 1 \right)$$

Where:

- \dot{m}_{in} is the instantaneous mass flow rate
- m_{cyl} is the instantaneous cylinder mass
- f is the engine frequency in rev/s

Table 4.5 Other Wolschni correlation coefficient used in WolschniGT model

	C_2
During cylinder gas exchange and compression	0
During combustion and expansion	0.00324

but it is possible to act on another parameter, the overall convection multiplier. This parameter by default is set to 1 and acts on the model by multiplying the output value. By varying this multiplier slightly, it is possible to increase or decrease the heat exchanged, which then results in a different exhaust gas temperature that affects the temperature upstream of the turbine (T3) and impacts combustion efficiency.

- Heat transfer coefficients: In addition to modeling the transfer between in-cylinder gases and the walls of the combustion chamber, the model requires the value of heat transfer coefficients between the walls of the cylinder and piston with the coolant and engine oil. The GT-Suite model in question imposes the temperature of oil and coolant (set directly as input) as a boundary condition, and then varying heat transfer coefficients leads to different wall temperatures that affect the actual heat exchanged. These heat transfer coefficients depend directly on the type of material but also on other parameters such as engine speed and load. In this case, the baseline model predicts a trend in heat transfer coefficients as a function of engine speed alone:

$$HTC = C_1 + C_2 * n$$

These parameters can be slightly modified to refine the same outputs described earlier (T3 and combustion efficiency) but have a much smaller influence. A better study could have been made if the temperatures of certain surfaces such as cylinder head and engine block were available among the experimental data.

Combustion parameters

In this model, combustion was modeled using Wiebe's approach. This is because more detailed models would increase the computational cost of the model, which is unacceptable since the main objective is the possibility of using it later in real-time. In addition, the study does not require a detailed analysis of pollutant emissions, so there is no need to lushly describe the combustion chemistry. In addition, it is much easier to calibrate the model since only four calibration parameters are acted upon with which the pressure profile inside the cylinder can be matched. The pressure profile is not present in the available experimental data while there is information on the maximum pressure in the chamber and the angle at which it occurs that is still sufficient to obtain good results.

- The MFB50 corresponds to the crank angle at which 50% of fuel mass is burned and, if is set as anchor angle, is the angle at which the peak of burn rate occurs (figure 4.4). Shortly after this angle usually the peak pressure occurs and therefore by changing this angle it is possible to "shift" the pressure profile over time (crank angles). Tuning this parameter then allows to match the angle that corresponds to the pressure peak.

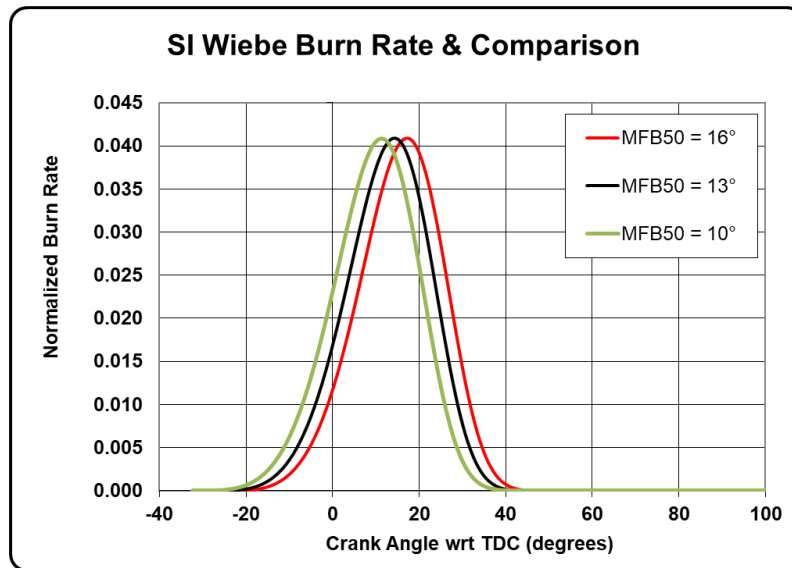


Figure 4.4 Burn rate comparison between different MFB50 chosen: greater is the MFB50, more advanced is the burn rate

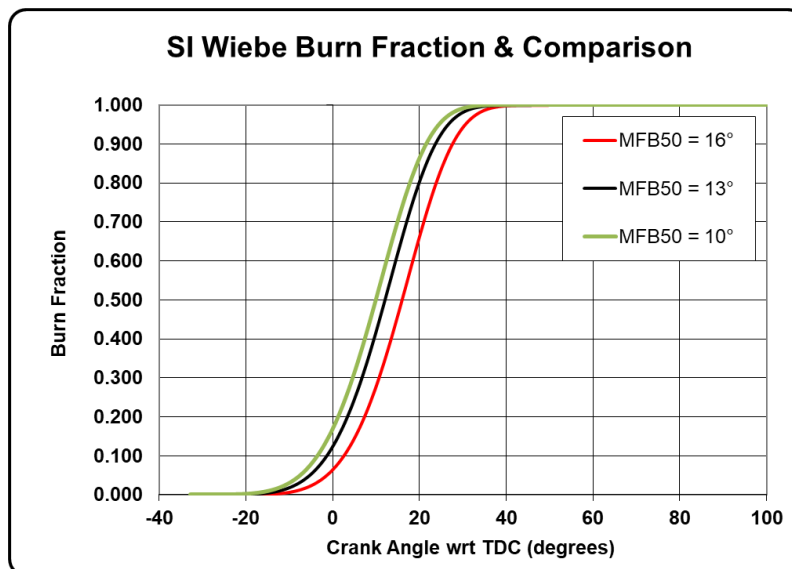


Figure 4.5 S-shape curve comparison between different MFB50 chosen

- Combustion duration in crank angle is usually defined as the difference between MFB90 and MFB10 and determines how quickly a given amount of fuel is burned. The faster it is burned the greater the amount of instantaneous energy released, higher is the peak of burn rate (figure 4.6). This results in a more abrupt rise in cylinder pressure, which then leads to a higher peak pressure. Therefore, this parameter can be varied to match the experimental peak pressure.

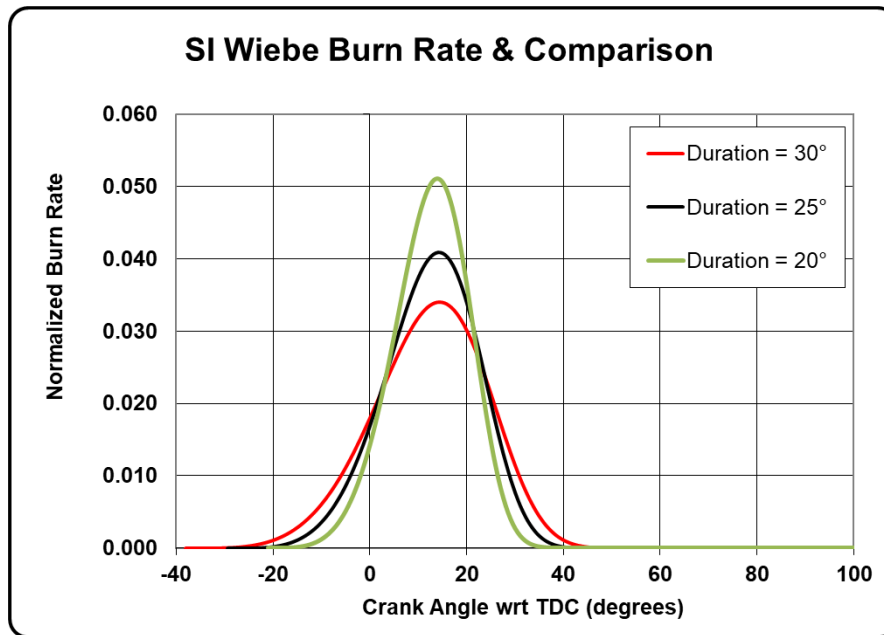


Figure 4.6 Burn rate comparison between different Combustion duration chosen: greater is the combustion duration, higher is the burn rate, therefore higher will be the peak pressure

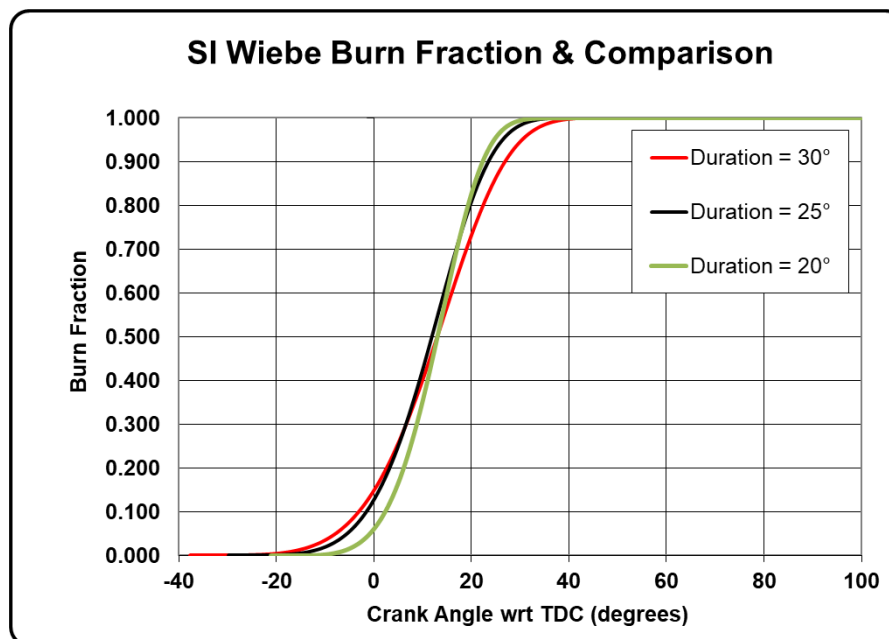


Figure 4.7 S-shape curve comparison between different combustion duration chosen: it can be seen as with lower duration the S shape is more vertical

- Wiebe exponent: This parameter affects the shape of the S (figure 4.9) and can be modified to best match the shape of the experimental pressure curve. In this case, not having the latter available, this parameter was set to an intermediate value of 4, which is usually a good compromise.

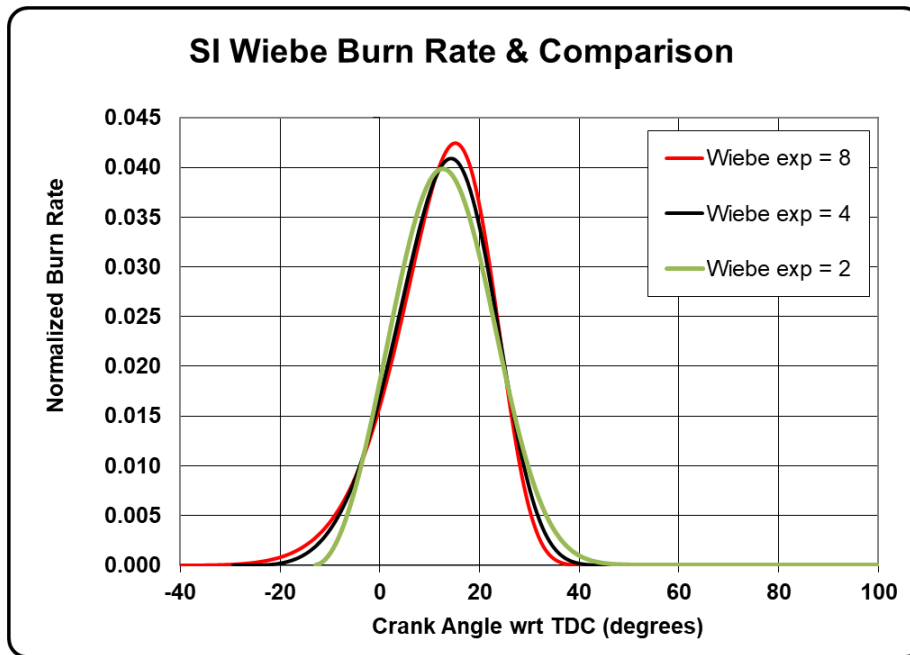


Figure 4.8 Burn rate comparison between different wiebe exponent chosen

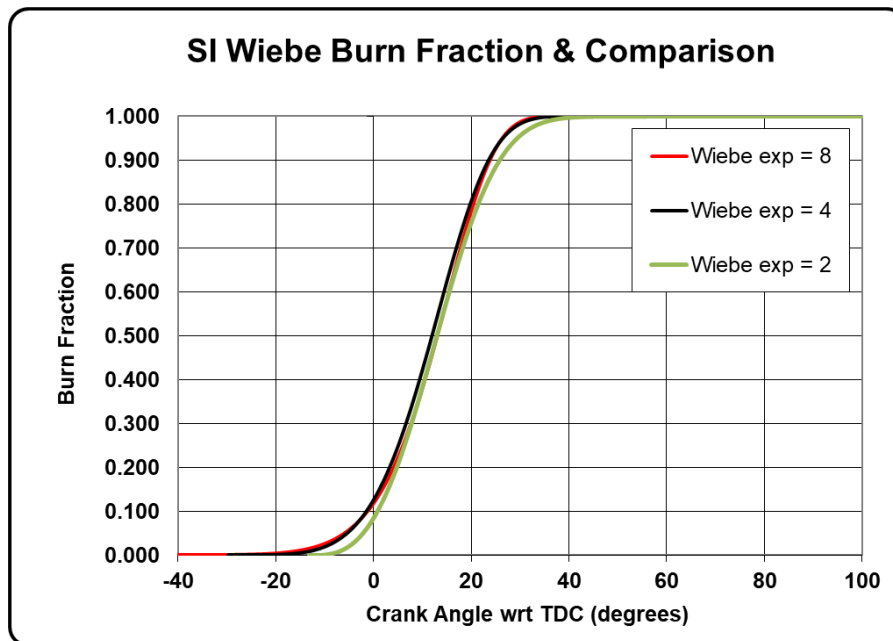


Figure 4.9 S-shape curve comparison between different Wiebe exponent chosen

- Fraction of fuel burned: By default this parameter is set to 1 and thus considers that all fuel is actually burned. In reality, combustion is never complete and leads to the formation of other species in addition to water and CO_2 . Although as mentioned before, this study does not focus on pollutant emission analysis, this parameter can be used to reduce combustion efficiency (reduced to a value less than 1). The shape of the burn profile in this case is not affected by the change in this parameter but is scaled so that at the end of combustion the fraction of fuel burned is as set (figure 4.11).

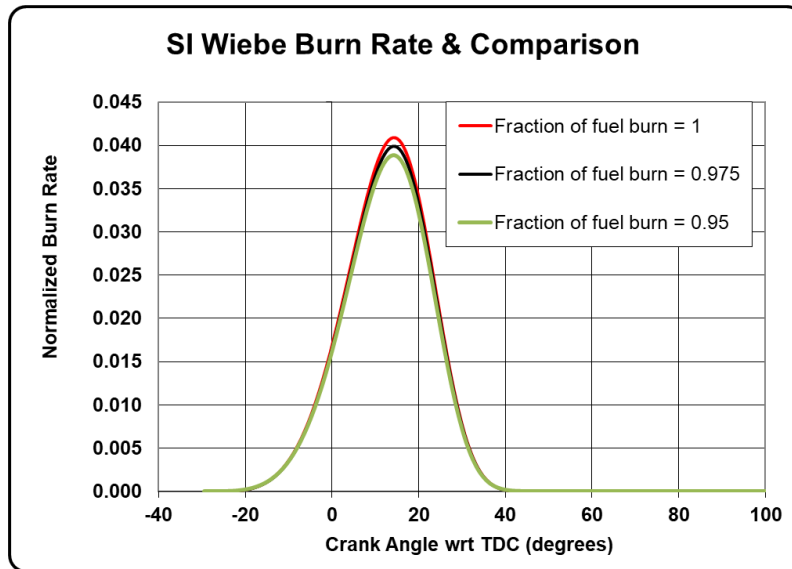


Figure 4.10 Burn rate comparison between different fraction of fuel burned: less fuel means less maximum burn rate

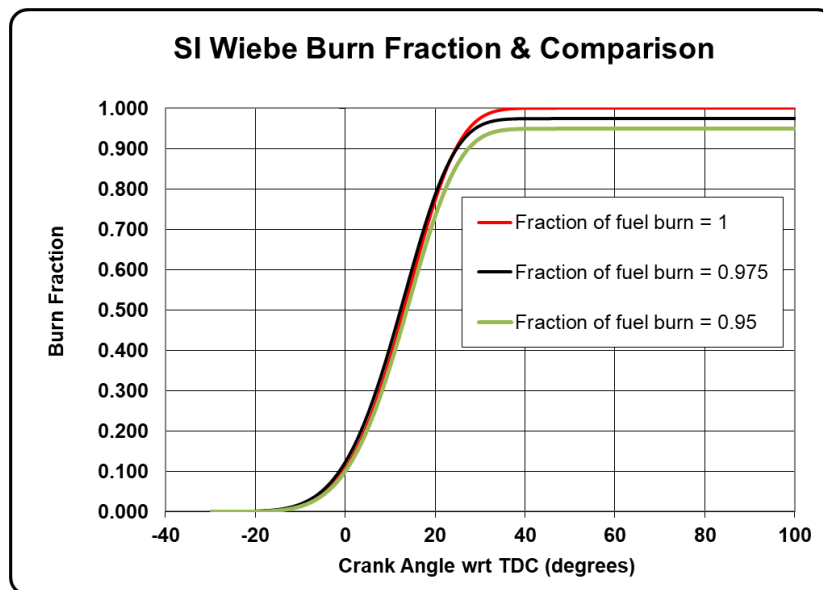


Figure 4.11 S-shape curve comparison between different fraction of fuel burned chosen

Other parameters

- Turbine mass multiplier: Turbine and compressor performance are modeled in GT-Suite using performance maps that are provided by the user. both compressor and turbine maps can be summarized as a series of performance data points, each of which describes the operating condition by speed, pressure ratio, mass flow rate, and thermodynamic efficiency. [22] The maps are configured so that if the speed and either the mass flow or pressure ratio are known, the efficiency and either the mass flow rate or pressure ratio (whichever is not known) can be found in the map. GT-Suite predicts the turbocharger speed and the pressure ratio (PR) across each turbine and/or compressor at each timestep, and therefore they are "known" with respect to the turbo

map. The mass flow rate and efficiency are then looked up in the table and imposed in the solution (figure 4.12).

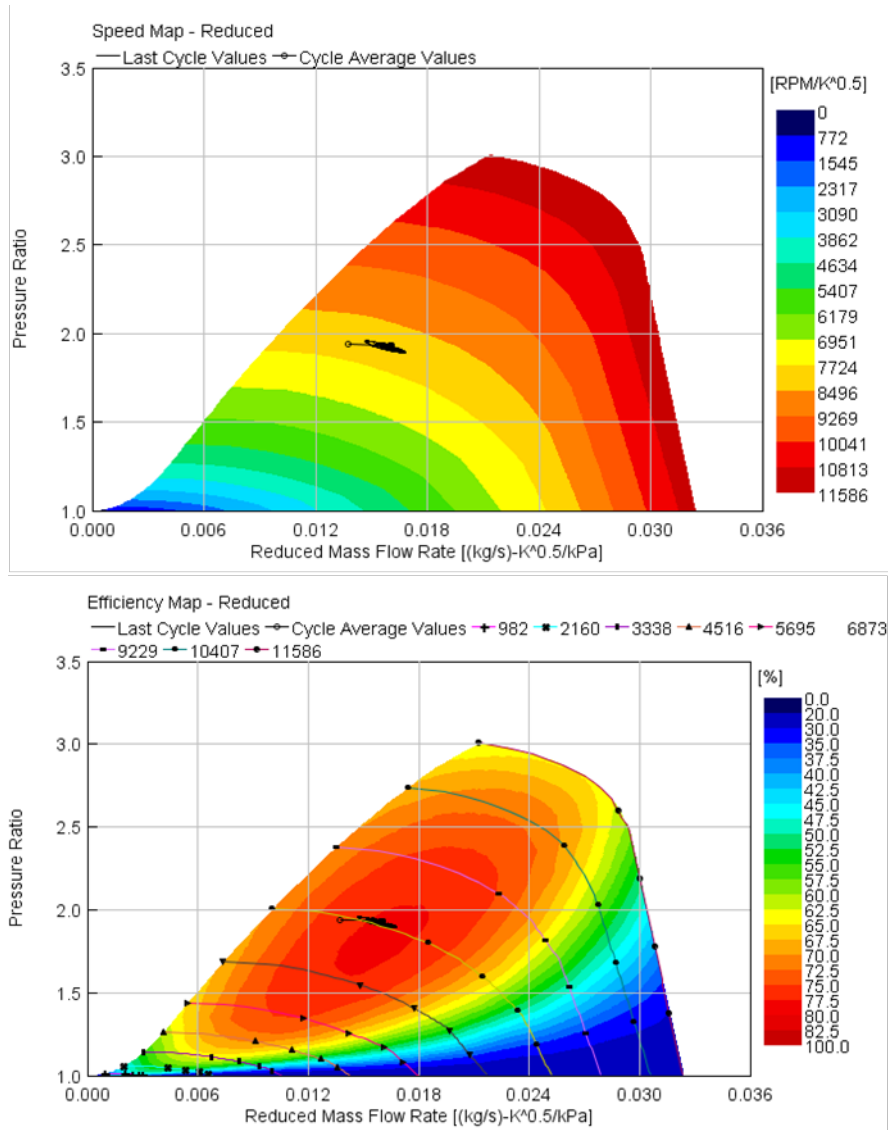


Figure 4.12 Example of compressor maps, GT-Suite at each time step predict pressure ratio and speed in a way to find the mass flow rate (upper figure) and then to find the efficiency (bottom figure)

The turbine mass multiplier is a parameter that the model use to multiply the mass flow rate funded by the interpolation on the turbine map of the instantaneous pressure ratio and speed, in this way the map is “scaled”. For the same mass flow rate, since the pressure downstream turbine (P4) is fixed, the pressure upstream (P3) will change. It can be used when the relation between pressure upstream of turbine, turbo-compressor speed and air mass flow rate does not match the experimental one.

- Intake valve opening and closing angles: The tool allows to enter for each operating point a valve lift profile i.e., it allows to configure lift and time (figure 4.13).

4.2 - Calibration parameters

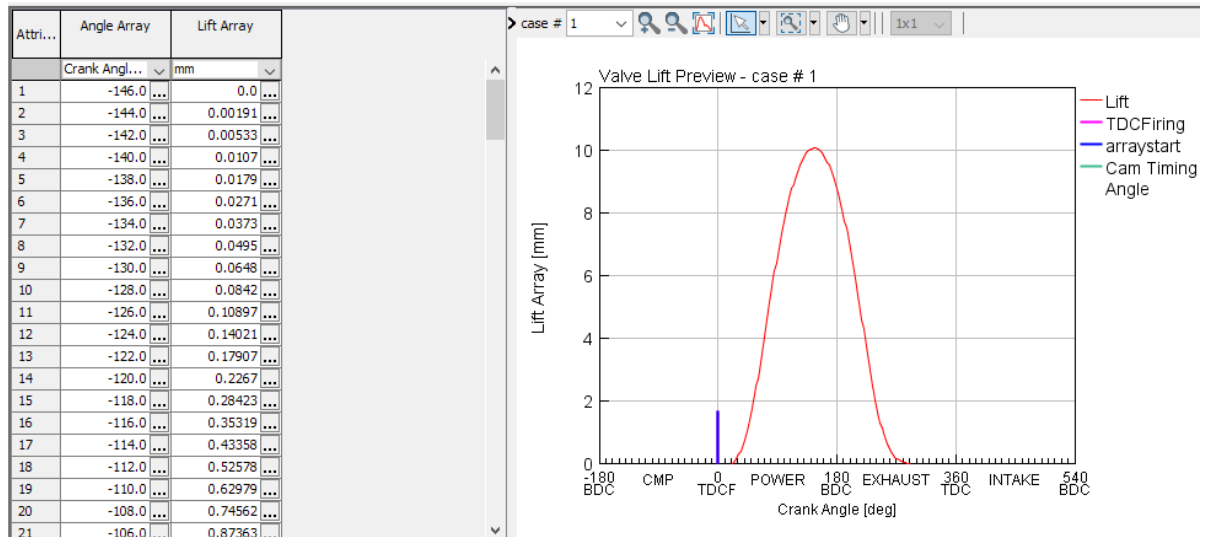


Figure 4.13 Example of valve lift and timing defined in GT-Suite valve object

Indeed, among the data, different profiles were available depending on the engine speed and the desired IVO and IVC (figure 4.14). The baseline model provides logic to identify the valves lift profile automatically based on the IVO and IVC parameters and engine speed defined in the case setup. In this way the VVA system can be simulated.

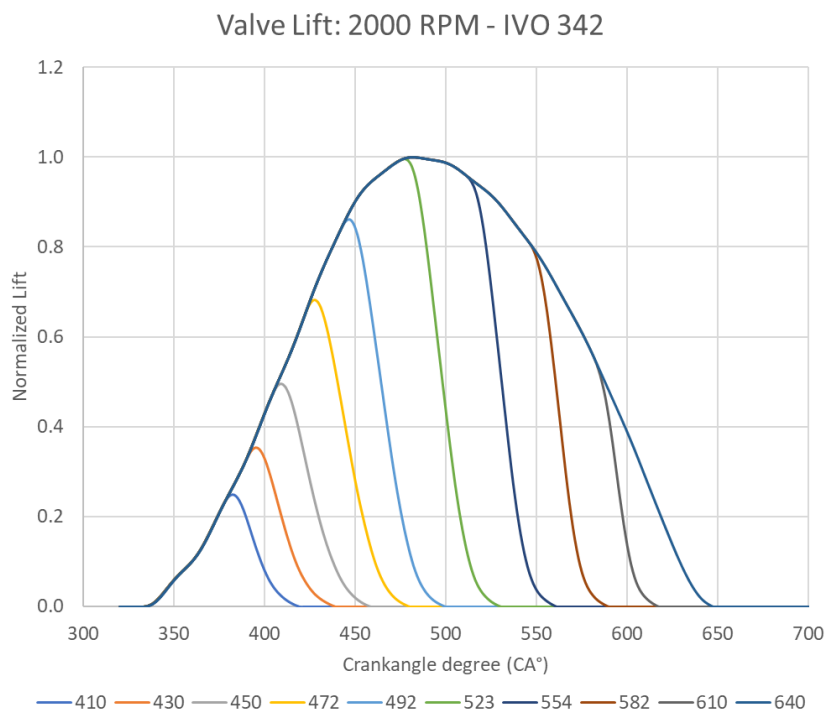


Figure 4.14 Example of the different lift profile available for the chosen IVO and engine speed, the model can interpolate between all these profiles based on IVO and IVC and engine speed

In the experimental data there are indications for the timing chosen for each operating point. These timings are called "electric angles" because they are defined directly in the control unit that

sends the signal to the solenoid valve. Some delays/variation can be present between these values that are extrapolated from the ECU and the true valve timing value. For these reasons, IVO and IVC are calibration parameters that can be tuned to match the experimental results.

4.3 Full load calibration

In the experimental data, the full load points available are 16 and are spread over the range from 1000 to 6000 rpm (figure 4.15).

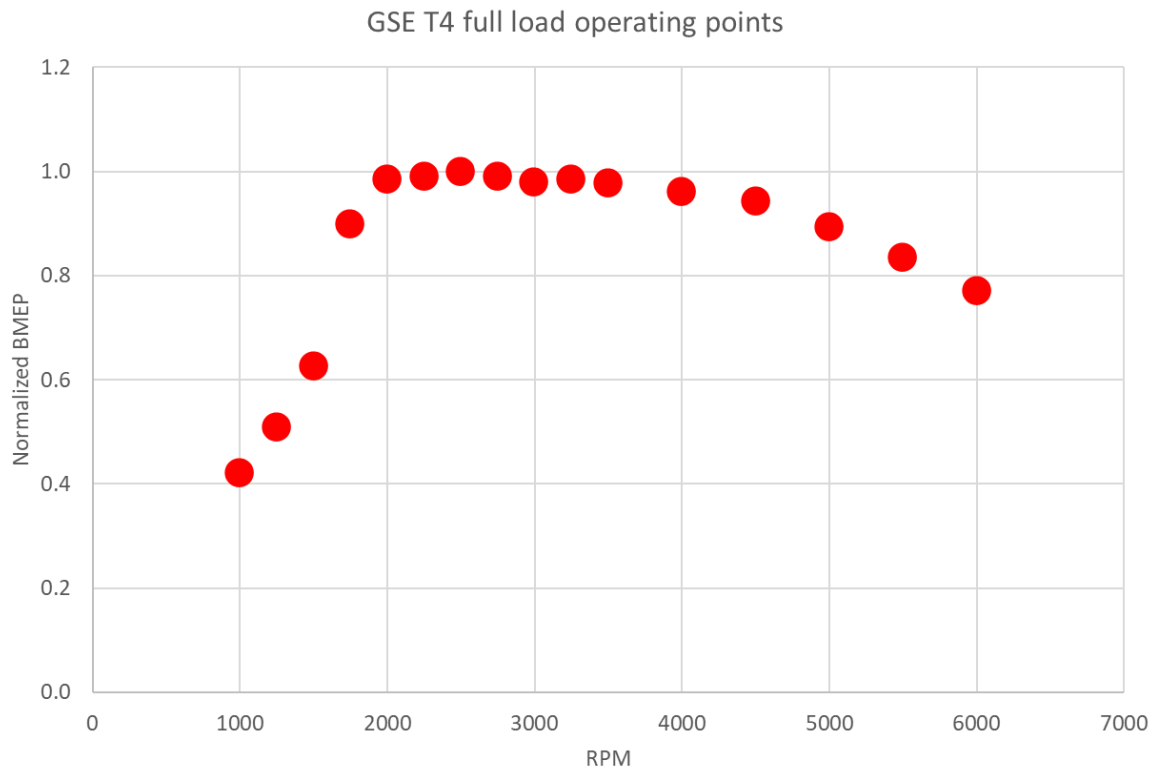


Figure 4.15 Full load point investigated

The logic for running a full load simulation involves the use of a PID controller to control the wastegate valve. There are values in the data regarding the wastegate valve angle, but in the GT-Suite model the wastegate has no physical meaning but is modeled as an orifice whose diameter is adjusted according to demand. For this reason, the controller, which has a particular template optimized for this very purpose (figures 4.16), can be set to adjust the valve to match the boost pressure (P2) from experimental data.

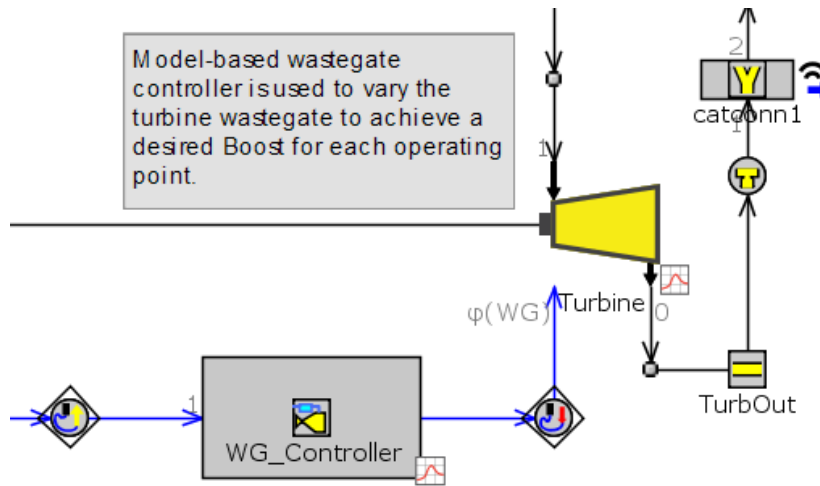


Figure 4.16 Example of wastegate controller connected to Turbine

4.3.1 Calibration methodology and results analysis

In the following figure are showed the results of the early Full load calibration.

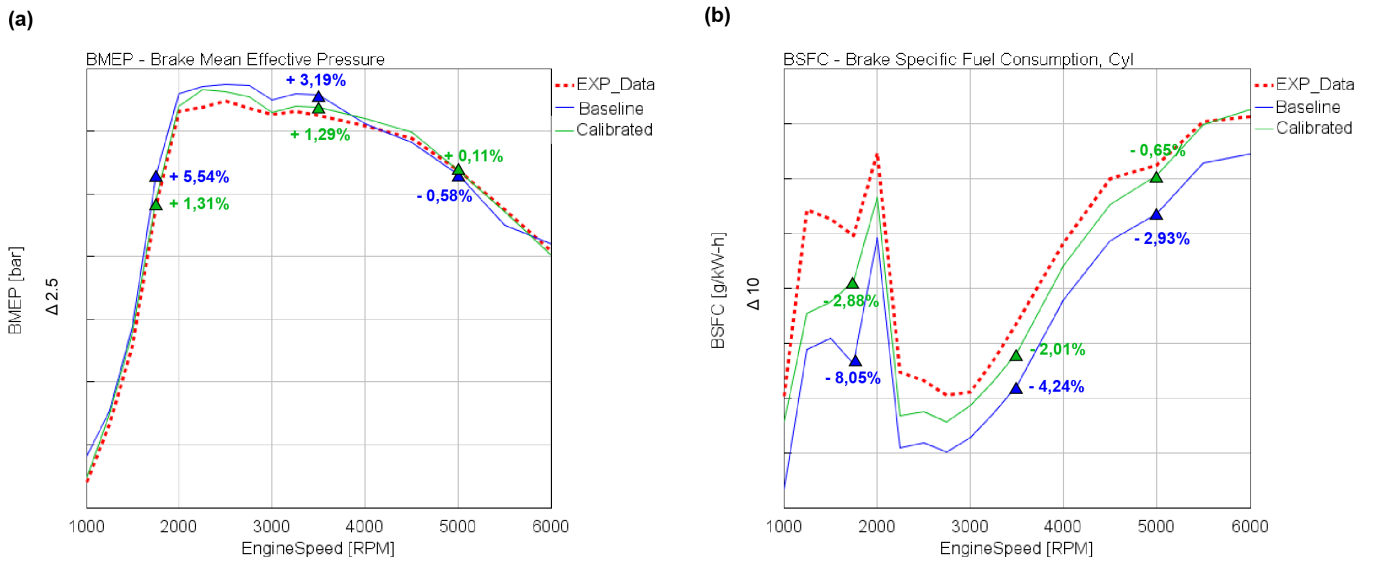


Figure 4.17 Comparison between experimental data (dashed red), the baseline model (blue) and calibrated one (green) on the BMEP(a) and BSFC (b)

4 - GSE-T4 Model calibration

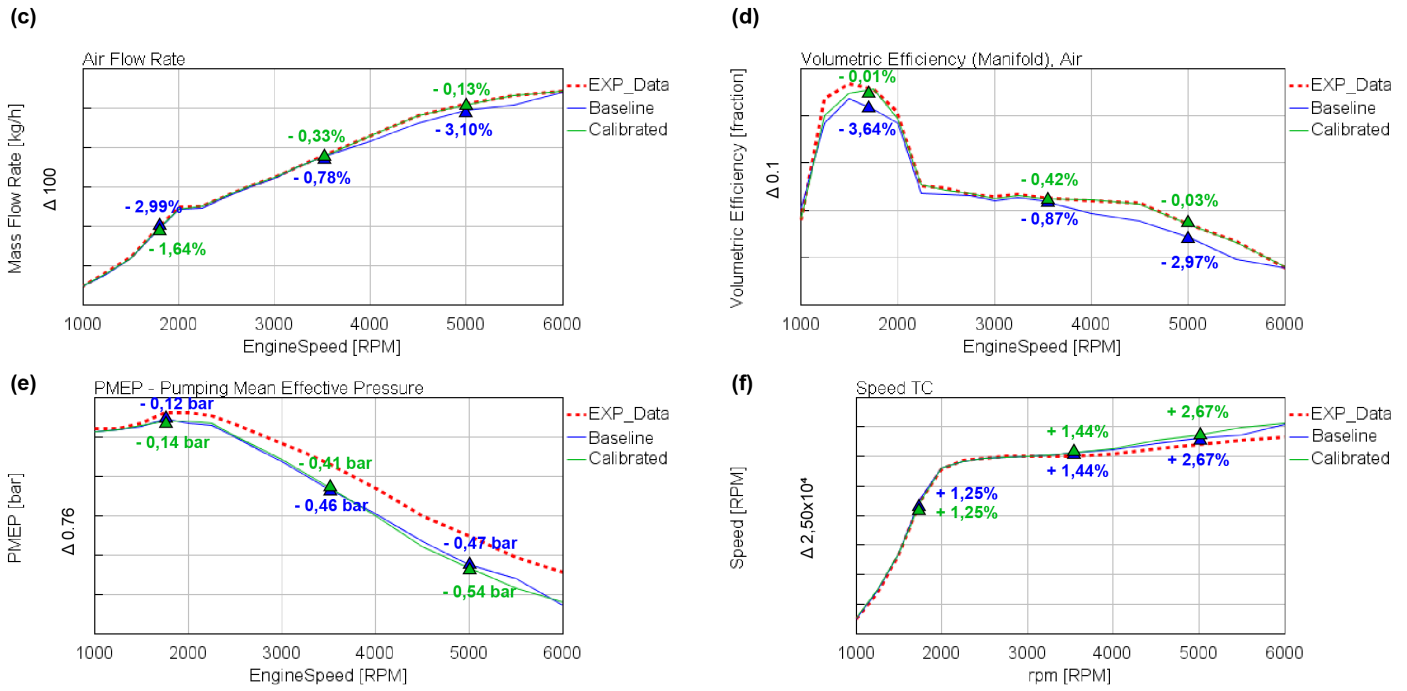


Figure 4.18 Comparison between experimental data (dashed red), the baseline model (blue) and calibrated one (green) on the Air mass flow rate (c), volumetric efficiency (d), PMEP (e) and speed of TC (f)

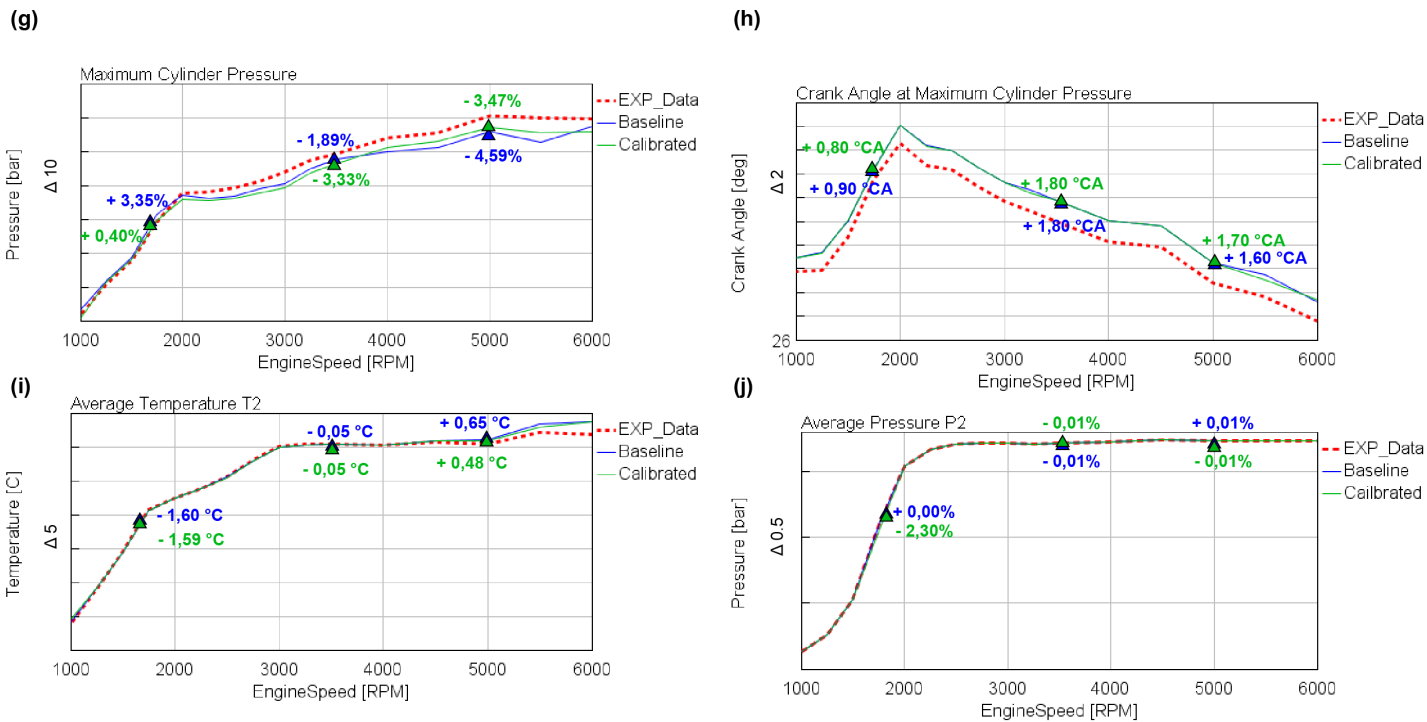


Figure 4.19 Comparison between experimental data (dashed red), the baseline model (blue) and calibrated one (green) on the Maximum cylinder pressure (g), crank angle at maximum cylinder pressure (h), temperature T2 (i) and boost pressure (P2)(j)

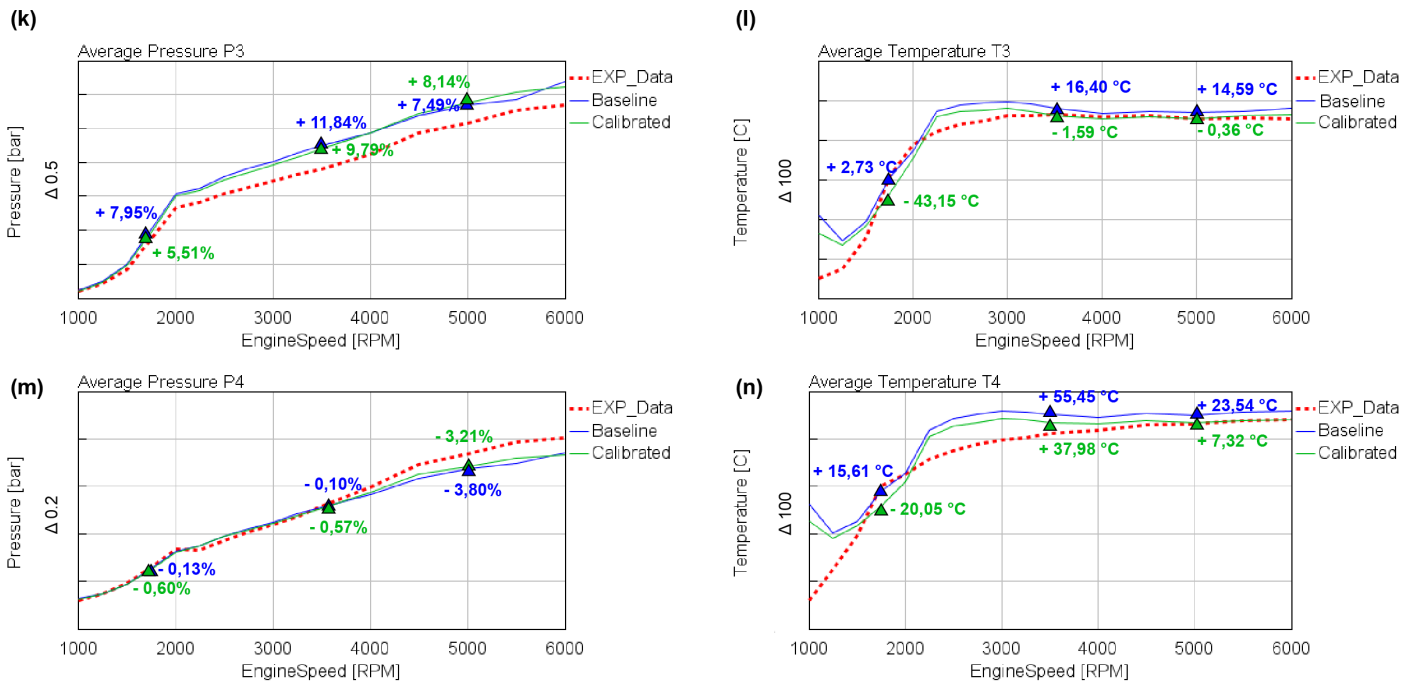


Figure 4.20 Comparison between experimental data (dashed red), the baseline model (blue) and calibrated one (green) on the pressure P3 and P4 and for the temperatures T3 and T4

From what can be seen from figure 4.17 (a) the BMEP follows the experimental curve although it is always higher up to 4000 rpm and then becomes lower just in the arc of the curve where lower volumetric efficiency can be seen. The BSFC (figure 4.17 b) is quite lower than the experimental one for the whole arc of the curve with 9% peaks around 1250 rpm. While P3 (figure 4.20 k) is consistently higher than the experimental model as is T3 (figure 4.20 i).

Since the baseline model was built on the basis of a full load test, the baseline model first simulation did not deviate much from the experimental data. For this reason, it was decided not to act on the calibration parameters such as the overall convention multiplier and heat transfer coefficients. Especially the former, by reducing the exhaust gas enthalpy and thus the energy available to the turbine, did not allow boost pressure to be achieved at various operating points in the engine map.

As for combustion, the baseline model provided already calibrated parameters. The trend of the maximum chamber pressure is well followed even if it tends to deviate a bit toward the high rpm (figure 4.19 g), while the maximum pressure angle maintains a constant delta (figure 4.19 h), perhaps due to a possible shift in the dyno measurement. For the same reasons discussed earlier it was not deemed necessary to act on the calibration parameters of the Wiebe function.

To improve the baseline model, the remaining parameters were acted upon:

- Fraction of fuel burned: By decreasing the fraction of fuel burned from 1 to 0.975, it was possible to obtain a load and BSFC curve closer to the experimental one (figure 4.17) and at the same time a lower T3 (figure 4.20 i) approaching especially at high rpm. In order not to lose too much enthalpy upstream of the turbine, it was decided not to decrease this parameter further. From figure 4.21 it can be seen that the wastegate at the 1750 rpm point is completely closed, stating that the turbo

has reached the maximum possible boost. With a lower value of fraction of fuel burned it would not have reached the target boost.

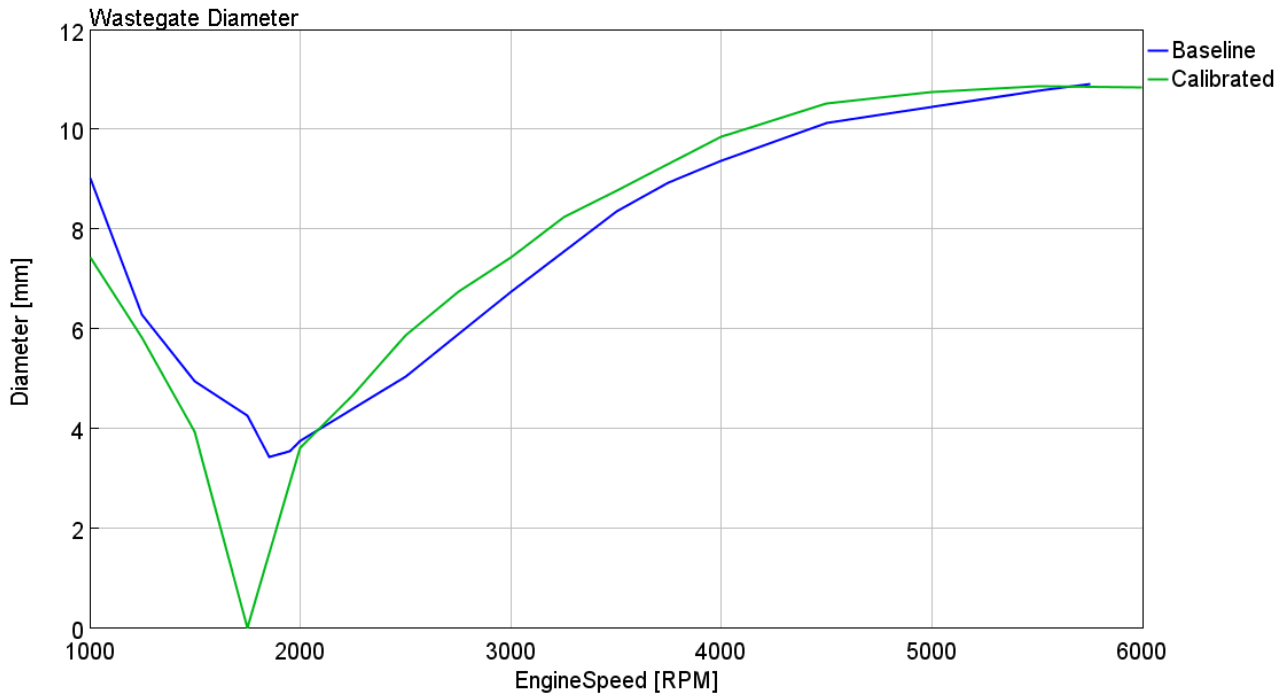


Figure 4.21 Wastegate diameter trend in baseline and calibrated model: it's possible to note how at 1750 rpm the wastegate is completely closed to have the maximum boost

- IVO and IVC: By slightly varying the opening and closing anchors of the inlet valves it was possible to obtain a volumetric efficiency curve and air flow rate as close as possible to the experimental one especially from 4000 rpm onwards thus also improving the load curve. Variations were performed through small full-factorial DOE for each operating point (table 4.6).

Table 4.6 Example of a small full-factorial analysis on IVO and IVC to match the volumetric efficiency and air flow rate

Case	IVO	IVC	Volumetric Efficiency deviation	Air mass flow rate deviation
1	275	570	+3%	+3%
2	275	574	+3%	+2%
3	280	570	+1%	+1%
4	280	574	0%	0%
5	285	570	-2%	-2%
6	285	574	-9%	-3%

- Turbine mass multiplier: An increase in volumetric efficiency caused P3 to rise further, to lower this value scaling the turbo map slightly helped. Despite this, the value of P3 still remains much higher than the experimental value, but increasing this value further means worsening the performance of the turbo compressor, which can no longer maintain the target boost pressure (wastegate totally closed).

It can be noted how PMEP at high rpm is nowhere near the experimental curve and the same for T3 at low rpm especially in the strange case of 1000 rpm where the curve does not follow the experimental trend. Further investigation may be needed to better understand these divergences.

4.4 Part load calibration

As far as part load points are concerned, the operating points (figure 4.22) were chosen based on an initial estimate of the operation of the PHOENICE vehicle. Precisely, the low rpm region of the engine map was considered, and the points were chosen uniformly. This is because it is expected that in the approval cycles the engine will operate mainly in this region.

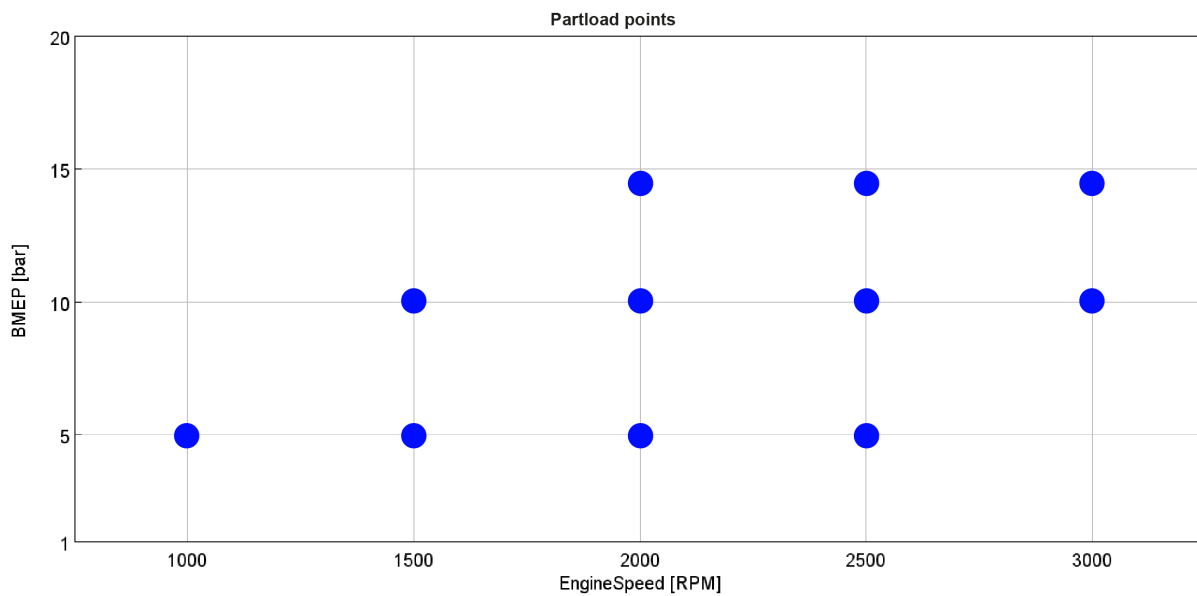


Figure 4.22 Part load operating point chosen

At part load points, the load is usually managed in the model by a PID controller acting on the throttle valve. Here too, the valve is not physically modelled, but the controller acts on the orifice diameter by decreasing it when necessary to match the load demand by reducing the air mass flow rate. This controller will operate simultaneously with the wastegate controller.

4.4.1 Calibration methodology and results analysis

In the following figures are showed the results of the part load calibration.

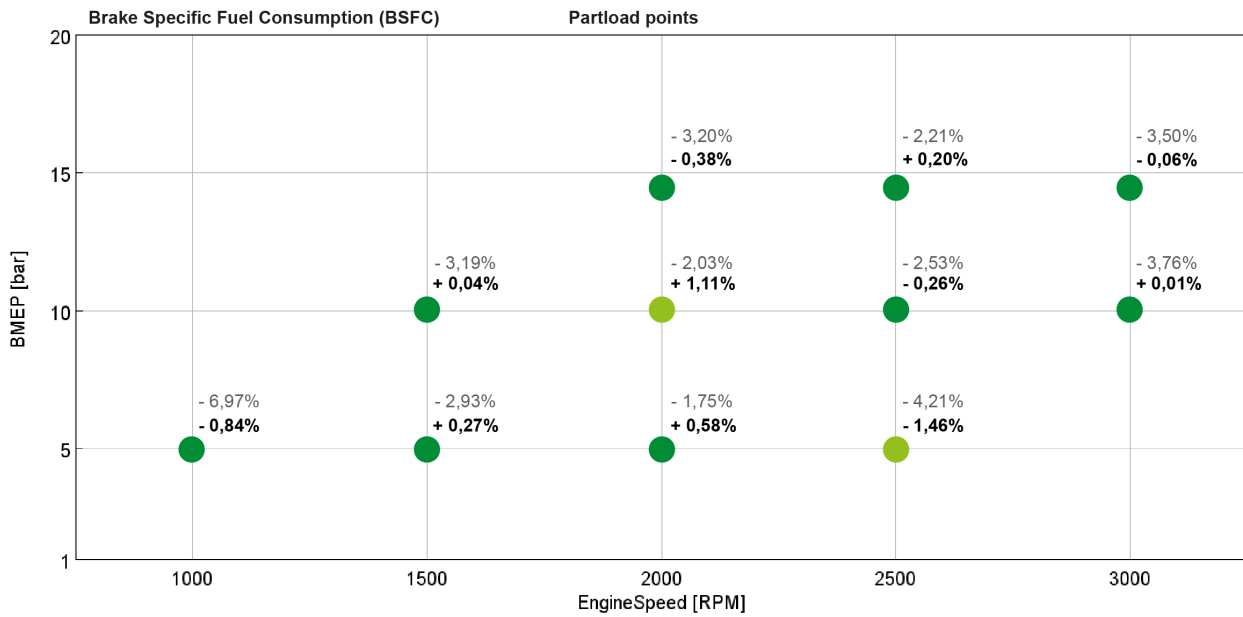


Figure 4.23 BSFC improvements respect the first attempt results, it's possible to notice that all the operating points were more efficient respect the experimental data. Errors are shown in percentage delta compared to the experimental data.

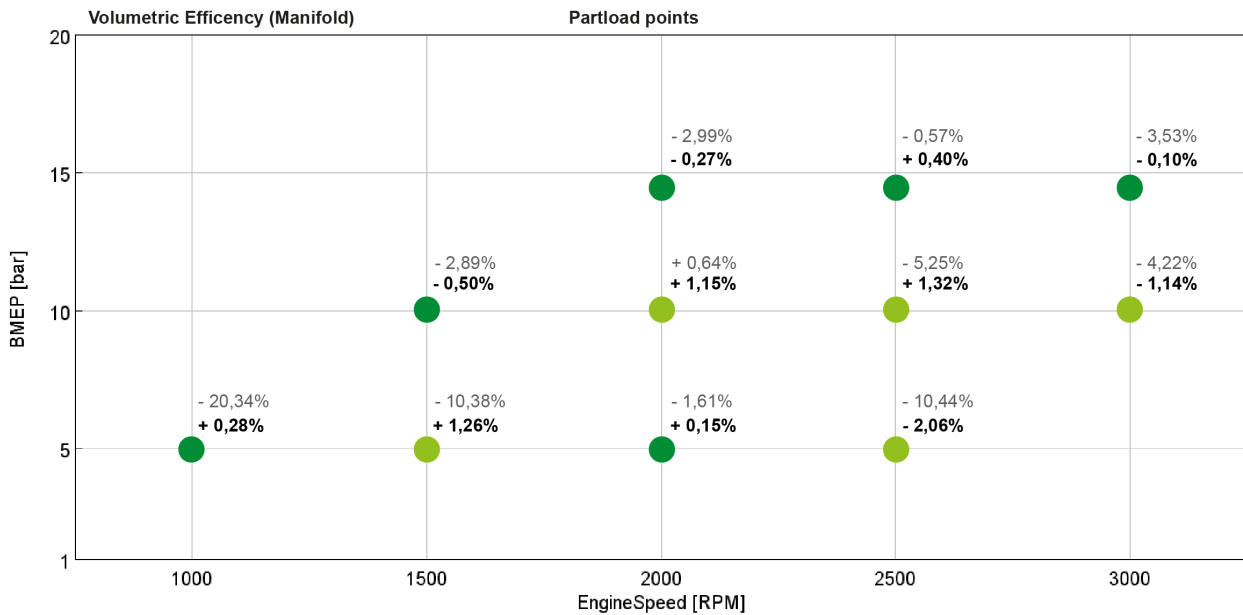


Figure 4.24 Volumetric efficiency improvements respect the first attempt results. Errors are shown in percentage delta compared to the experimental data.

4.4 - Part load calibration

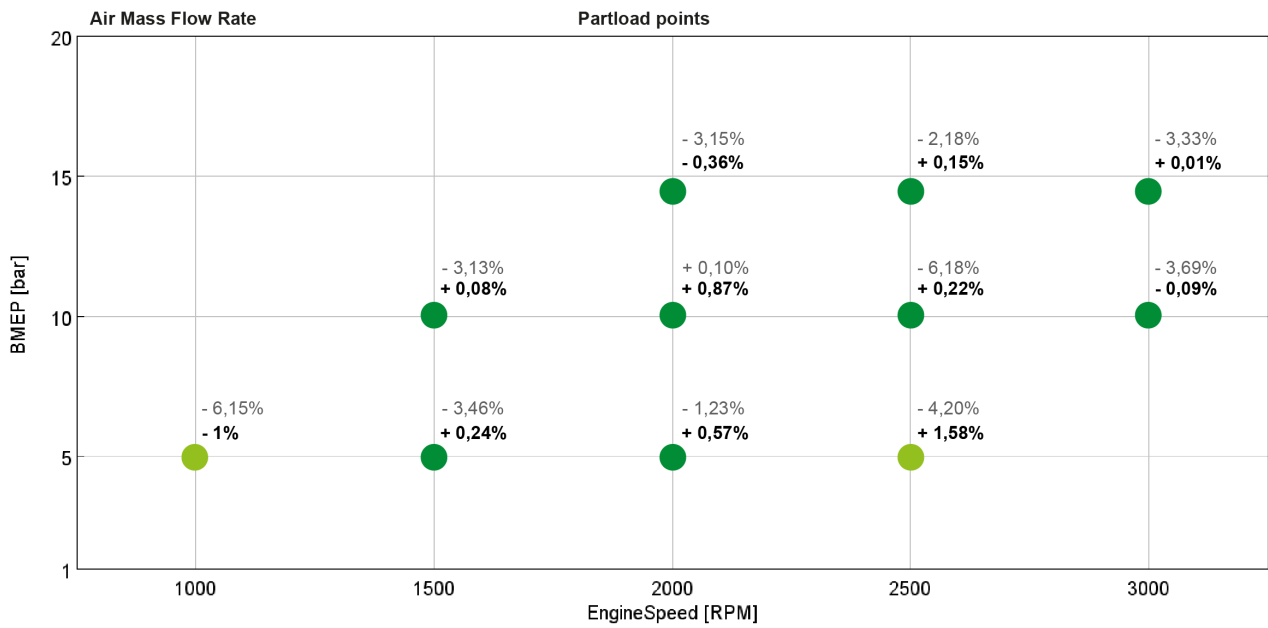


Figure 4.25 Air mass flow rate improvements respect first attempt results. Also from here It can be noticed how much the first attempt is more efficient respect the experimental data. Errors are shown in percentage delta compared to the experimental data.

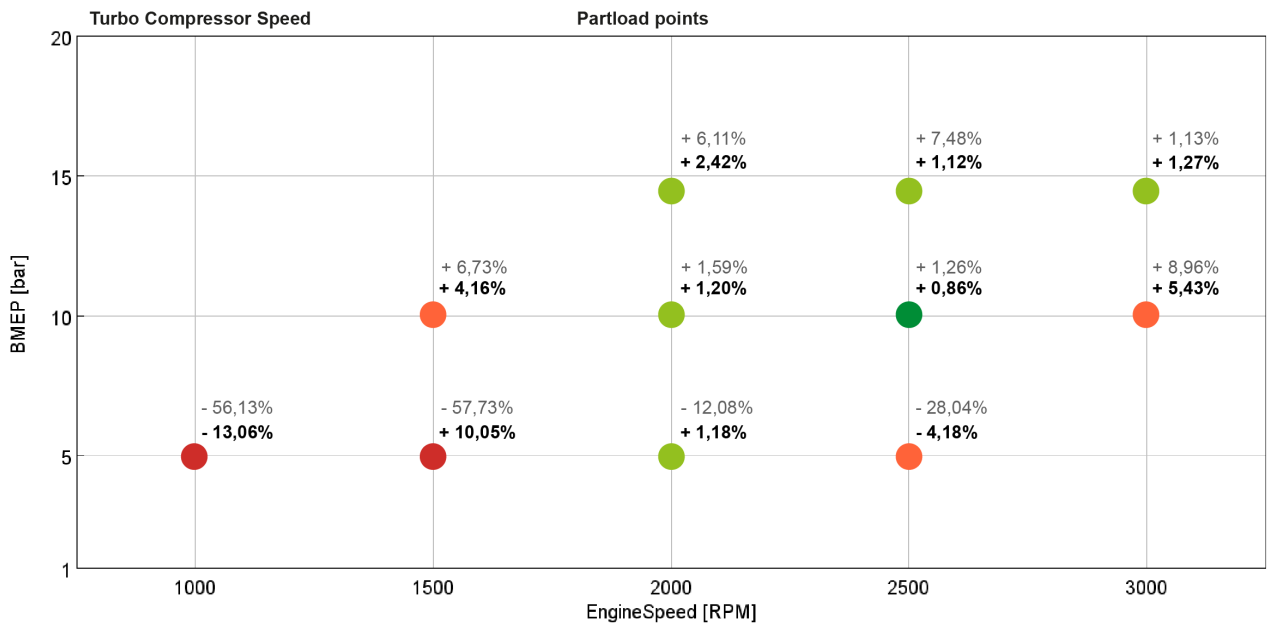


Figure 4.26 Turbo compressor speed percentage deviation respect experimental data. It can be notice how in some point the first attempt was quite far from the reality

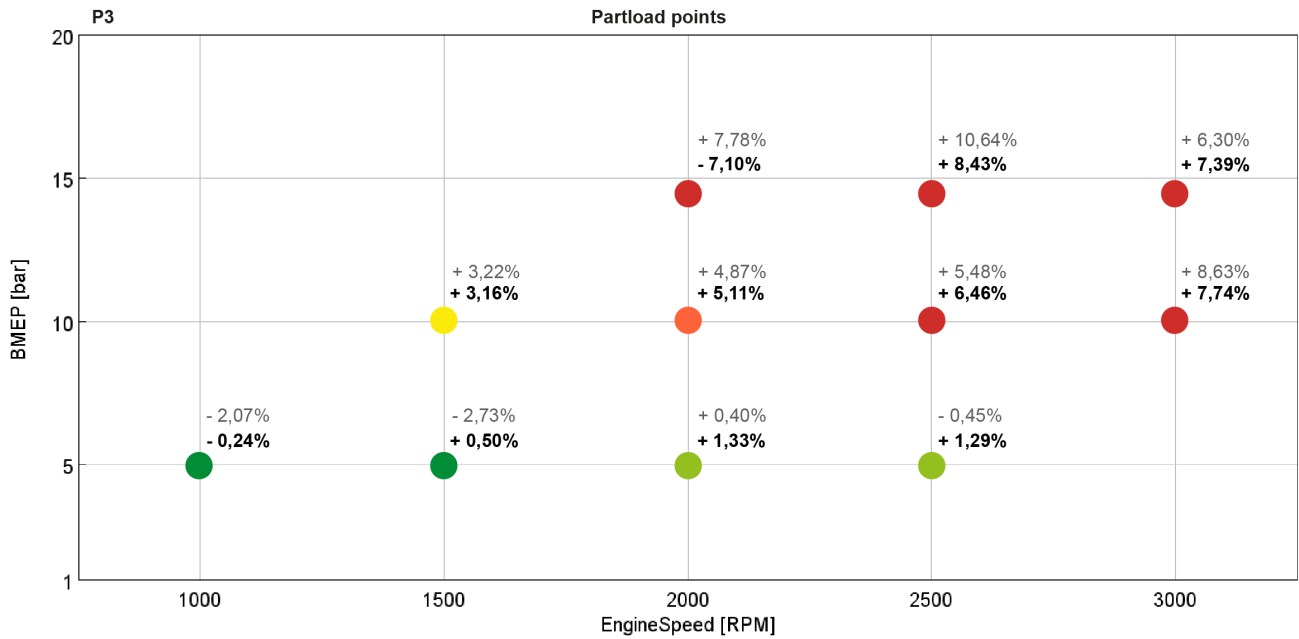


Figure 4.27 P3 deviation in percentage respect experimental data. It can be noticed how the trend is similar to the full load calibration where P3 deviate as much load and speed are increased

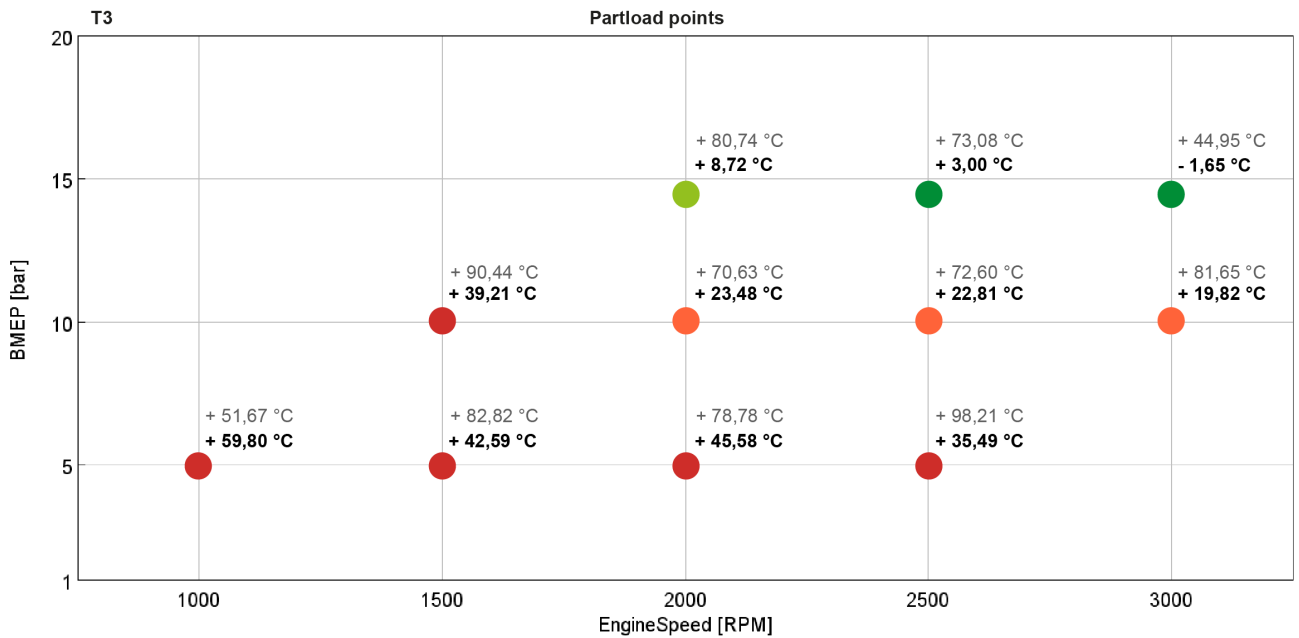


Figure 4.28 T3 deviation in absolute values respect the experimental data. The first attempt predicted a significantly higher exhaust gas temperature than was actually the case. After calibration at some points this delta was reduced considerably if not almost to zero.

4.4 - Part load calibration

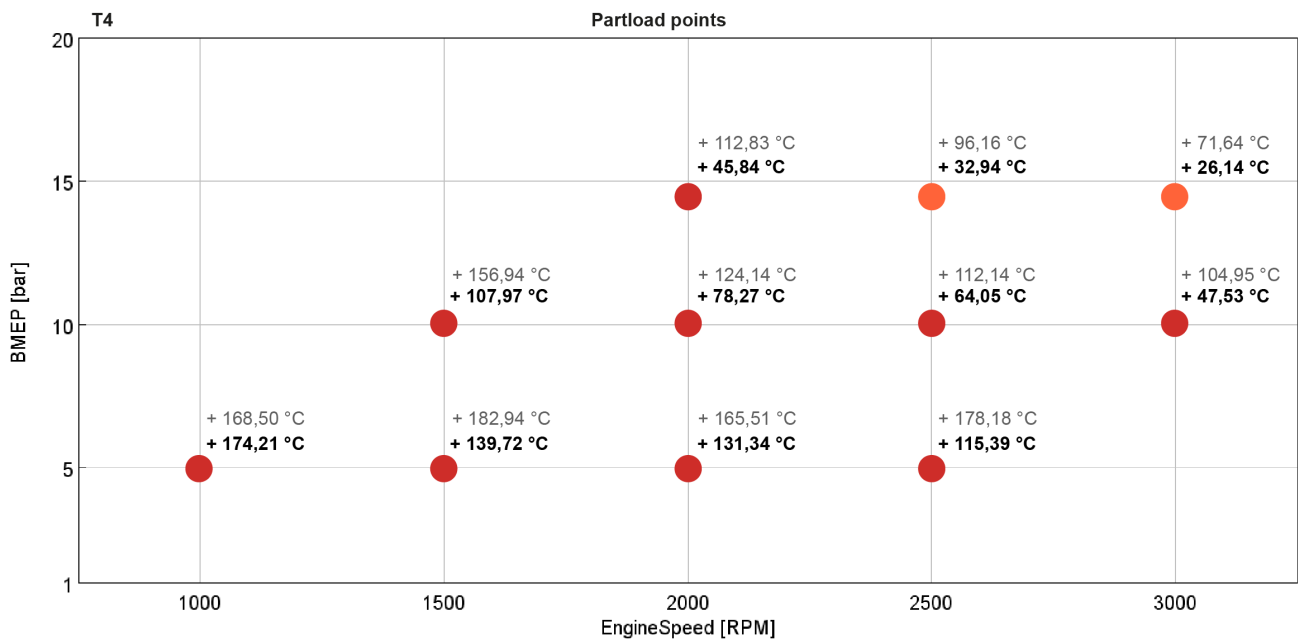


Figure 4.29 T4 deviation in absolute values respect the experimental data. It can be noticed how the model predicts far less cooling of exhaust gases than in reality. This could be partly explained by a position of the sensor further downstream of the turbine than where it was considered in the model.

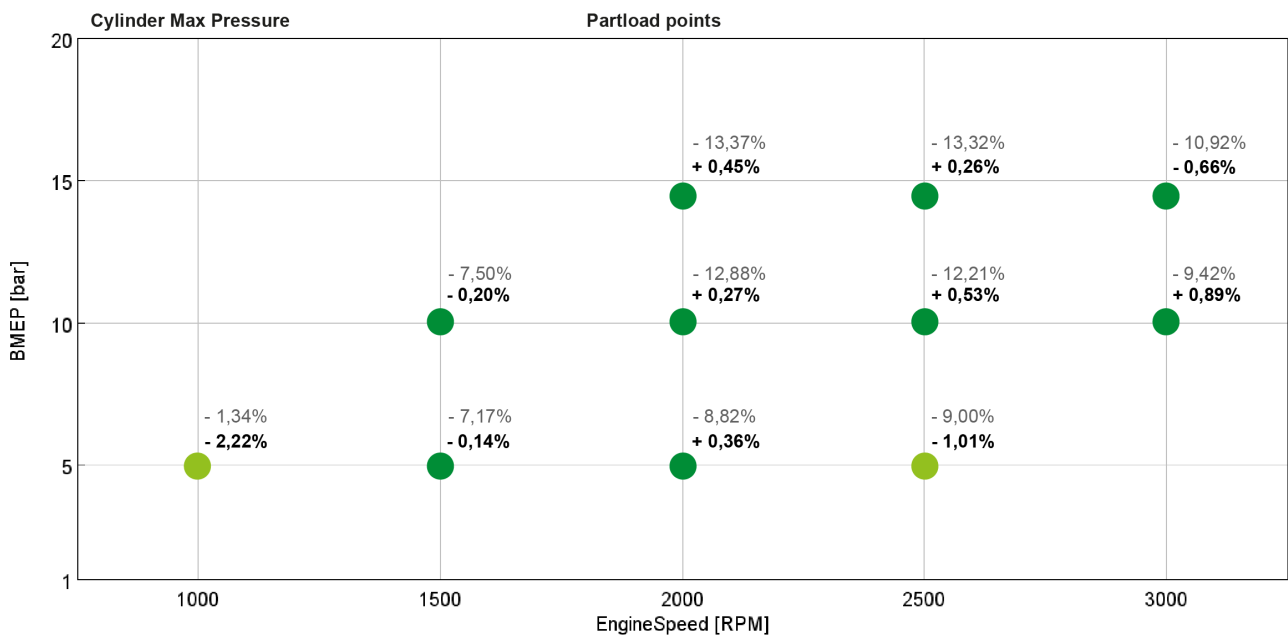


Figure 4.30 Max cylinder pressure error percentage deviation respect the experimental data. After calibration of combustion parameters, the maximum cylinder pressure is almost equal to the real one

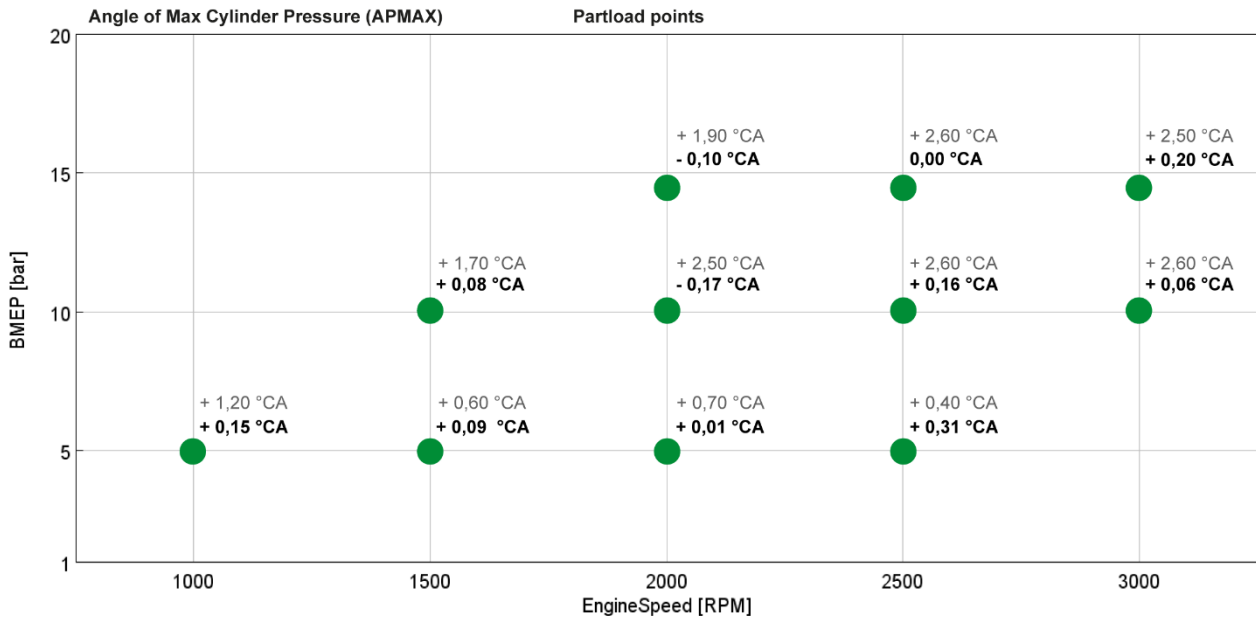


Figure 4.31 Angle of max cylinder pressure deviation in absolute value respect the experimental data. After calibration

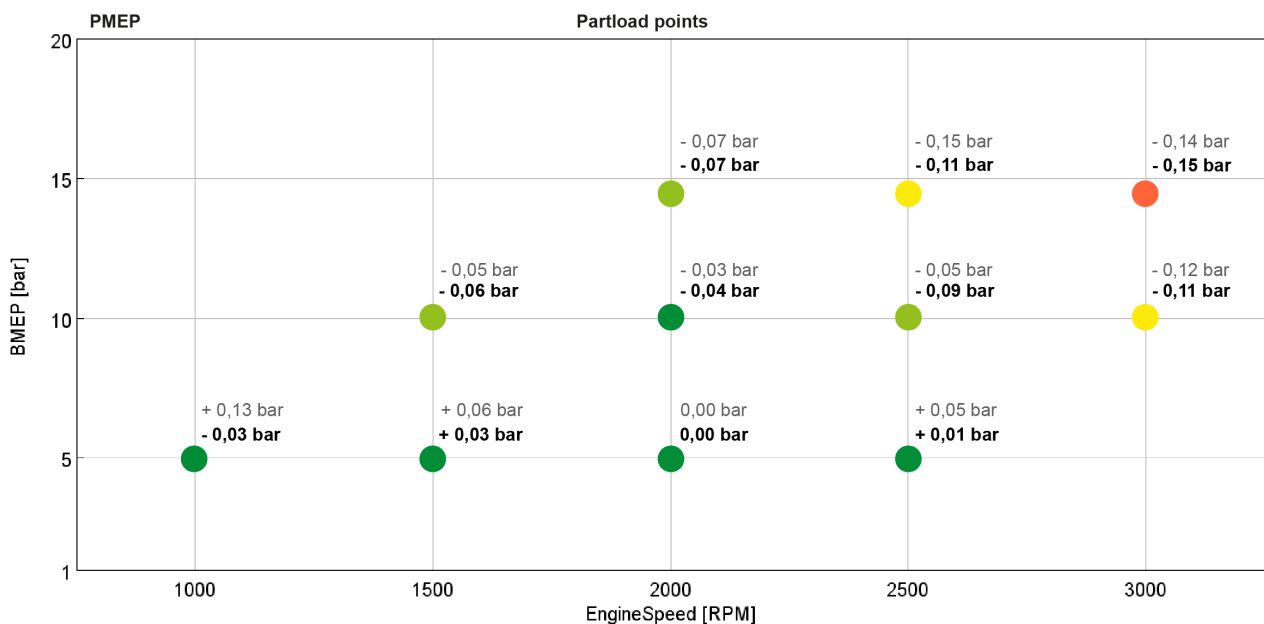


Figure 4.32 PMEP deviation in absolute vales from experimental ones.

In this case the effort in terms of calibration was much more demanding. In fact, with the input parameters taken from the experimental data, a large divergence compared to the bench test was found. In some cases, the throttle controller could not even match the required load, and the same happened with the wastegate controller in the case of boost. After calibration in all cases the controllers manage to match the two required parameters. The most critical value is definitely T3 and then T4 (figure 4.28 and 4.29). The model predicts less loss in terms of waste heat than in reality and especially less temperature loss downstream of the turbine. While the latter can be explained by the fact that the sensor was placed further downstream than the flow split considered in the model, T3 depends very much on the losses in heat transfer in the combustion chamber.

The calibration strategy for each operating point was set up as follows:

1. In a first step a full-factorial DOE with IVO and IVC parameters was performed around the ECU parameters in order to be able to match target BMEP and experimental boost pressure (in the graphs above, the first attempt results refer precisely to the condition in which BMEP and boost pressure are matched in order to have a fair comparison).

Table 4.7 Example of how changing IVC, the BMEP and boost targets can be matched both in the operating point considered. *These angles refer to the one suggested by ECU data

Case	IVO	IVC	BMEP deviation	Boost pressure deviation
1	324*	653*	-7%	0%
2	324	630	0%	-5%
3	324	640	0%	0%

In table 4.7, it can be seen that in order to reach the BMEP target, the IVC had to be reduced. By analysing the flow in the cylinder (figure 4.33), it can be seen the amount of back flow (air leaving the cylinder and returning to the intake manifold) due to the excessive delay in closing the intake valve.

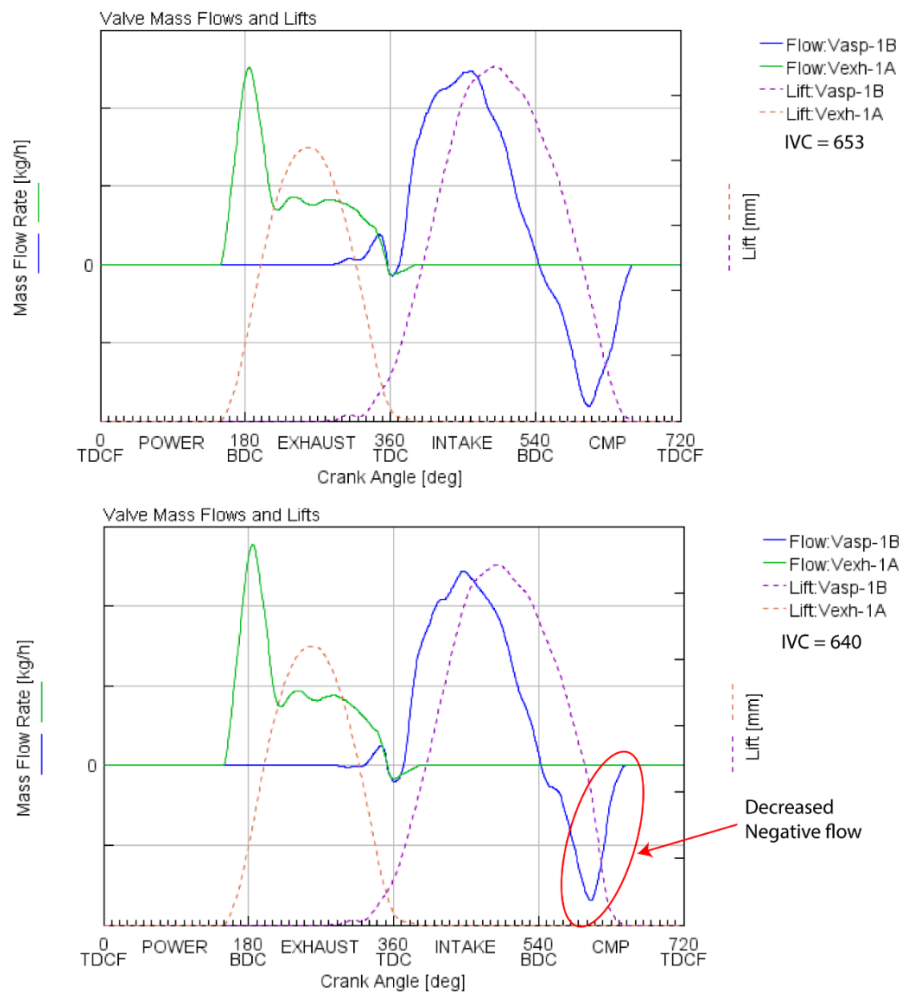


Figure 4.33 Graph of mass flow rate and valve lift vs crank angle degrees in one cycle. In green the flow across the exhaust valve is depicted and in blue the mass flow across the intake valve. It can be noticed how anticipating the IVC the back flow decrease

This phenomenon limits the maximum achievable air flow rate and thus the maximum achievable load despite the throttle valve being fully open. Conversely, an IVC that is too early leads to having to close the throttle valve too much, thereby increasing the pressure drop across the valve itself. This forces the turbocharger to generate even more boost (wastegate closes) to achieve the same target boost downstream of the throttle until the maximum boost is reached for the same operating point (wastegate fully closed) (table 4.8).

Table 4.8 Example of some results obtained changing the IVC: anticipate too much the IVC bring to an excessive pressure drop across the throttle valve

Case	IVO	IVC	Pressure drops across throttle valve (bar)	Wastegate diameter (mm)	Throttle orifice diameter (mm)
1	324	635	0.15	0	12
2	324	640	0.09	2.3	20

- Once a pair of IVO and IVC values satisfying BMEP, boost pressure and volumetric efficiency was obtained, the overall convection multiplier was acted upon. Compared to the full load calibration, it was preferred to act on this parameter with respect to the fraction of fuel burned because it allowed the gas temperature to be drastically lowered without excessively affecting the combustion efficiency and thus the BSFC. Whenever this parameter was raised, the energy of the exhaust gas upstream of the turbine decreased and thus the maximum boost pressure guaranteed by the compressor. In addition, the combustion efficiency decreases, and the air flow required to achieve the same load increases and consequently the throttle valve opens more. For this reason, a further variation of IVO and IVC may have been necessary. Once a configuration that met the BMEP, pressure and volumetric efficiency targets was found, if the T3 temperature was higher and the BSFC lower than the experimental ones, a further increase of the convection multiplier could be attempted. This was done until the BSFC value matched the experimental one (table 4.9) and the model was able to guarantee the target BMEP and boost pressure.

Table 4.9 Example of how the overall convection multiplier influence the BSFC and the temperature upstream turbine: in that case the value 1.4 allow to match the BSFC with a satisfactory temperature delta respect the experimental one

Case	Convection multiplier	IVO	IVC	BMEP deviation	BSFC deviation	Delta T3 deviation (°C)
1	1	324	640	0.0%	-3.8%	+81.7
2	1.2	324	640	-3.3%	-0.7%	+35.8
3	1.2	324	632	0.0%	-1.2%	+40.9
4	1.4	324	632	0.0%	-0.1%	+20.4
5	1.5	324	632	0.0%	+1.5%	+6.9

Acting in this way at each operating point coincided with an optimal convection multiplier value (figure 4.34). To ensure robustness of the model and thus the possibility of obtaining satisfactory results at other operating points as well, by interpolation the following law was formulated as a function of load and engine rpm:

$$\text{Convection Mult.} = 1 + (n/1000) * 0.091125 + \text{BMEP} * 0.013$$

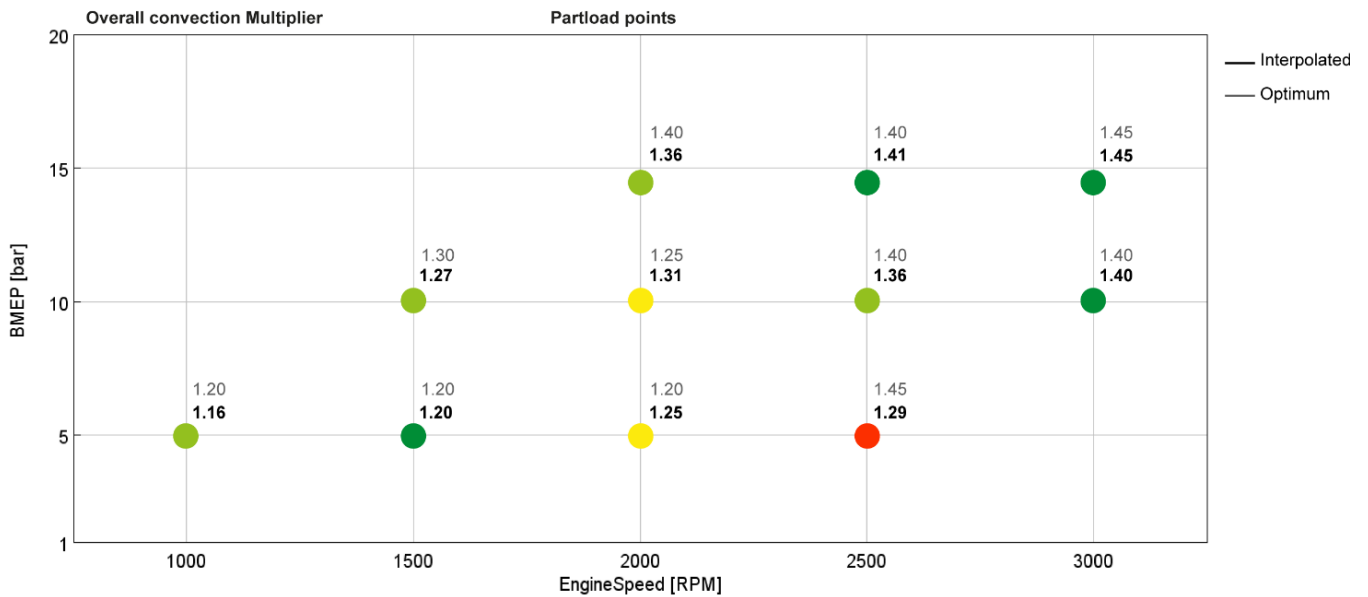


Figure 4.34 The overall convection multiplier defined with the above expression compared to the optimal value founded through the calibration procedure. A great deviation is present only on the 2500x5 point

The only point that does not follow the trend is the 2500 rpm at 5 bar, but even with a lower value than the optimum, there was a lower absolute error in T3 than the other points at 5 bar but a slightly lower BSFC than the experimental one.

- The third step involves calibrating the maximum pressure inside the cylinder and the angle at which the peak is present. To match these data, the Wiebe parameters (table 4.10) were manually intervened. Increasing or decreasing the MFB50 respectively resulted in a pressure peak farther or closer than the top dead center (TDC), while decreasing or increasing the combustion duration resulted in a higher or lower pressure.

Table 4.10 Example of combustion parameter tuning to match max cylinder pressure and angle of peak pressure

Case	MFB90-10	MFB50	Max cylinder pressure deviation	Angle of peak pressure deviation
1	23.01	7.55	-9.4%	20.4%
2	25.01	4.45	0.9%	0.3%

Of course, these parameters also had minor influences on all the other validation variables, so the strategy did not necessarily follow this linear path but could retrace one of the steps several times.

As for P3, the trend remained the same as for Full Load calibration: the divergence becomes more noticeable as rpm and load increases (figure 4.27), while other values such as pumping losses (figure 4.32) were found to be not too affected by the calibration parameters.

The results of this calibration can be considered sufficient to be able to make an initial setup of the HiL bench since the plant model will then be updated with a representative model of the PHOENICE engine, which as mentioned above, anticipates the integration of many features aimed at increasing the overall efficiency of the engine.

5 Implementation of the PHOENICE features

5.1 Model updates

In this chapter, the pre-calibrated model is updated with PHOENICE features, and an initial optimization is performed to evaluate the theoretical benefits in terms of fuel reduction and thus GHG emissions. The optimization consists of analyzing possible valve timing strategies in a model that carries numerous updates:

- The compression ratio is increased from 10.5 to 13.5.
- A long-pressure EGR loop is introduced that allows exhaust gases downstream of the turbine to re-enter the loop before the turbo compressor and then finally return to the combustion chamber (figure 5.1). This loop differs from the high-pressure loop, which instead takes exhaust gases upstream of the turbine and brings them downstream to the compressor (figure 5.2).

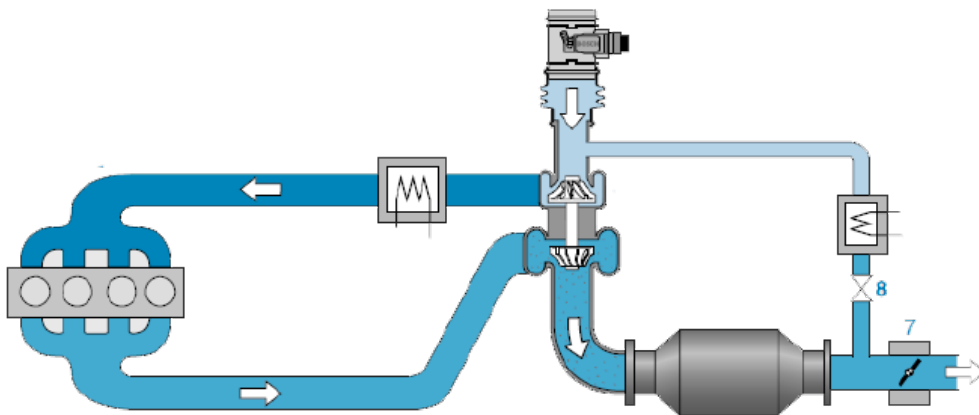


Figure 5.1 Example of low pressure EGR loop

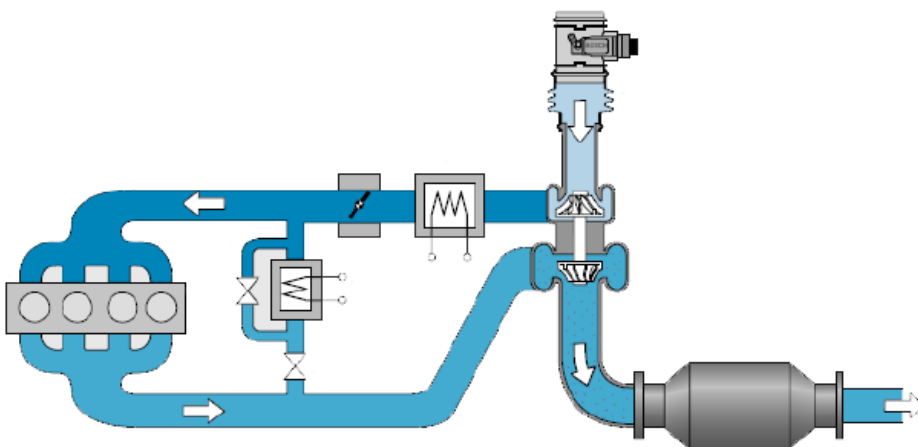


Figure 5.2 Exampre of high pressure EGR loop

- The turbocharger changes types and maps. The Phoenix engine will be equipped with a variable geometry turbine (VGT).
- Lambda values will no longer be stoichiometric, but combustion will be lean with added EGR to take advantage of Dual Dilution Combustion Approach (DDCA).
- In this context, combustion will also be totally different due to the new Swumble™ concept. Since the data needed to simulate this new charge motion inside the cylinder will not be available, the burn rate profile derived from the first experimental bench data will be imposed. For this reason, optimization will focus only on the points that were investigated on the bench (Figure 5.3).

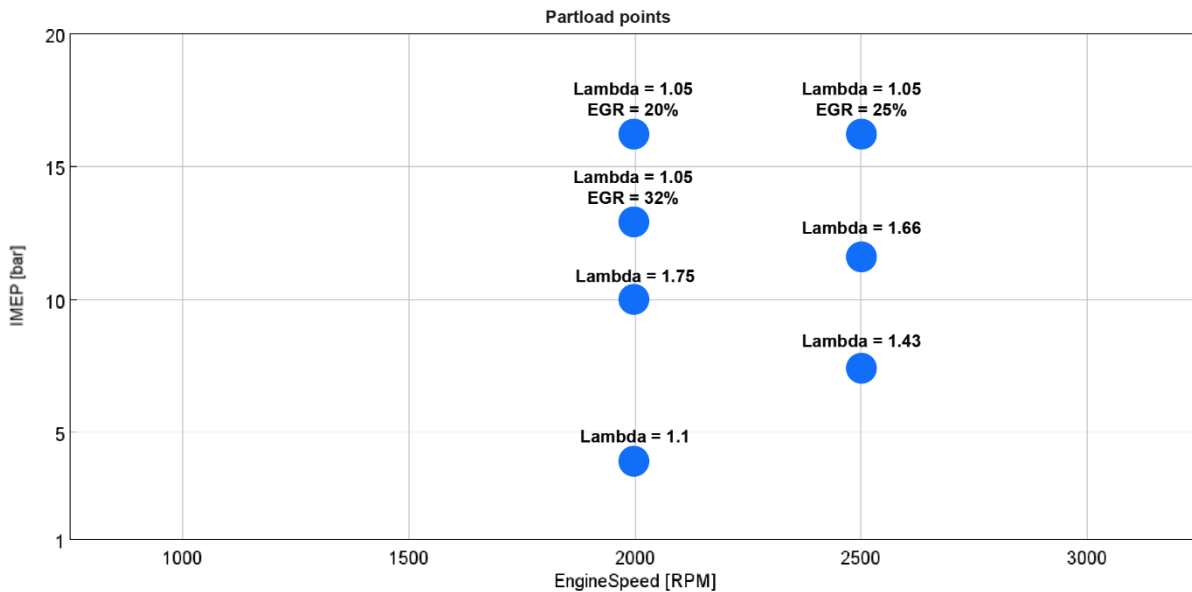


Figure 5.3 PHOENICE experimental data on which optimization is carried on

5.2 Control strategy definition

Since EGR was introduced, a new controller that regulates the EGR valve has been incorporated into the model. Furthermore, the VGT turbine allows more flexibility than a conventional turbine because it allows boost regulation without the losses associated with the wastegate valve. For this, a control strategy must be defined that regulates the behavior of the controllers within the model.

The idea for exploiting the VGT's potential to the full is to control the load by adjusting the rack of the VGT so as to avoid the losses due to the closing of the throttle valve. In reality, this type of strategy is followed, but in order to ensure a satisfactory transient response, it is preferred to maintain light control over the throttle valve as well. Even in the model, control via the VGT alone is not so accurate in matching the required BMEP (figure 5.4). For this reason, a multiplier to the BMEP target sensed by the VGT controller was applied so that the throttle control could also intervene to match the true BMEP value set.

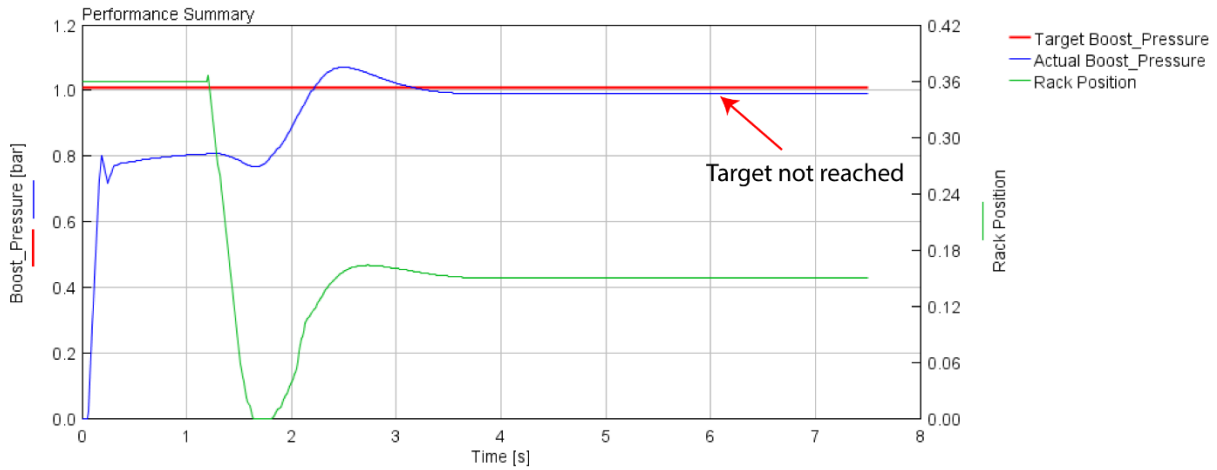


Figure 5.4 Example of problems in reach target BMEP of the VGT controller

Another factor to consider is the EGR flow, which is also very high at some operating points. Being a low-pressure loop, to guarantee a certain EGR flow the turbo compressor must guarantee a higher mass flow. For this reason, the VGT strategy must also take into account the amount of EGR required to match the experimental data (figure 5.5 and 5.6).

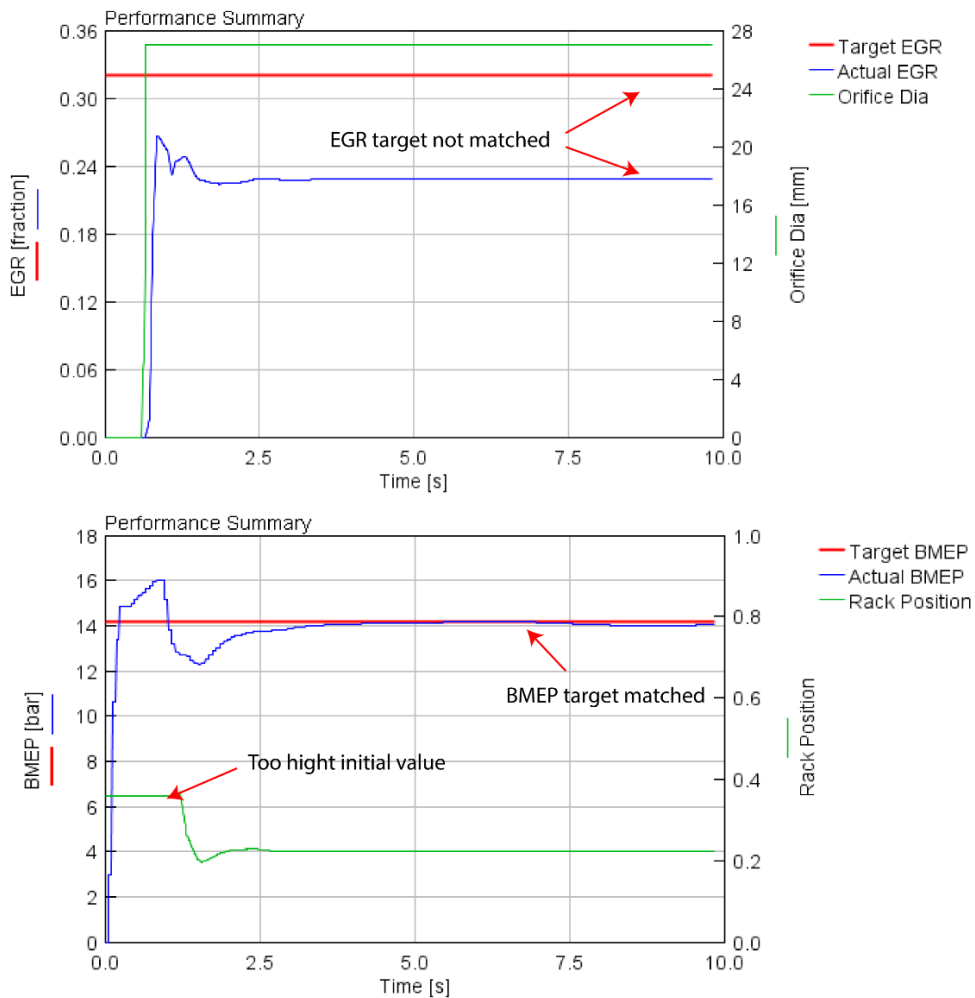


Figure 5.5 Case in which EGR fraction target can't be matched due to low total mass flow rate given by the turbine

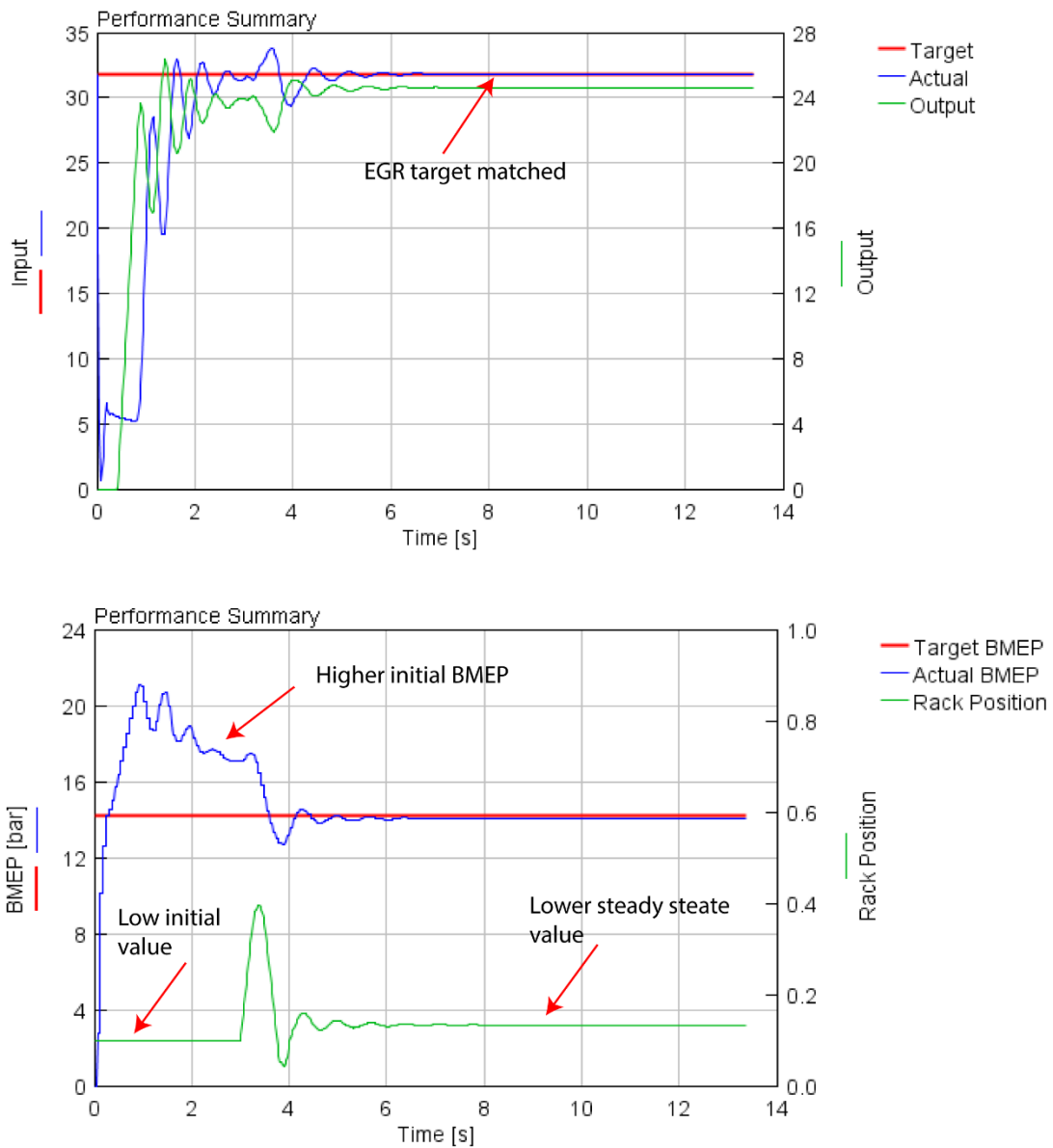


Figure 5.6 Example of how the problem of EGR matching is resolved: the rack of VGT is set to a initial very low value in a way to guarantee the correct mass flow rate. Then, when EGR target is matched, the VGT controller can start to regulate to match the target BMEP

GT-Suite allows the implementation of even sophisticated logic that allows controllers to interact during the simulation of an operating point. To implement the strategy described above, the logic described in figure 5.7 was implemented.

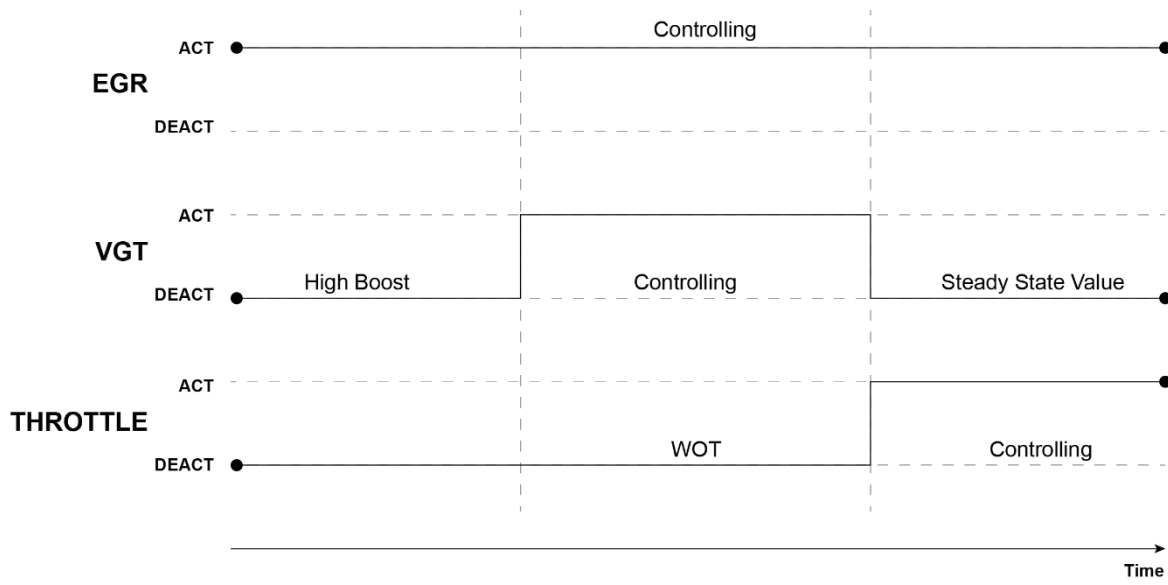


Figure 5.7 Controller strategy used for model optimization

Figure 5.8 shows the results of a simulation where all targets were matched.

5.2 - Control strategy definition

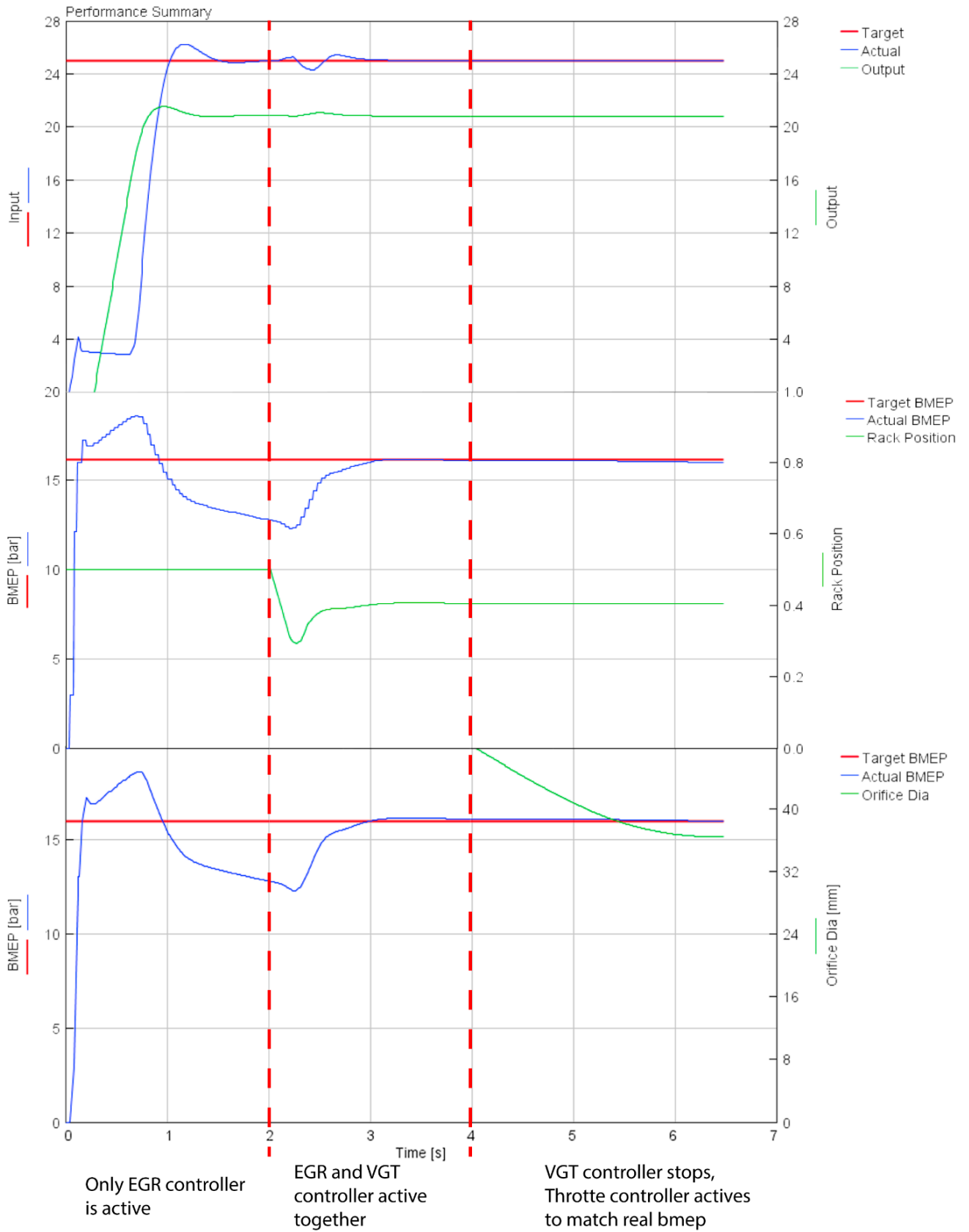


Figure 5.8 Results obtained with the previous explained strategy. It can be seen when the controller starts to work and when are deactivated

5.3 Optimization methodology

For each operating point a full factorial DOE was launched to investigate valve timing with IVO from 250° to 380° and IVC from 480° to 620° after TDC firing (i.e., after the piston has reached top dead center and combustion has occurred). The results can be divided into two main cases:

The points with load above 10 bar: these are characterized by either very lean combustion or high EGR flow. In both situations the required mass flow rate is significantly higher than in the stoichiometric case (or without EGR) and at the same time the exhaust gas temperature is significantly lower. This means less energy available to the turbine, which must also provide more mass flow rate. This results in a very high closure of the turbine blades that accelerate the flow but create high exhaust backpressure compared to less boost pressure.

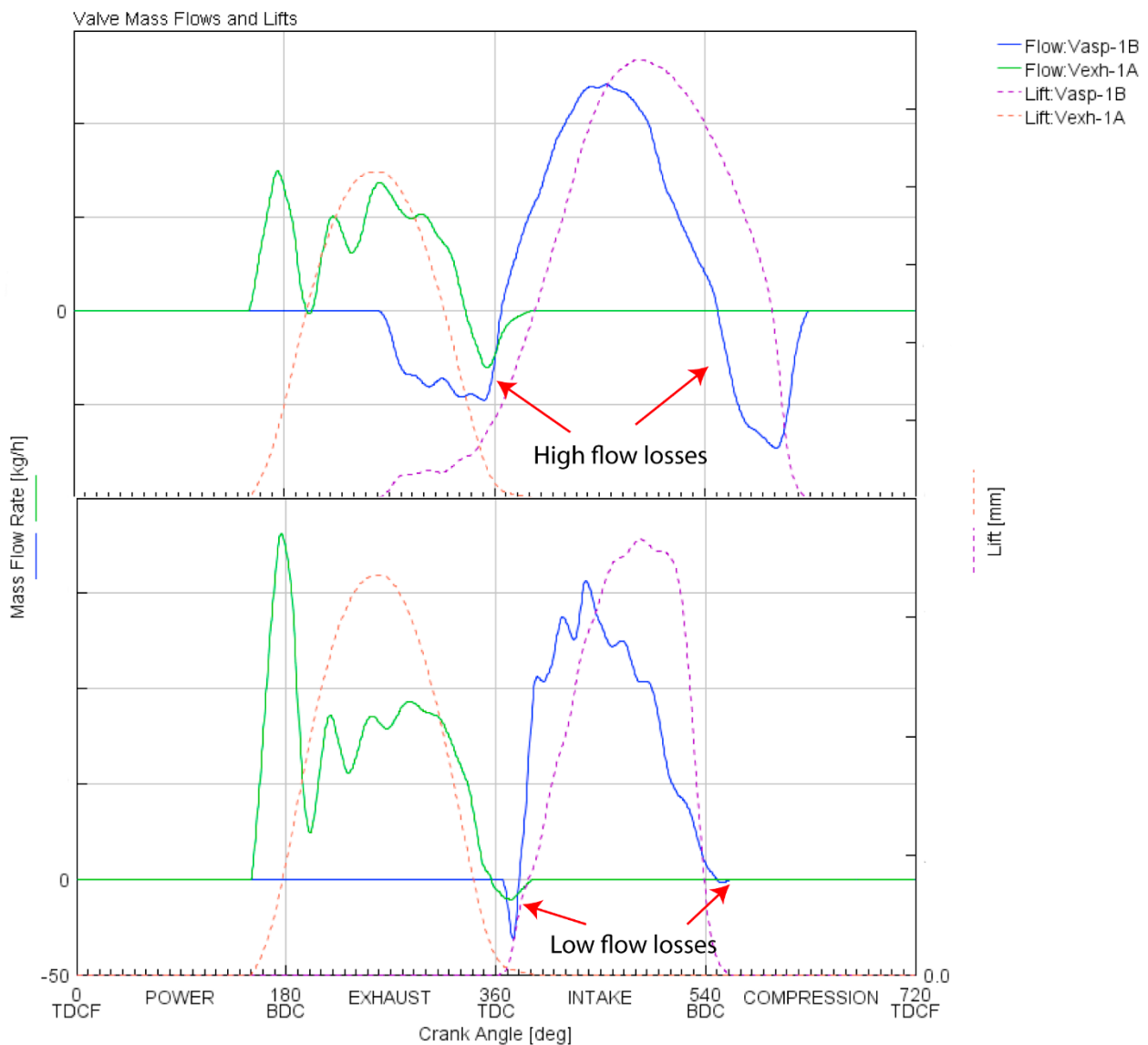


Figure 5.9 The upper graph shows how EIVO and LIVC are detrimental due to much air flow losses. This is caused by the higher exhaust-intake pressure delta. A more conventional strategy is illustrated in the below where the losses are much less

Going to analyze the mass flow rate values across the valves (figure 5.9) it is possible to see how much reverse flow is generated under these conditions. This disfavors the use of Miller timing (EIVC or LIVC) and valve overlap (EIVO) and that is why the lower BSFC in these cases coincides with IVO and IVC angles not too far from the TDC and BDC, respectively (figure 5.10).

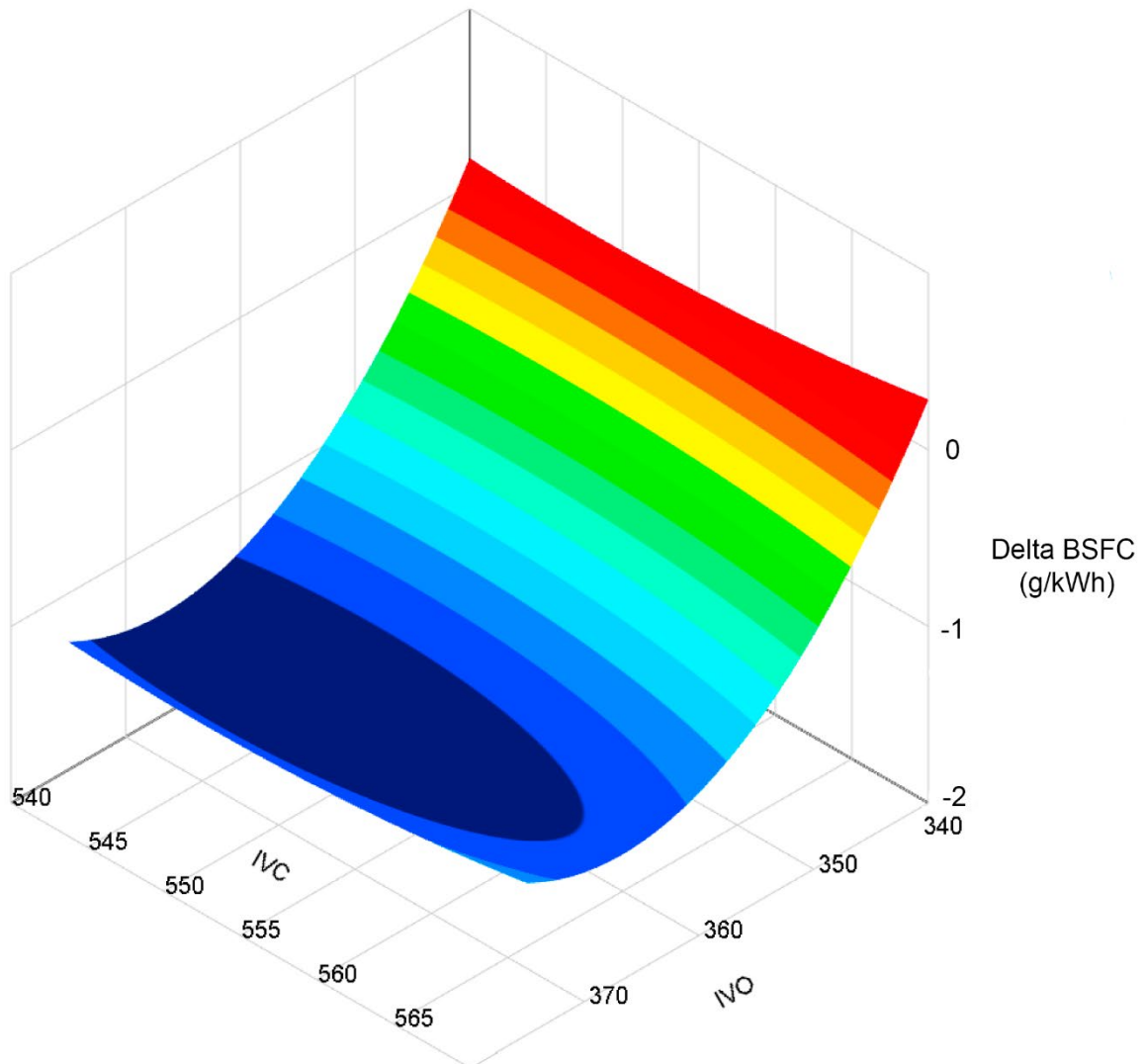


Figure 5.10 Results of full-factorial DOE analysis on IVO and IVC for a high load point (2000x14). It confirms that conventional timing angle guarantee the minimum BSFC. The graph is restricted to a narrow window of IVO and IVC due to the impossibility to match the target BMEP (engine in full-load condition) outside this region

Opposite case are the lower load operating points: In these cases, the EGR is not present and to achieve the required load the VGT fully opens the vanes to decelerate the flow and simultaneously the throttle valve also acts. The exhaust backpressure is no longer so high, and the timing millers (EIVC and LIVC) are both a suitable solution to reduce losses due to the throttle valve and thus reduce fuel consumption (figure 5.11).

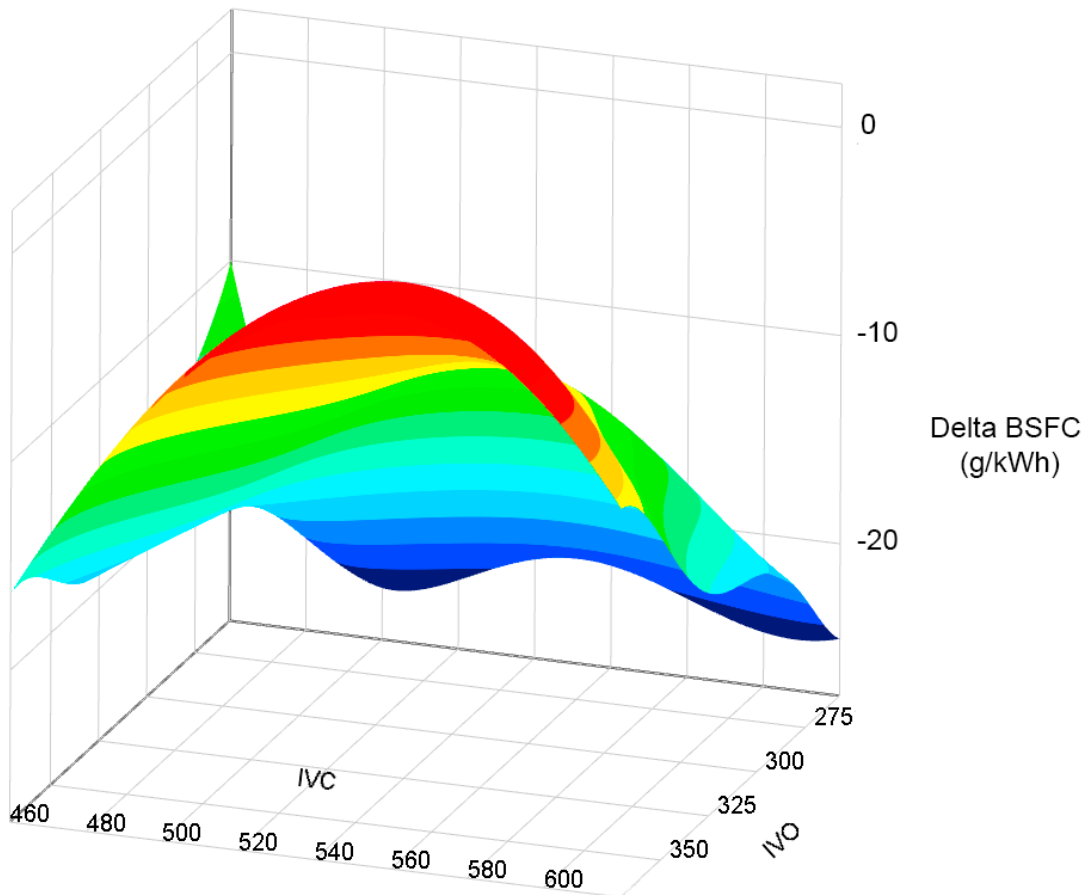


Figure 5.11 Results of full-factorial DOE analysis on IVO and IVC for a low load point (2000x5). It confirms that conventional timing angle guarantee the minimum BSFC

The IVO and IVC angles found to provide the lowest BSFC are shown in table 5.1.

Table 5.1 Optimized IVO and IVC angle for each operating point

Point	IVO	IVC
Rpm x BMEP	°CA after ftDC	°CA after ftDC
3000 x 16	350	550
3000 x 14	330	550
3000 x 7	260	600
2000 x 16	370	550
2000 x 14	370	550
2000 x 10	370	540
2000 x 5	257	600

As can be seen, only at the lowest load points (3000x7 and 2000x5) is it convenient to use an early IVO and a late IVC to decrease throttling, while the other operating points need to maximise the airflow inside the chamber in order to reduce the back pressure generated by the VGT as much as possible.

5.4 Results and analysis

After optimization of each operating point a comparison with the calibrated model of GSE-T4 can be appreciated in the following pictures.

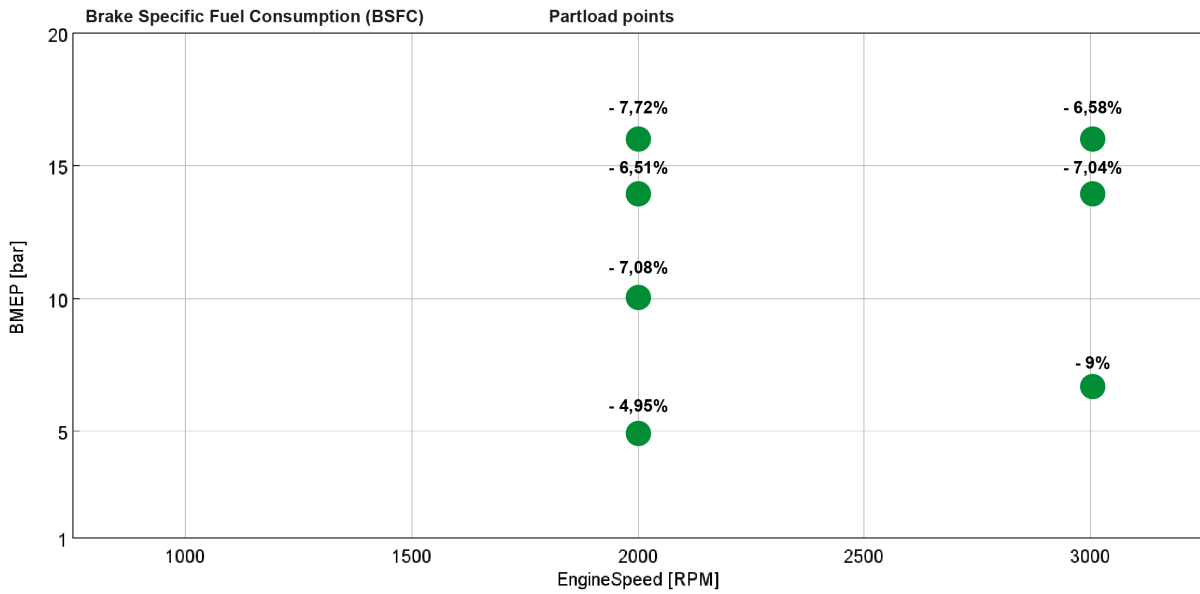


Figure 5.12 BSFC gain for each operating point: best results obtained in the 3000x7 point due to the combination of Miller timing and high charge dilution

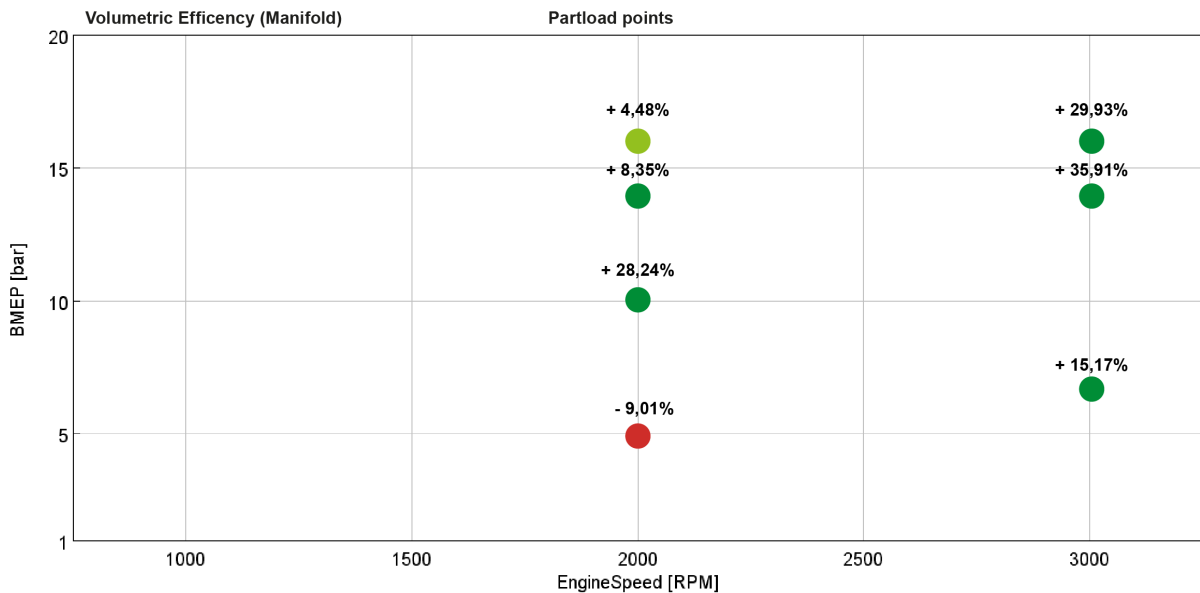


Figure 5.13 Volumetric efficiency in the manifold deltas: in this case the all mass flow rate (air + gases) is considered: the gain corresponds to all the point in which high dilution or high EGR rate is present

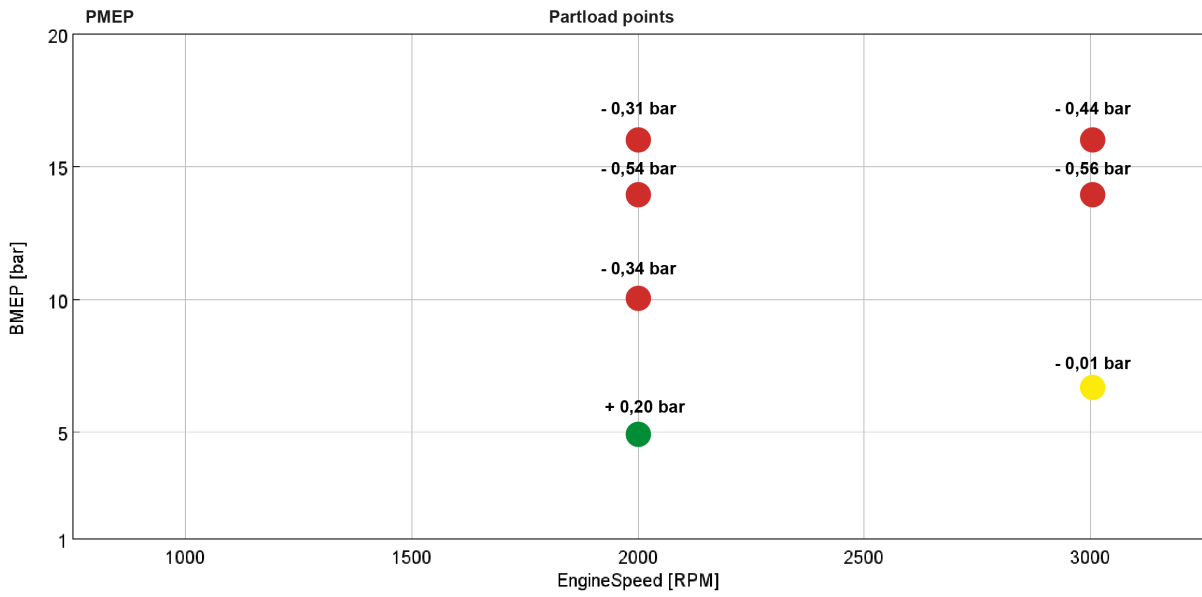


Figure 5.14 Pumping losses deltas: in general, the pumping losses are increased due to increased back pressure (P3) respect the boost pressure (P2). A gain is evinced only where no boost pressure is needed and EIVO can be used to decrease throttling

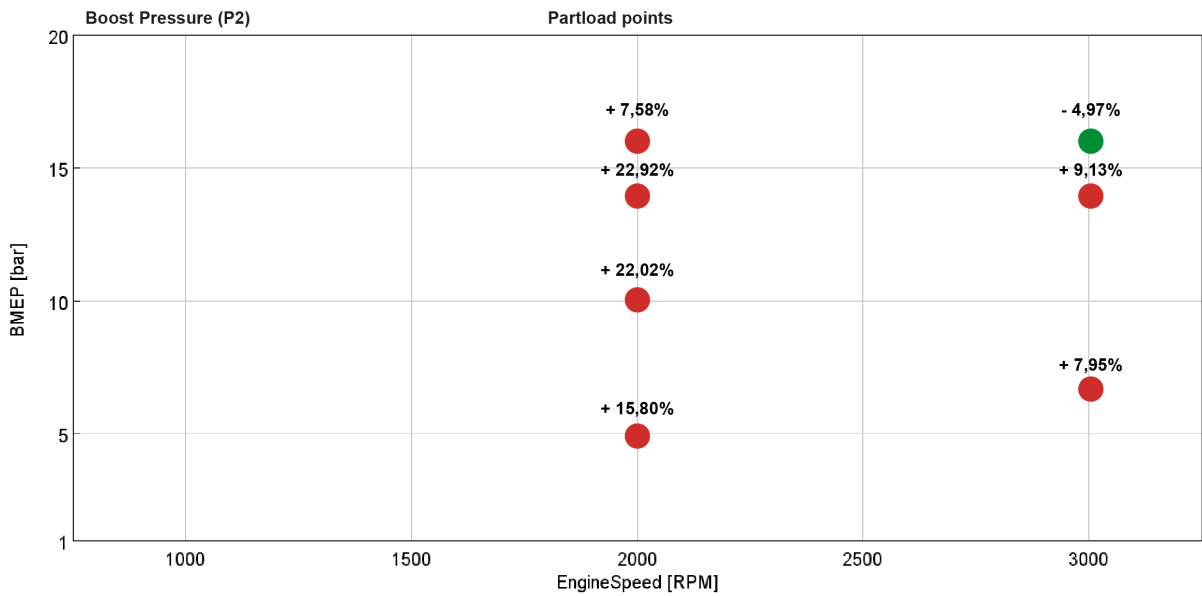


Figure 5.15 Boost pressure in general is higher due to increased mass flow rate demand

5.4 - Results and analysis

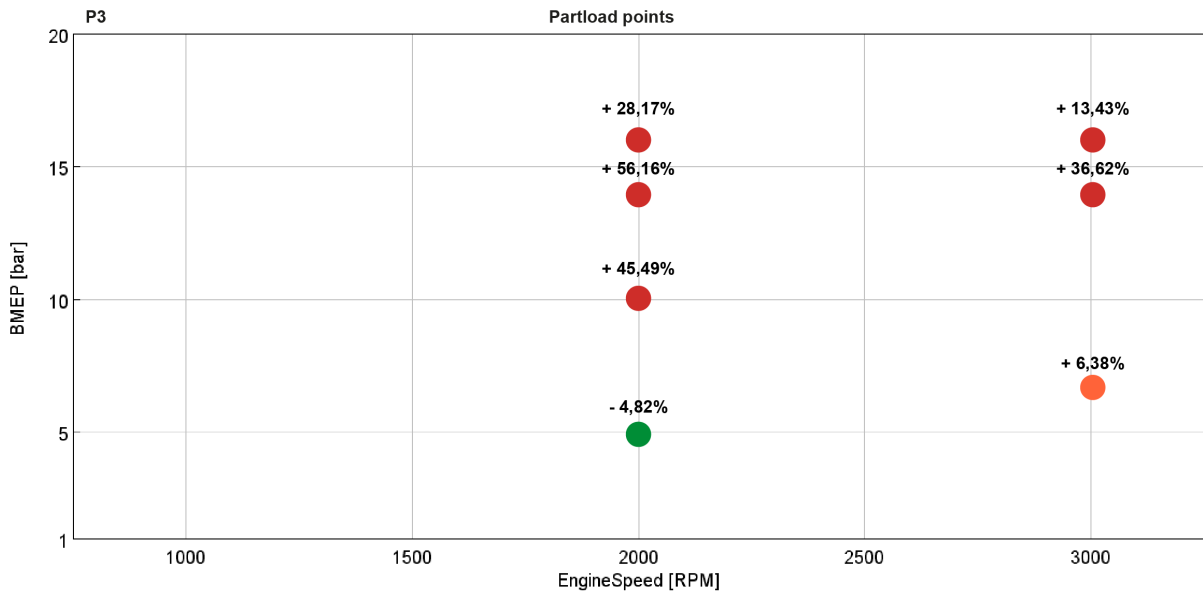


Figure 5.16 As for P2 also P3 is in general higher due to increase mass flow rate demand

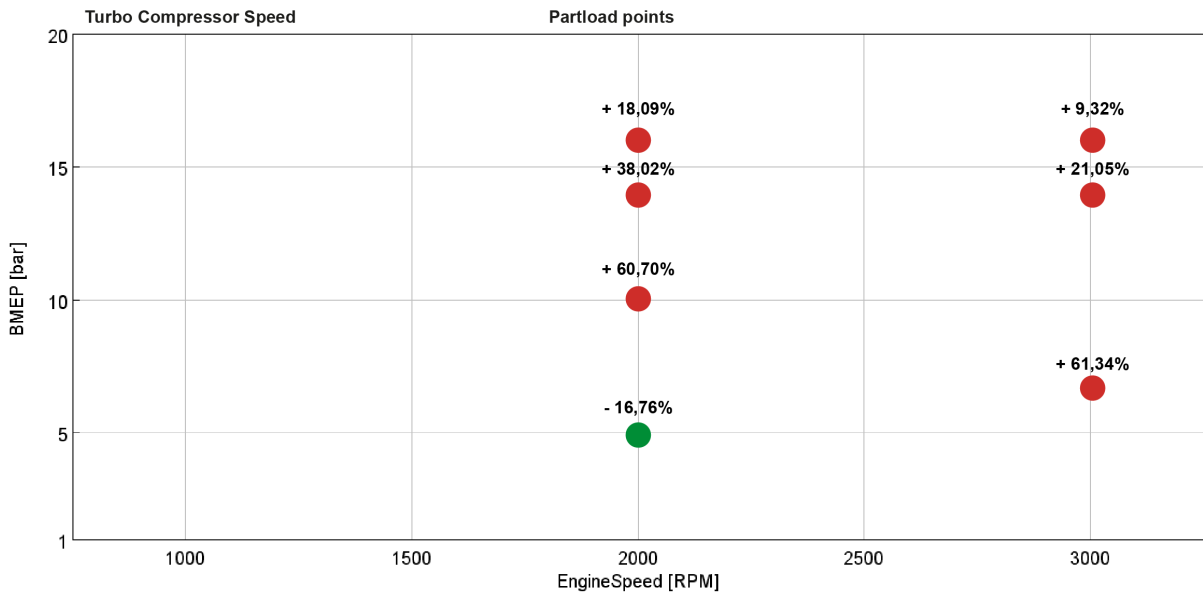


Figure 5.17 The turbo compressor speed confirms the trend showed earlier, the turbo has to guarantee much more mass flow rate

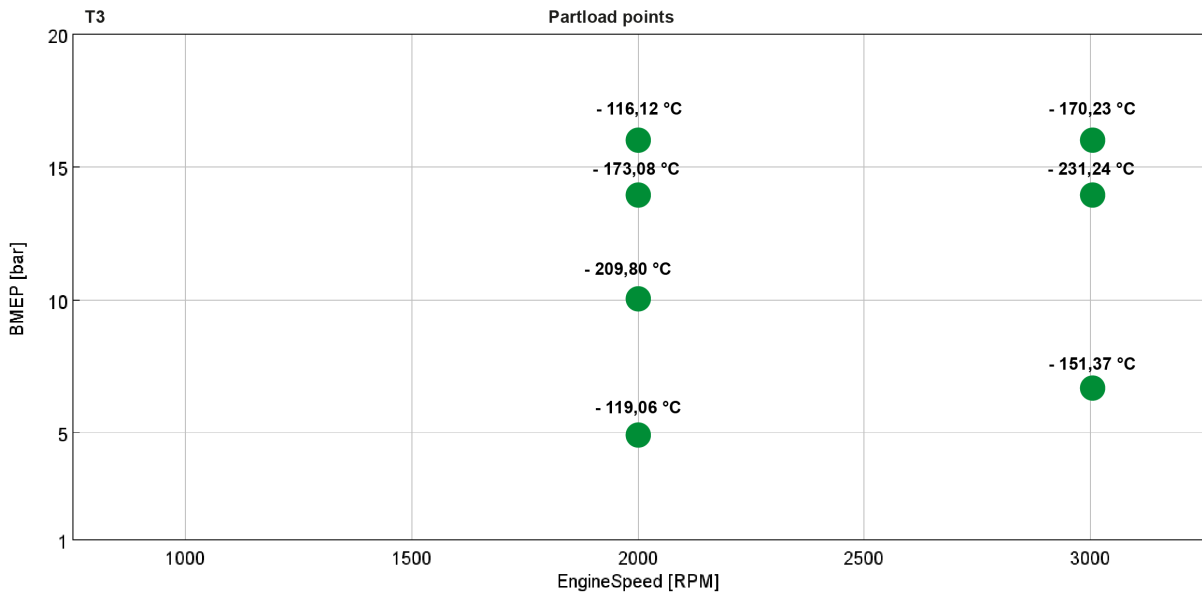


Figure 5.18 The lean combustion brings a considerable decrease of gas temperature respect the GSE-T4 model

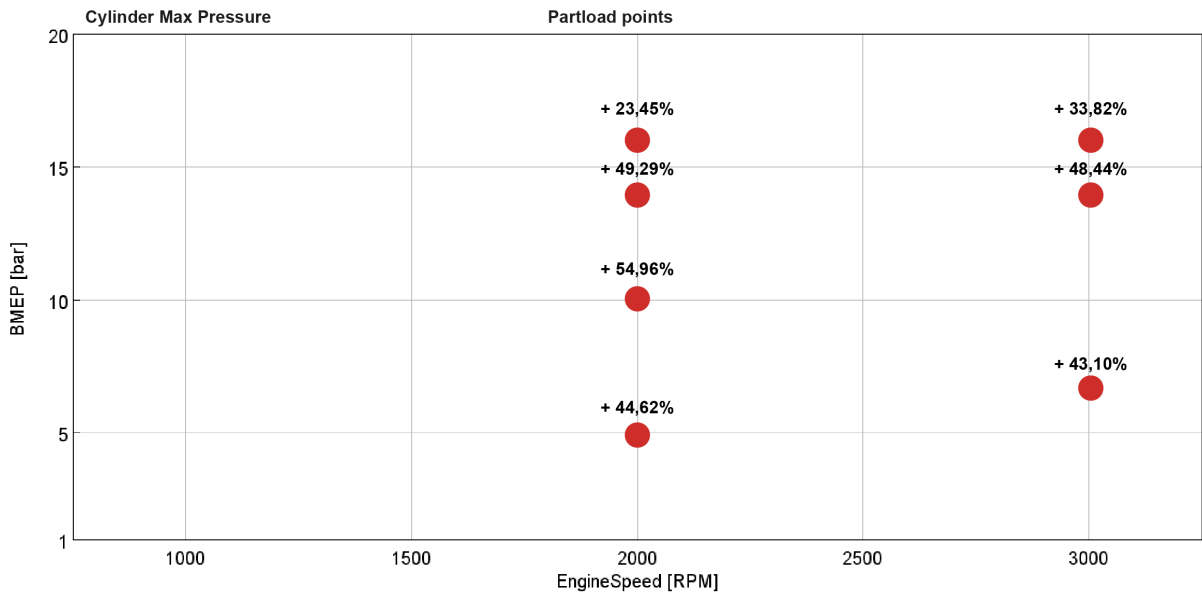


Figure 5.19 Due to increased back pressure and compression ratio the cylinder pressure is much higher respect the GSE-T4

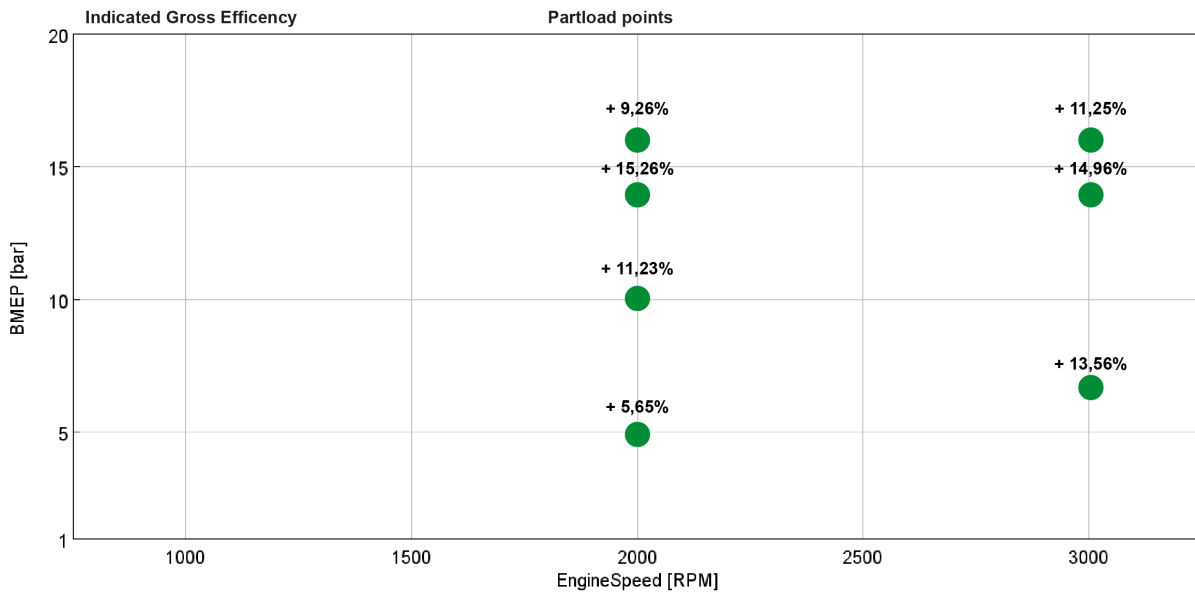


Figure 5.20 The overall efficiency gains for each operating point

As can be seen at the mid to high load points that have a high air-fuel ratio (or high EGR) the boost pressure and back pressure are very high (figure 5.16 and 5.17). The turbo compressor speed is much greater due to the increased mass flow rate needed (figure 5.18). These values combined with an increased compression ratio, lead to much higher in-cylinder pressure than the GSE-T4 model (figure 5.19). In addition, this produces even higher pumping losses (figure 5.15). All this, however, is counterbalanced by the high charge dilution that allows much lower temperatures to be reached inside the cylinder which results in a much lower upstream turbine gas temperature (figure 5.18). This leads to avoid detonation phenomena in the first place, despite the high chamber pressure, and also decreases losses due to heat transfer by increasing combustion efficiency to such an extent that it generates a lower average consumption around 7% (figure 5.12).

At the low load points, it can be seen that the use of EIVO leads to a good decrease in pumping losses (figure 5.14) in the case of 2000x5 or at least counterbalance the exhaust-pressure difference (3000x7) which together with slightly lean combustion still allows lower fuel consumption to be achieved (figure 5.14).

These first results are very promising and show a gain in indicated gross efficiency of up to almost 6% when considering the internal combustion engine alone (figure 5.20). If variables such as energy regeneration via the turbo's electric motor or via the Exhaust gas to coolant Heat Recovery system (EHRS) are included, the overall efficiency of the vehicle can increase even further. However, this first optimisation uses the combustion profile derived from experimental data as a constant input without taking into account possible changes in the profile due to problems in combustion stability caused by aggressive EIVO and LIVC strategies or detonation phenomena due to reaching high in-cylinder pressure. The model assumes that the new type of in-cylinder motion (the Swumble™) is capable of avoiding these types of problems, but experimental confirmations with these types of VVA time strategies will be necessary to continue the development of the model.

Conclusion

In the global energy scenario, the transportation sector, and thus also the automotive sector, is in the midst of a transition to a new mix of technologies to ensure that GHG emissions are properly abated. In this context, technologies flanking today's gasoline engines have made it possible to achieve the target currently envisaged. Turbo direct injection engines with variable valve actuation system such as the GSE T4 represent the state of the art in today's passenger car engines. In this work, it was possible to appreciate the reasons behind these design choices but also their limitations. The constraint of stoichiometric combustion to properly operate the three-way catalyst results in high losses due to heat transfer. The slow attainment of the light-off temperature of the catalyst also represents the major limitation to bring down the pollutant emissions that stand at the beginning of the driving cycle. This is where the PHOENICE project fits in with the goal of eliminating these constraints. By harnessing the electrical energy from the hybrid part of the vehicle, it is possible to incorporate technologies that increase the flexibility of operation of the internal combustion engine. On the other hand, also, PHOENICE focuses heavily on virtual vehicle development with the goal of providing new standards to speed up the whole development process.

This thesis work focused on both aspects. Calibration of the 1D CFD engine model of the GSE T4 led to satisfactory results that will allow the model to be used as a virtual environment in the HiL bench for its initial setup. Subsequently, the PHOENICE ECU software will be developed on this platform in parallel with its hardware and in parallel with its virtual environment as well. Indeed, the model will be constantly updated and will support the development of the real engine on the dyno. In this work, through an availability of an initial dyno test, a first look was taken at the benefits that the PHOENICE modifications brought in terms of efficiency. The results show a considerable increase in efficiency (up to a +6%) corresponding to a decrease in brake specific fuel consumption (up to a -9%) achieved through lean combustion with the addition of an EGR system and a variable geometry turbine. But when considering the use of an electrified catalytic converter and a heat recovery system, the overall efficiency of the vehicle could bring an even greater improvement over the technology present today. PHOENICE with this new concept of combustion engine development geared toward a hybrid architecture will provide what may be a new standard for the development of future hybrid cars toward an increasingly efficient future.

References

- [1] International Energy Agency, «World Energy Outlook 2021,» 2021.
- [2] «United Nations Climate Change,» 2022. [Online]. Available: <https://unfccc.int/process-and-meetings/the-paris-agreement/the-paris-agreement>.
- [3] «European Union Official Website,» 2016. [Online]. Available: https://joint-research-centre.ec.europa.eu/welcome-jec-website/jec-activities/well-wheels-analyses_en.
- [4] International Energy Agency , «Global EV Outlook,» 2022.
- [5] E. Béziat, «Le Monde,» Le Monde, 9 June 2022. [Online]. Available: https://www.lemonde.fr/en/economy/article/2022/06/09/following-historic-vote-internal-combustions-engine-are-set-to-disappear-in-europe_5986231_19.html.
- [6] International Energy Agency, «Global Fuel Economy Initiative,» 2021.
- [7] P. Mock, «Raising the bar: French and Italian manufacturers are leading on electric vehicle target announcements,» International council on clean transportation, 7 January 2022. [Online]. Available: <https://theicct.org/publication/market-monitor-eu-jan-to-dec-feb22/>.
- [8] E. Spessa, *Material of course of Design of a engine and control system*, 2020.
- [9] European Commission, Directorate-General for Energy, «EU energy in figures,» Publications Office, 2021. [Online]. Available: <https://data.europa.eu/doi/10.2833/511498>.
- [10] M. Peter , U. Tietge, S. Wappelhorst, G. Bieker, J. Dornoff e M. R. Bernard, «Market monitor: European passenger car and light commercial vehicle registrations, January–December 2021,» ICCT, 2022.
- [11] H. Jääskeläinen, «Miller Cycle Engines,» 2019. [Online]. Available: https://dieselnet.com/tech/engine_miller-cycle.php.
- [12] F. Germanetti e F. Millo, «Engine Emission Control Lecture Notes,» 2019.
- [13] T. Leroy, X. Gautrot, L. E. Martinez Alvaredo e L. Nowak, «SWUMBLETM 3-Cylinder High Efficiency Gasoline Engine for Future Electrified Powertrains,» IFP Energies nouvelles, 2020.
- [14] European Commission, «PHEV towards zero Emissions & ultimate ICE efficiency,» 2020. [Online]. Available: <https://cordis.europa.eu/project/id/101006841>.
- [15] F. Daudo, «FCA FireFly: l'erede del FIAT FIRE,» Autotecnica.org, 28 March 2019. [Online]. Available: <https://www.autotecnica.org/fca-firefly-t3-t4-turbo-benzina/>.
- [16] D. Stefano, *Material of course: Combustion Engine and their application to vehicles*, 2020.
- [17] C. Curtale, *Simulazione termo-fluidodinamica 1d di un motore lamborghini v12 a ciclo otto: calcolo di prestazioni*, Politecnico di Milano, 2017/2018.

- [18] K. Lamberg, J. Richert e R. Rasche, «A New Environment for Integrated Development and Management of ECU Tests,» dSPACE GmbH, 2003.
- [19] Gamma Technologies, *GT-Suite Manual: General and adadvanced simulation*, Gamma Technologies, 2020.
- [20] Gamma Technologies, *GT-Suite Manual: Flow Manual*, Gamma Technologies, 2020.
- [21] Gamma Technologies, *GT-Suite Manual: Engine Performance*, Gamma Technologies, 2020.